SLAC-254
UC-34d
(E)

SELECTED STUDIES OF CHARMONIUM DECAYS*

Melissa Eve Bronwen Franklin

Stanford Linear Accelerator Center
Stanford University
Stanford, California 94305

August 1982

Prepared for the Department of Energy

under contract number DE-AC03-76SF00515

Printed in the United States of America. Available from the National Technical Information Service, U.S. Department of Commerce, 5285 Port Royal Road, Springfield, VA 22161. Price: Printed Copy A06, Microfiche A01.

---

* Ph.D. Thesis.

ABSTRACT

Selected Studies of Charmonium Decays

Melissa Eve Bronwen Franklin, Ph.D.

Stanford University, 1982

We present two analyses involving decays of the charmonium states, $\psi(3095)$ and $\psi'(3684)$. We have measured the ratio of branching ratios of six strong decays of the ψ and ψ' and compared them with the theoretical prediction of perturbative quantum chromodynamics and the non-relativistic quark model. In four cases there is good agreement and in two cases theory and experiment differ by more than an order of magnitude. We also present an observation of the $\theta(1640)$ in the radiative decay $\psi \to K^+K^-\gamma$, and the measured branching ratios,

$$B(\psi\to\theta\gamma)B(\theta\to K^+K^-) = (6.0\pm.9\pm2.5)\times10^{-4}$$

and

$$B(\psi\to f'(1516)\gamma)B(f'\to K^+K^-) = (.9\pm.3\pm.5)\times10^{-4} \quad .$$

ACKNOWLEDGEMENTS

The acknowledgement, written in haste and by a frantic mind, enters the thesis like a baby squirrel, naked and fuzzy, ensconced in its admiration of the world. Having come to terms with this, I will begin. I acknowledge my thesis advisor, Gary Feldman, for being just what I needed in an advisor, and being it best. I would like to thank Martin Perl, leader of group E, for being completely supportive. My parents I couldn't have done without. Together and independently I thank them for a seemingly endless store of support and perspective. I also acknowledge the Mark II collaboration, including visiting aliens, (of which there were many) and the technical and support staff, for absolutely everything more or less, but particularly for its elegance. I would like to thank theorists: Nathan Isgur for teaching me Feynmans Q.M.'s. Mark Srednicki for his inspiring clarity. Subhash Gupta, Michael Chanowitz, Stan Brodsky, Jonathan Rosner and Frank Close for helpful and fun discussions of my thesis work. My fellow graduate students Michael Levi, Carl Zaiser and Kevin Einsweiler I thank for physics discussions which were helpful and often pleasantly absurd. I thank George Trilling for help with this analysis. All of SLAC for being a friendly and inspiring place to work. I thank my friends who saw me through various graduate school catalysed chemical reactions, familiarly, pre-post adolescence. Mary James for technical discussions of all kinds and for being my friend; Roger Miller, Joe Marsetti, Joe Sodja and David Fryber-

ger. Eric Linstadt for arming me with Philip K. Dick books during the last leg of my thesis and for various quotes well timed. Eric Junior. The Campo Bello social theorists, Lou-head, Roger Hutchins, Ian Hacking Peter B., Jonathan G., Jay, Roz, Eddy, Jodi and Havoc. I thank my reading committee including Fred Gilman and David Ritson. I especially acknowledge Sid R. Spocaine II and his brother Persi for encouragement, cooking and mostly for rekindling my enthusiasm for physics.

CONTENTS

Chapter I

INTRODUCTION

In this thesis two separate analyses are presented. Both involve decays of the charmonium states, $\psi(3096)$ and $\psi'(3684)$. The first analysis is a measurement and comparison of branching ratios of six hadronic decays of the ψ and ψ'. A theoretical calculation based on the non-relativistic quark model and perturbative quantum chromodynamics is made and compared to the relevant experimental results. In four cases which we have measured, (and many more previously measured) there is agreement, and in two cases there is not. No explanation of the disagreement between theory and experiment is found. The second analysis invovles a search for the radiative decay,

$$\psi \rightarrow \theta(1640)\ \gamma \hookrightarrow K^+K^-$$

The $\theta(1640)$ has previously been seen only in the decay,

$$\psi \rightarrow \theta(1640)\ \gamma \hookrightarrow \eta\eta$$

A resonance is found and its measured mass, width and spin are found to be consistent with the $\theta(1640)$. The branching ratio $B(\psi\rightarrow\theta)\times B(\theta\rightarrow K^+K^-)$ is measured. Another resonance is seen in this decay, consistent with the SU(3) spin 2^{++} nonet member, the $f'(1516)$. Finally the branching ratio $B(\psi\rightarrow f'\gamma)\times B(f'\rightarrow K^+K^-)$ is measured.

Chapter II

THEORETICAL MOTIVATIONS

2.1 STRONG DECAYS

The current theory of strong interactions, quantum chromodynamics, (QCD)[1], classifies the $\psi(3095)$ and the $\psi(3684)$ as bound states of a charmed and anti-charmed quark. They are called states of charmonium in analogy to the electron-positron bound states in positronium. They are considered $SU(3)_{colour}$ singlets with quantum numbers $J_{PC} = 1^{--}$ and $I_G = 0^{-}$. Figure 2.1 is an energy level and angular momentum diagram for the charmonium system. The $\psi(3095)$ from here on called the ψ is the 1^3S_1, or ground state of the system and the $\psi(3684)$ from here on called the ψ' is the first radially excited state of the system, 2^3S_1.

The ψ is supposed to decay into hadrons in three ways. It can decay through a virtual photon into a quark anti-quark pair. The quarks then dress themselves to emerge as hadrons. See Fig. 2.2.

---

[1] QCD: A descriptive summary of the theory is given in: Appelquist, Barnett and Lane, Annual Review of Nuclear and Particle Science, Vol. 28, 387 (1978); and in J.D. Bjorken, SLAC-PUB-2372 (1979).

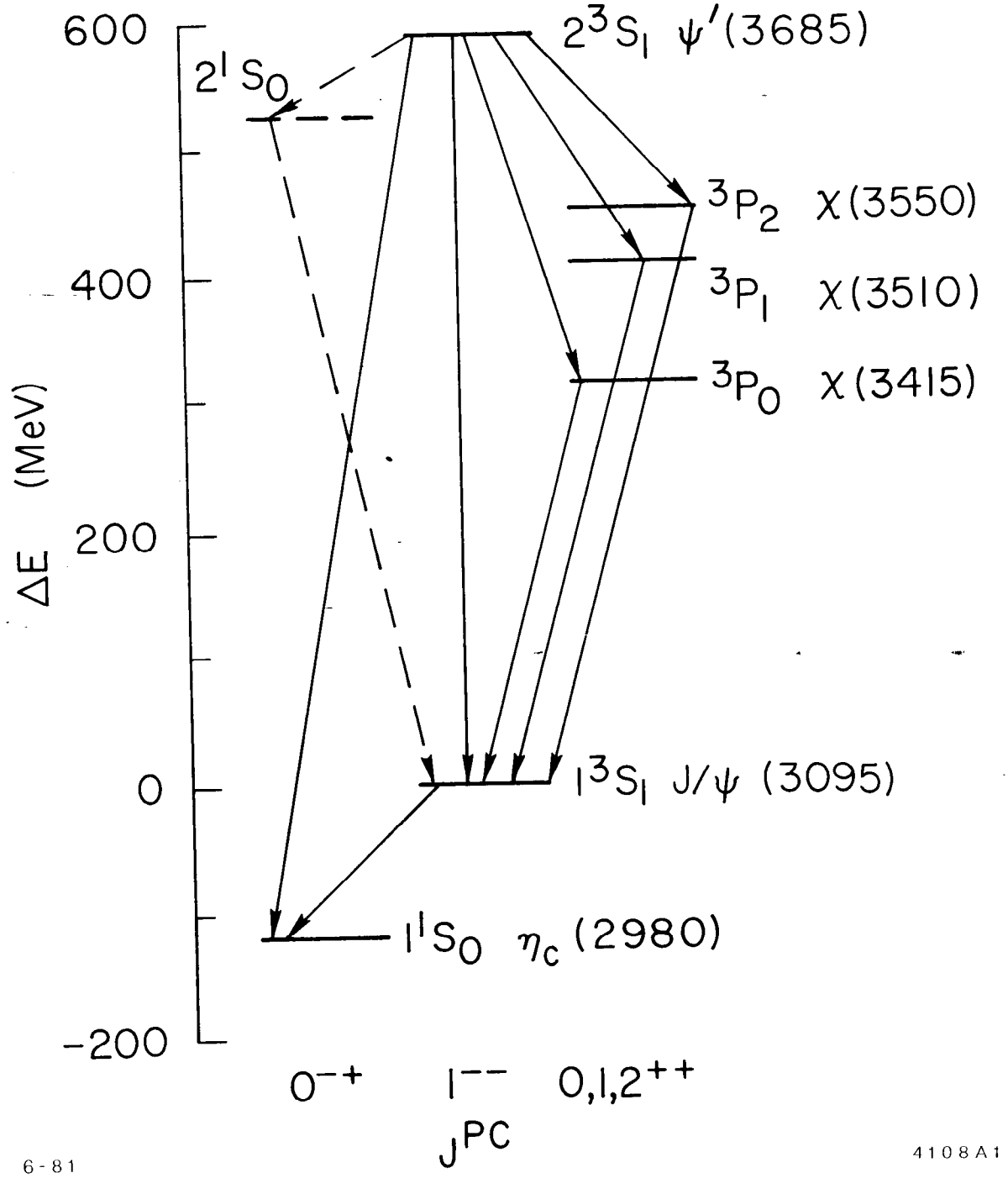

Figure 2.1: Charmonium energy level diagram. All experimentally verified states are shown.

$$e^+ e^- \rightarrow \gamma \rightarrow \psi \rightarrow \gamma_v \rightarrow \text{hadrons} \qquad \text{(a)}$$

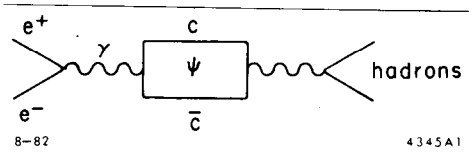

Figure 2.2

It can decay via three[3] gluons, which in turn produce hadrons. See Fig. 2.3.

$$e^+ e^- \rightarrow \gamma \rightarrow \psi \rightarrow g\ g\ g \rightarrow \text{hadrons} \qquad \text{(b)}$$

2.3

Figure 2.3

The third possibility is that the ψ decay into two gluons and one photon as in Fig. 2.4.

$$e^+ e^- \rightarrow \gamma \rightarrow \psi \rightarrow g\ g\ \gamma \rightarrow \gamma + \text{hadrons} \qquad \text{(c)}$$

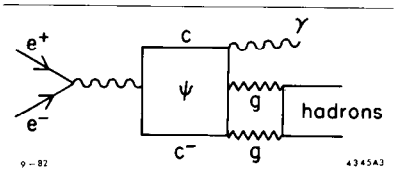

Figure 2.4

---

[3] Note:The ψ cannot decay via one gluon because gluons carry colour and colour is a locally conserved symmetry. It cannot decay via two gluons by charge conjugation conservation. The two gluon system is an eigenstate of the charge conjugation operator with eigenvalue +1. The ψ itself is an eigentstate of C with eigenvalue -1. As charge conjugation is a conserved symmetry the ψ cannot decay into a state of postive C such as the two gluon state. Therefore the the fewest number of gluons the ψ can decay to is three.

One way in which this third possibility can happen is via the resonant state η_c (Fig. 2.5).

$$e^+ e^- \rightarrow \gamma \rightarrow \psi \rightarrow \gamma X,\ X \rightarrow g\ g \rightarrow \text{hadrons} \qquad (d)$$

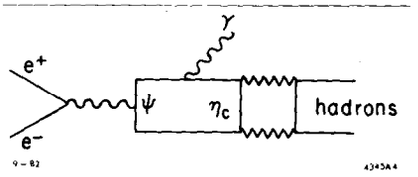

Figure 2.5

The ψ' can decay in all the ways stated for the ψ as well as by the emission of two gluons from one of the quarks. This leaves the quarks in the ground state of charmonium ψ, which then decays by one of the previously discussed routes into hadrons as in Fig. 2.6. The two gluons create a positive charge conjugation state, like $\pi\pi$.

$$e^+ e^- \rightarrow \gamma \rightarrow \psi' \rightarrow \pi\ \pi\ \psi,\ \psi \rightarrow \text{hadrons} \qquad (e)$$

Figure 2.6

In the first part of this thesis we are interested in the strong, isospin conserving decays of the ψ and ψ', reaction (b). The rate for

this decay is calculable in lowest order perturbation theory of QCD under certain assumptions.

We must assume that:

1) The quark-gluon coupling constant squared, α_s^2 is small compared with 1 in order to motivate the use of a perturbation expansion in α^2.

2) There are no significant contributions to the decay amplitude from the Feynman diagrams which include three-gluon verticies.

3) The charmed quarks behave in a non-relativistic manner within the bound state, so that we don't have to make relativistic corrections to the naive non-relativistic quark model. This approximation can be made due to the heavy masses of the charmed quarks.

4) The annilhilation takes place at a point. This last assumption states that the width $\Gamma(\psi \rightarrow \text{hadrons})$ depends only on the wavefunction of the ψ at the origin squared, $|\Psi(0)|^2$, and its mass. The origin is defined as the point where the separation between the quark and anti-quark is zero. Given all the above assumptions we can use lowest order perturbation theory and draw from the quantum electrodynamical analysis of positronium decays to calculate the width:

$$\Gamma\ (\psi \rightarrow 3 \text{ gluons})$$

The width for the decay of the triplet or orthopositronium state into three photons is:[3]

$$\Gamma(^3S_1 \rightarrow \gamma\gamma\gamma) = \frac{16(\pi^2-9)}{9\pi} \frac{\alpha^3|\Psi(0)|^2}{M^2} \qquad (1)$$

---

[3] A derivation of this formula is given in: Jauch and Rohrlich, Theory of Photons and Electrons, Addison Wesley, Reading, Mass.

where $\alpha = 1/137$ is the electromagnetic coupling constant, M is the positronium mass and $\Psi(0)$ is the wavefunction of the $^3S_1$ positronium state at the origin. The prescription to go from three photons to three gluons in the final state is to replace

$$\alpha^3 \quad \text{by} \quad 5\alpha_s^3/18$$

This can be shown using SU(3) colour symmetry[4]. If the ψ is the $^3S_1$ state in question, then

$$\Gamma(\psi \to ggg) = \frac{40(\pi^2-9)}{81\pi} \frac{\alpha_s^3 |\Psi(0)|^2}{M_\psi^2} \qquad (2)$$

where $\Psi(0)$ is now the wavefunction at the origin of the ψ. Two further assumptions are made. The first is that the probability that the three gluons decay to hadrons, is equal to 1. The second is that the strong coupling constant α_s does not change appreciably from 3.1 GeV to 3.7 GeV.

We have picked for analysis final states which are produced predominantly through the three gluon decay. These are states of negative or undefined G-parity, such as states with an odd number of pions or which include kaons and pions. The G-parity operator is defined as;

$$G = C \exp(iI_2\pi) \quad \text{and} \quad G|\pi\rangle = -|\pi\rangle$$

where I_2 is the second component of the isospin operator.

---

[4] Applequist and Politzer, PRL 34, 43 (1975).

Negative G-parity states can also be produced via the non-isospin conserving electromagnetic decay (a) of the ψ. The photon has quantum numbers , $I_g = 1_+, 0_-$ and can therefore produce final states with isospin 1 or 0. The amplitude for this QED process is proportional to α^4. The ratio of cross-sections,

$$\frac{\sigma(e^+e^- \to \psi \to \gamma \to \text{HADRONS})}{\sigma(e^+e^- \to \psi \to \gamma \to \mu^+\mu^-)} = 2.7 \pm 0.5 \quad . \qquad (3)$$

This ratio is the same on and off the ψ resonance because the Feynman diagrams can be factorised. The ratio was measured off-resonance[5]. So by measuring $\sigma(e^+e^- \to \psi \to \gamma \to \mu^+\mu^-)$ on resonance we determine $\sigma(e^+e^- \to \gamma \to \psi \to \text{hadrons})$. We find an 18% contribution to the total hadronic width of the ψ from (a). We are looking for the portion of these electromagnetic decays which will result in decays to final states with isopin 0 and G-parity negative. Two arguments suggest the same result:

1. For isospin I=1, the third component of isospin I_z can be 0, -1, or +1, whereas for I=0, I_z can only be 0. Naively then 1/4 of the time the electromagnetic decay produces I=0 final states and thus 1/4 × 18% = 4.5% of the observed decays will be due the to electromagnetic decays (a).

2. Another way to show this is to look at the vector meson couplings to γ, $G_v \propto 1/\gamma_v$ where v labels the particular vector meson. From experiment[6],

---

[5] J.L.Siegrist, Phd. Thesis, SLAC Report No. 225, October 1979. (Unpublished)
[6] F.J.Gilman, SLAC-PUB 1600, June 1975.

$$\frac{1}{\gamma_\rho{}^2} : \frac{1}{\gamma_\omega{}^2} : \frac{1}{\gamma_\phi{}^2} = 7.2 : 1.0 : 1.7$$

The isospin of the ω and ϕ is 0 and the isospin of the ρ is 1. The photon couples three times more strongly to I=1 than to I=0. Therefore approximately 4% of the I=0, hadronic final states are due to (a). For final states with undefined G-parity the above arguments do not apply. For final states such as $K^+K^-\pi^0$, the fraction of events produced through a photon is unknown. I will ignore this electromagnetic contribution throughout unless otherwise stated.

What has actually been measured are not the partial widths , but rather the branching ratios:

$$B(\psi \to X) = \frac{\Gamma(\psi \to X)}{\Gamma_t(\psi)} \qquad (4)$$

where X is a particular final state, Γ_t is the total width of the ψ and $\Gamma(\psi \to X)$ is the partial width. We can construct the ratio of the branching ratios from the ψ and ψ'.

$$Q \equiv \frac{B(\psi' \to X)}{B(\psi \to X)} = \frac{\Gamma(\psi' \to X)\ \Gamma_t(\psi)}{\Gamma(\psi \to X)\ \Gamma_t(\psi')} \ . \qquad (5)$$

From (2), making the assumption that the ratio of partial widths is equal to the ratio of light hadronic widths from the ψ and ψ', we have,

$$\frac{\Gamma(\psi' \to X)}{\Gamma(\psi \to X)} = \frac{|\Psi'(0)|^2\ M_\psi{}^2}{|\Psi(0)|^2\ M_{\psi'}{}^2} \ . \qquad (6)$$

This assumption is open to question. We make it because there are no theoretical calculations of the particular partial widths we are looking

at and because there is no reason to think that it is otherwise. Since the electromagnetic annihilation of the ψ to electron pairs occurs at a point in the non-relativistic quark model, the width is proportional to the square of the wavefuntion of the ψ at the origin:

$$\Gamma(\psi \to \gamma \to e^+e^-) \propto \frac{|\Psi(0)|^2}{M_\psi^2} \quad . \qquad (7)$$

This means that by measuring the leptonic widths of the ψ and ψ' we obtain the ratio of their wavefunctions at the origin. To measure the leptonic and total widths of the ψ and ψ', we use the fact that

$$\Gamma(\psi \to e^+e^-) = \frac{M^2}{6\pi^2} \int \sigma_{tot}(\psi)\, dE \qquad (8)$$

and

$$\Gamma_t(\psi) = \frac{\int \sigma_{tot}\, dE\ \Gamma(\psi \to e^+e^-)}{\int \sigma(\psi \to e^+e^-)} \qquad (9)$$

and integrate the measured total and leptonic cross-sections. From Mark I data taken at SPEAR[7,8]:

$$\frac{\Gamma(\psi \to e^+e^-)}{\Gamma_t(\psi)} = 0.069 \pm 0.009$$

and

$$\frac{\Gamma(\psi' \to e^+e^-)}{\Gamma_t(\psi')} = 0.0093 \pm 0.0016$$

substituting back into equation 5, we find:

---

[7] Boyarski et al., Phys. Rev. Lett. 34, 1357 (1975).
[8] V.Luth et al., Phys. Rev. Lett. 35, 1124 (1975)

$$Q = \frac{\Gamma(\psi' \to e^+e^-)\ \Gamma_t(\psi)}{\Gamma(\psi \to e^+e^-)\ \Gamma_t(\psi')} = 0.135 \pm 0.023 \quad .$$

This then is the ratio expected by perturbative QCD. It is the goal of this thesis to measure this ratio for various decay modes and compare these experimental results with the prediction.

2.2 RADIATIVE DECAYS

Though the ψ resonance was discovered simultaneously in the data of two experiments in November of 1974[9], it was not until 1976 that the first radiative decay of the ψ,

$$\psi \to \eta\ \gamma \ ^{10}$$

was observed. The dominant decay of the ψ into hadrons was thought to be via three gluons. In 1975 Chanowitz[11], Okun and Voloshin[12], and Applequist et al.[13], suggested that an obvious extension of the three gluon decay was the decay ocurring via two gluons and one photon. They calculated the ratio of widths:

$$\frac{\Gamma(\psi \to \gamma gg)}{\Gamma(\psi \to ggg)} \sim 10\%$$

---

[9] Augustin et al., Phys. Rev. Lett. 33, 1453 (1974);J. J. Aubert et al., Phys. Rev. Lett. 33, 1404 (1974).
[10] Bartel et al., Phys. Lett, 64B, 483 (1976)
[11] M. Chanowitz, Phys. Rev. D12, 918 (1975).
[12] ITEP-95, (1976).
[13] Applequist et al., Phys. Rev. Lett. 34, 365 (1975).

assuming the photon to be real ($q^2 = 0$). In 1977 Brodsky et al.[14] suggested that the these two gluon, one photon decays of the ψ were a place to look for gluon bound states. The two gluons can form a quark-antiquark bound state as in Fig. 2.7.

Figure 2.7

which would decay to hadrons. The two gluons can also, by the non-Abelian nature of QCD, couple to a third gluon, and so forth, forming a gluon bound state, familiarly called a glueball. See Fig. 2.8.

Figure 2.8

A glueball, it is thought, would be distinguishable by both its refusal to fit into the quark antiquark SU(3) multiplet arrangement and its flavour independent decays to hadrons. There are now (1982) two possible candidates for glueballs. One is the $\iota(1420)$ seen[15] in the decay $\psi \to \gamma KK\pi$ and the other is the $\theta(1640)$[16] observed in the decay, $\psi \to \eta\eta\gamma$. In this thesis we have focussed on this second possibility.

---

[14] S. Brodsky,T. A. DeGrand, R.R.Horgan, and D.G.Coyne, Phys. Lett. 73B (1978).
[15] C. Edwards et al., Phys. Rev. Lett. 49, 259 (1982).
[16] C. Edwards et al., Phys. Rev. Lett. 48, 458 (1982).

Chapter III

THE DETECTOR

This analysis was performed on data taken at the SPEAR electron positron storage ring at the Stanford Linear Accelerator Center with the Mark II magnetic detector during the fall of 1978 (cycle 1) and the spring of 1979 (cycle 2). The SPEAR storage ring and the Mark II detector are described in detail elsewhere[1]. What follows is a brief description of the detector noting in particular, attributes relevant to this analysis.

Figure 3.1 is a cross-sectional schematic sliced in the x-y plane, of the detector. Figure 3.2 is an expanded isometric diagram of the detector. Travelling radially outward from the e^+e^- interaction point a particle travels through $\simeq$ 7 cm of vacuum, the beam pipe, the pipe counter, the central drift chamber, the time of flight scintillators, the magnet coil, the liquid argon shower counters and the muon counters.

The charge,momentum, energy, and type of a particle escaping the interaction region are found by employing five types of detector.

---

[1] R. Schindler, Ph.D. Thesis, SLAC-Report No. 219, (1979) (unpublished).

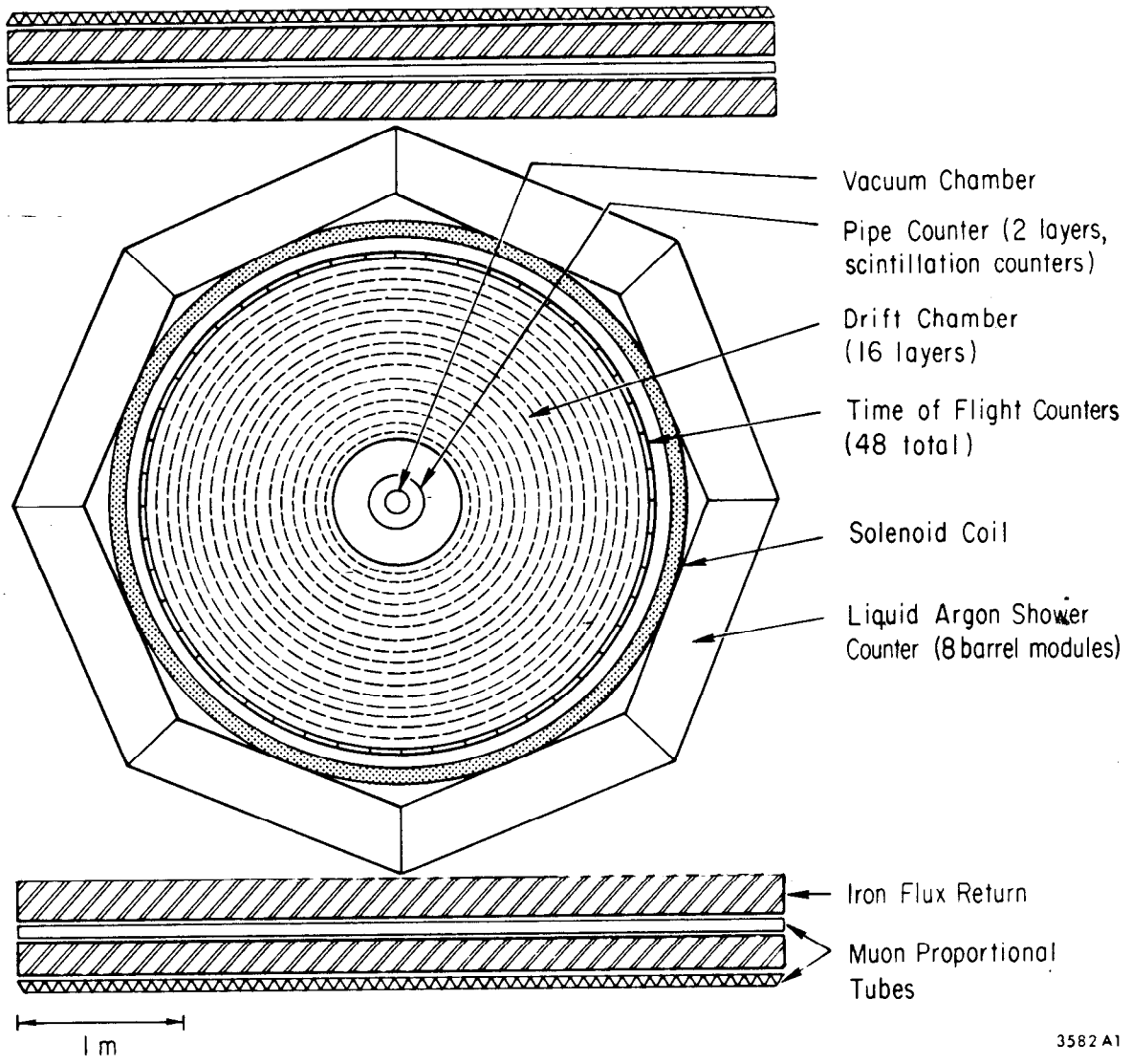

Fig. 3.1: The Mark II detector, schematic cross-section.

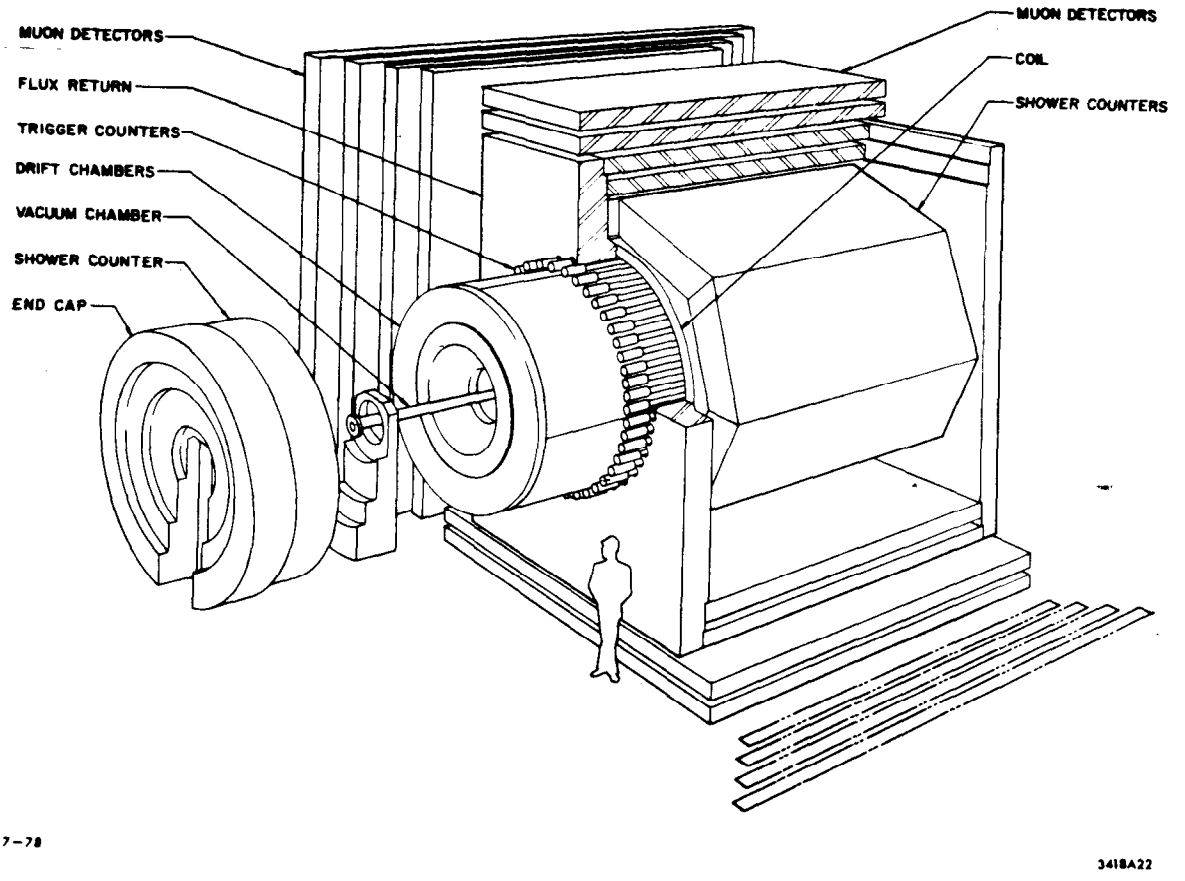

Fig. 3.2: The Mark II detector. An expanded isometric outline with human scale included.

1. SCINTILLATION COUNTERS

Hugging the .21 mm thick corrugated stainless beam pipe are two layers of semi-cylindrical .6cm thick plastic scintillator. This set of four counters comprise the pipe counter. The pipe counter is required in the primary trigger and is used as a cosmic ray veto.

There is a set of 48 344.2cm by 20.3cm by 2.5cm scintillation counters arranged in a cylinder about the beam axis, at a radius of 1.515 metres. They are viewed by photomultiplier tubes at both ends. Both end to end timing and a pulse height analysis are performed on the phototube signals to measure the flight time of charged particles travelling through the detector. This time of flight (TOF) system is used to identify the type of particle being tracked by assigning to it a mass consistent with its velocity and path length in the drift chamber. The TOF resolution σ is defined by the rms width of the gaussian curve describing the TOF residual. The residual is defined as the expected time minus the measured time. The σ for hadrons is $\simeq$ 300 picoseconds; the σ for electrons is $\simeq$ 270 picoseconds. Figure 3.3 is a plot of the TOF residual. This system can distinguish, at the 1 σ level, between π's and e's with momentum below 300 MeV/c, between π's and K's below 1.3 GeV/c and between protons and kaons below 2 GeV/c.

2. DRIFT CHAMBERS

Lying coaxial with the beam line, and situated inside the TOF system and outside the pipe counter in a 4.16 kilogauss solenoidal magnetic field, is the central cylindrical drift chamber which is used to measure

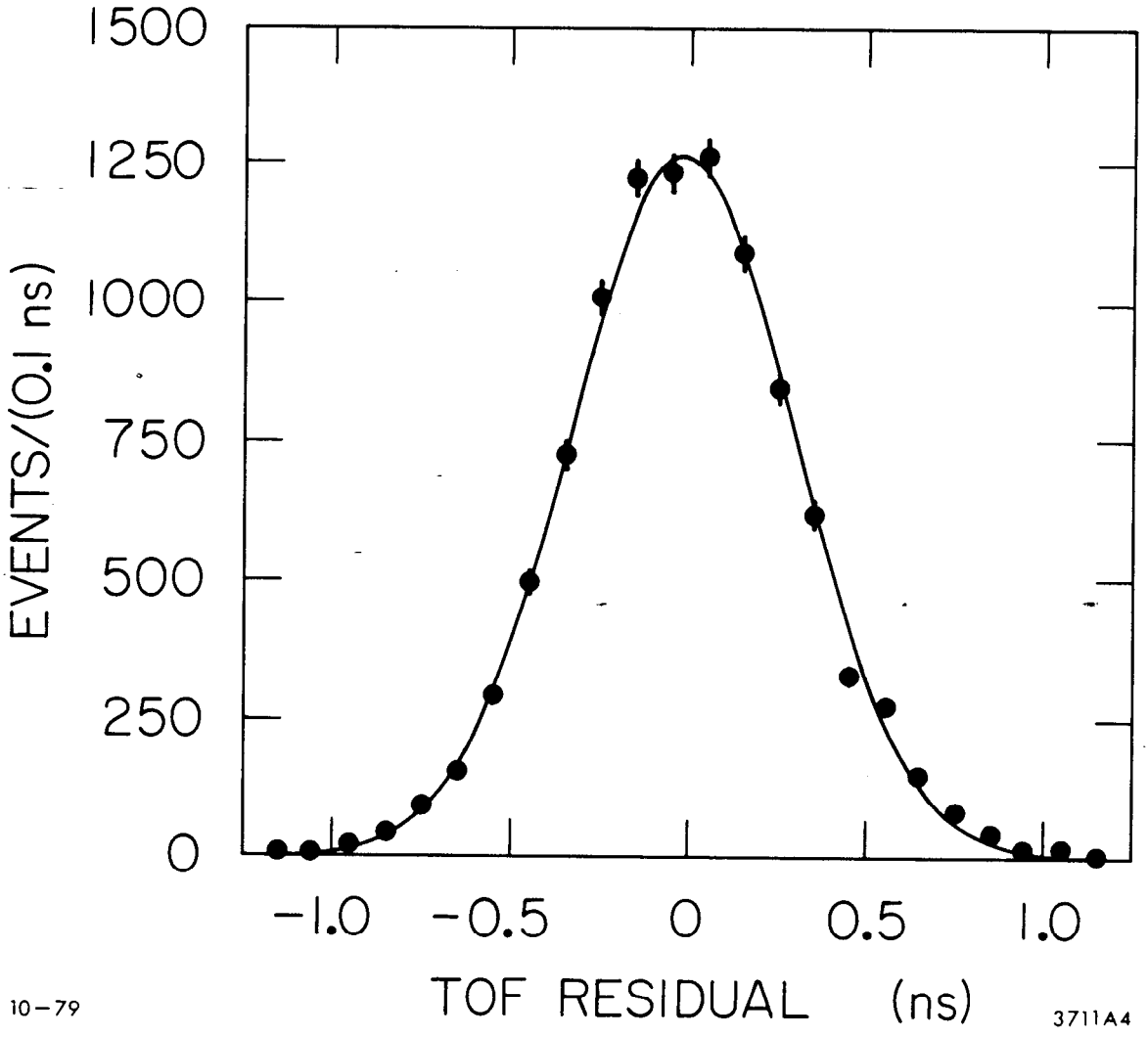

Fig. 3.3: Time of flight resolution for muons from ψ decays.

the momentum of charged particles. It covers ≃ 85% of 4π steradians. There are 16 layers in all. Six layers have sense wires strung parallel to the beam line and the remaining 10 have sense wires strung at an angle of ≃ 3° relative to these. That is, one end of these stereo layer wires is rotated by $\delta\phi = 3R/L^{\circ}$ with respect to the other end, where L is the length of the wire, and R is the radius of the wire from the beam line. All 16 layers together allow a three dimensional reconstruction of the path of a charged particle. The mean spatial resolution is ≃ 220 microns. The rms momentum resolution is

$$\delta p/p = \sqrt{[(.015)^2 + (.005p)^2]}$$

The first term under the square root is due to multiple scattering in the material of the detector and the second term is momentum dependent and is due to the single drift chamber cell spatial resolution.

3. LIQUID ARGON CALORIMETER

There are eight liquid argon shower counter modules arranged in an octagon , coaxial to the beam line, outboard of the magnet coil, which cover ≃ 64% of 4π steradians of solid angle. This coverage does not include the liquid argon south endcap which was not used in this analysis. The LA system is used to detect electromagnetic showers made by photons and leptons and hadronic showers made by interacting hadrons. In this analysis they are used to identify photons and to separate electrons from hadrons. Each module in the octagon is a lead strip-liquid argon sandwich, 18 layers long. Each layer consists of 2mm of lead followed by 3mm of liquid agron. A particle goes through 14 radiation

lengths of lead and liquid argon if it travels normally through a module. Alternating layers of the lead stips are held at ground potential, while the remainder are held at high voltage to collect charge from ionization. This charge is integrated over time and amplified to produce the liquid argon signals. In these layers the lead is in strips between 3.8 and 5.2 cm wide (depending on the layer) producing a mean angular resolution of σ = 8 milliradians. The strips run at 45°, 90° and 0° relative to the beam line providing 3-dimensional spatial reconstruction of neutral tracks. The energy resolution is measured to be $\delta E/E = 14\%/\sqrt{E}$. A complete description of the liquid argon system is given by Abrams et al.[1]

4. PROPORTIONAL MUON TUBES

The muon detection system consists of four sections of steel-proportional tube sandwiches, arranged in a rectangle about the central detector. The muon system is used to identify muons, by ranging out all more highly interacting particles in the steel. There are three layers. The first two layers of steel are 23 cm thick and the last layer on the top section is 30cm thick. μ's with momentum greater than 1 GeV will be detected as μ's. The magnet flux return on the top and bottom of the detector (refer to Fig. 3.1) is used as the first layer of absorbing steel. The proportional counters are extruded aluminum triangular tubes with the anode wires strung either parallel to the beamline or at 90° to it. Pions are sometimes misidentified as muons in two ways. To

---

[1] G.S.Abrams et al., IEEE Transactions on Nuclear Science NS-25,309 (1978).

begin with the pion has a small probability of not interacting in the steel. When this happens the pion is called a punch-through pion. Pions also have a small probability of decaying via, $\pi^- \rightarrow \mu\nu$, before they reach the muon counters, and are then identified as μ's. In this analysis the muon system is used only to reject μ's.

There are three layers of multi-wire proportional chambers at the north end of the detector which are not used in this analysis and therefore will not be further discussed.

5. MAGNET

The magnet is a two layer aluminum wound solenoid, $\simeq$ 1.4 radiation lengths long, which sits between the central drift chamber and the liquid argon modules. It provides a 4.16 kilogauss solenoidal magnetic field z direction, which is held constant to .2%. The field was mapped before the installation of the magnet with a Hall probe and is monitored during data taking by a probe which works on the principle of nuclear magnetic resonance.

Chapter IV

TRIGGER, NORMALISATION AND MONTE CARLO

4.1 THE TRIGGER

The trigger consists of two levels of requirements. The first level demands that a coincidence occur involving a hit in both layers of either half of the pipe counter, a beam crossing signal, and hits in four out of six layers in the central drift chamber. Events which satisfy this primary trigger are sent on to the secondary trigger, which finds tracks according to a well specified track finding algorithm[1], classifies them, and counts them. For our analysis the secondary trigger, which was programmable, required one track with at least 4 out of 6 of the axial layers of the drift chamber to fire and another track with at least 3 out of the 5 innermost layers of the drift chamber to fire. The secondary trigger rate was low, $\simeq$ 1-3 Hertz, which made the triggering efficiency for $\geq$ 2 prong events $\simeq$ 99%. That is, almost no events were lost due to trigger inefficiencies caused by trigger rate. For a complete and detailed description of the Mark II trigger, see Himel[1].

---

[1] Himel,T.M., Thesis, SLAC Report No. 223 , (1979).

4.2 THE NORMALIZATION

The number of produced ψ''s in our data sample was calculated[1] by measuring the number of detected events of the type;

$$\psi' \rightarrow \pi^+\pi^-\psi, \quad \psi \rightarrow \ell^+\ell^-$$

The efficiency for detecting these events was calculated using the Mark II Monte Carlo program in which the π^+ and π^- were thrown according to a distribution which included their final state interaction. Using the branching ratios

$$B(\psi' \rightarrow \pi^+\pi^-\psi) \quad \text{and} \quad B(\psi \rightarrow \ell^+\ell^-)$$

measured[2] by the Mark I collaboration at Spear, and the Monte Carlo generated efficencies; the number of produced ψ' events derives directly from the number of the above events observed. The resulting number of produced ψ''s in the data sample is;

$$(1.02 \pm .04 \pm .17) \times 10^6,$$

where the first error is due to uncertainty in the calculation of the detection efficiency and the second error comes from the error in the measured branching ratios.

To measure the number of produced ψ's in our data sample, a clean sample of ψ's was obtained for study by selecting events at the ψ',of the type,

$$\psi' \rightarrow \pi^+\pi^-\psi,$$

---

1 Himel,T.M., Thesis, SLAC Report No. 223, October 1979.
2 Particle Data Group, Phys. Lett. 75B (1978)

in which the π^+ and π^- satisfy the detector trigger independently of the decay products of the ψ, (which are not necessarily observed). These events are selected by requiring that two oppositely charged pions be observed and that the missing mass recoiling against them be that of the ψ. This provides an unbiased sample of ψ's with which we measure the ψ detection efficiency. The fraction of such events in which the ψ decay products satisfy the detector trigger is the ψ detection efficiency. This method then gives a relationship between the number of ψ's detected and the number of ψ's produced. This relationship is checked by running the Monte Carlo program for various exclusive decays of the ψ and measuring their respective detection efficiencies. Measured branching ratios are used to obtain the number of produced ψ's in the sample in each case. The number calculated by this method agrees with the number of the previous method to within 5%.

The total number of produced ψ's then is

$$427{,}000 \pm 21{,}000$$

The Mark II detector at Spear accumulated data corresponding to 1.3×10^6 produced ψ's. However, half of this data was taken whilst the liquid argon shower detection system was inoperational. Since the following analysis relies heavily on photon detection this half of the data was not used. In summary we have a sample of 427,000 produced ψ events with complete liquid argon shower counter information, approximately 200,000 ψ's with seven of the eight liquid argon modules working. We also have another 640,000 ψ's taken when the liquid argon system was totally inoperational. The total data sample corresponds to 1,300,000 produced ψ's.

For the ψ', all data was taken with the complete liquid argon calorimeter working. Table 4.1 is a summary of ψ and ψ' data taken with the Mark II detector.

Table 4.1

Sample	Fraction of LA Shower Counters Operational	Number of Produced Events
ψ : 1	8/8	427,000
ψ : 2	7/8	200,000
ψ : 3	0/8	640,000
ψ'	8/8	1.02×10^6

4.3 THE MONTE CARLO

The Monte Carlo method is used to compute efficiencies and acceptances in this analysis. The Mark II Monte Carlo randomly generates "events", consisting of 3-momentum vectors thrown according to user specified final state hypotheses and user specified momentum distributions. For final states not involving resonances, Lorentz invariant phase space distributions were generated. The program then tracks the

"particles" defined by the momentum vectors and masses through a simulated detector. The simulation includes almost all of the Mark II's relevant attributes. It includes:

(a) Energy losses as the charged tracks pass through material in their paths.

(b) A measured distribution of vertex positions for the events.

(c) The probability that photons will convert in the detector.

(d) The probability that particles will interact in the detector and estimates how they will interact. This includes multiple scattering and nuclear interactions.

(e) The measured cross-sections for interactions for e^+e^-, etc.

(f) The measured lifetimes of the produced particles.

(g) Measured detector resolutions for the TOF and drift chamber systems.

(h) The probability that the leptons bremsstrahlung.

(i) The liquid argon calorimeter efficiency and energy resolution.

It generates liquid argon raw data, and showers the particles travelling through the liquid argon modules, using an electromagnetic showering Monte Carlo package called EGS[1].

---

[1] R.L.Ford and W.R.Nelson, Computer Programs for the Monte Carlo Simulation of Electromagnetic Cascade Showers, SLAC Report No. 210, 1978

Chapter V

EVENT SELECTION

We measure the branching ratios from the ψ and the ψ' to the following final states:

$$\pi^+\pi^-\pi^0$$

$$K^+K^-\pi^0$$

$$p\bar{p}\pi^0$$

$$2\pi^+2\pi^-\pi^0$$

$$\pi^+\pi^-\omega$$

$$3\pi^+3\pi^-\pi^0$$

The event selection criteria and methods of analysis are quite similar for these different modes. We will describe here in detail the methods common to all these analyses.

In all cases we require that a π^0 be detected in the final state. A photon which decays from a π^0 appears as a signal in the liquid argon (LA) shower counter with no associated charged track in the drift chambers. The definition of a π^0 is two observed photons in the LA whose invariant mass is $115 < M(\gamma\gamma) < 165$ MeV/c^2. Noise in the liquid argon shower detection system in conjunction with energy deposited in the modules from charged tracks in an event can cause spurious signals in the liquid argon system. These signals of non-existent photons are called fakes. The energy spectrum of fakes peaks at about 150 MeV/c. Figure

5.1 shows the photon energy spectrum in events of the type, $\psi' \to \pi^+\pi^-\psi$, $\psi \to \ell^+\ell^-$ in which no photons are expected. These are by definition fakes. These pose a serious background to signals in which two photons are required. It is possible that a fake will combine with a real photon to form a π^0 signal. A number of cuts are made to diminish the number of fakes which contaminate the real photons. The first is a momentum cut. We require that photons have momentum greater than 150 MeV/c (unless explicitly noted). The second is that only photons found in one of the eight liquid argon barrel modules be allowed. This is needed because the liquid argon endcap was very noisy and therefore not useful for this analysis. Each liquid argon shower counter module has 16 layers, containing both lead and liquid argon. To minimise the cost of electronics to read out the system, many of the layers are combined and read out together. In this way, the counter is divided into six sections. Figure 5.2 shows the ganged schematic of the liquid argon system.

A clean sample of photons was analysed to determine a photon signature in the shower counters. This resulted in a set of cuts on photons which reject fakes. If the summed energy in layers 1 and 2 divided by the total energy < .05 GeV and the energy of the photon < .300 GeV

or

the energy in layers 1, 2 and 3 < .15 GeV

or

the energy in layers 1 and 3 < .01 and the energy of the photon < .3 GeV,

then the photon is rejected as a fake.

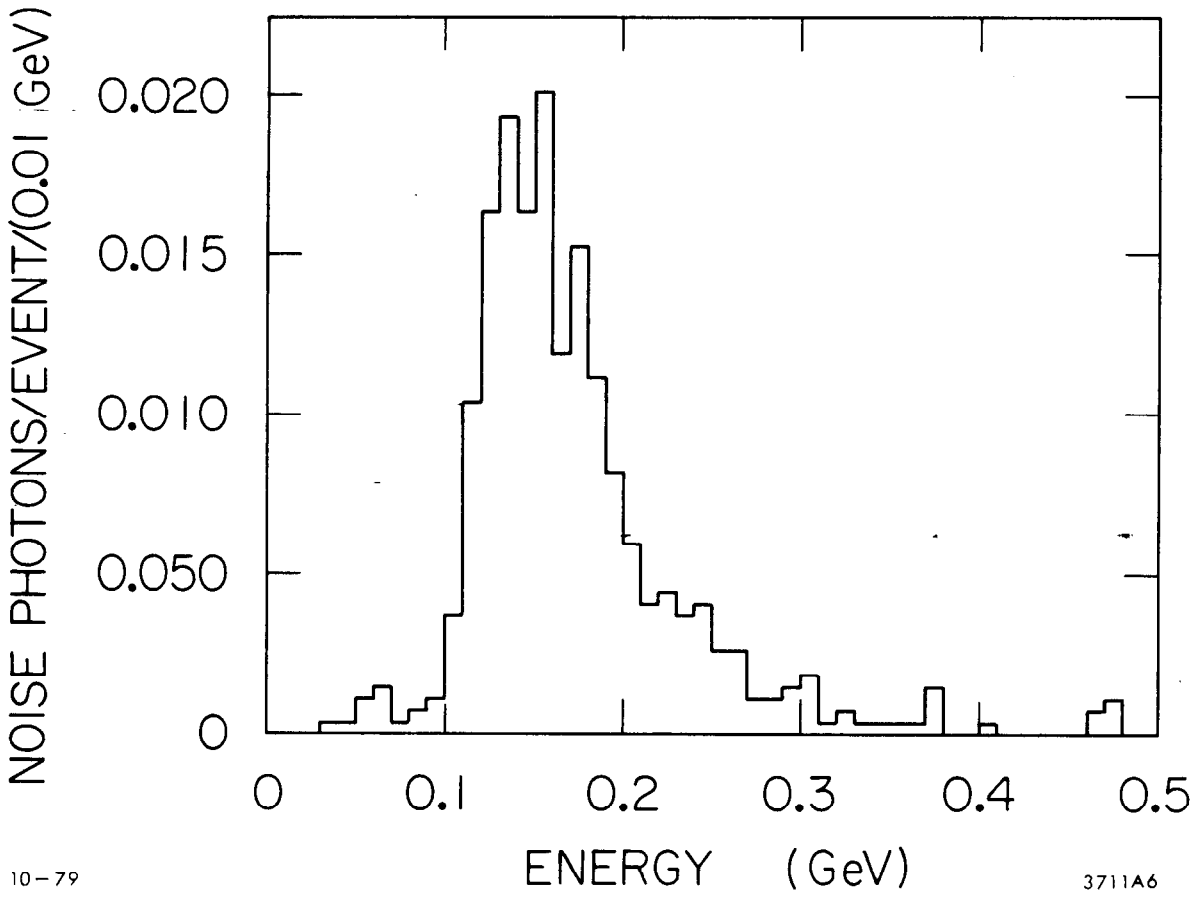

Fig. 5.1: Energy spectrum of fake photons observed in the decay $\psi \to \pi^+\pi^-\psi$, $\psi \to \mu^+\mu^-$.

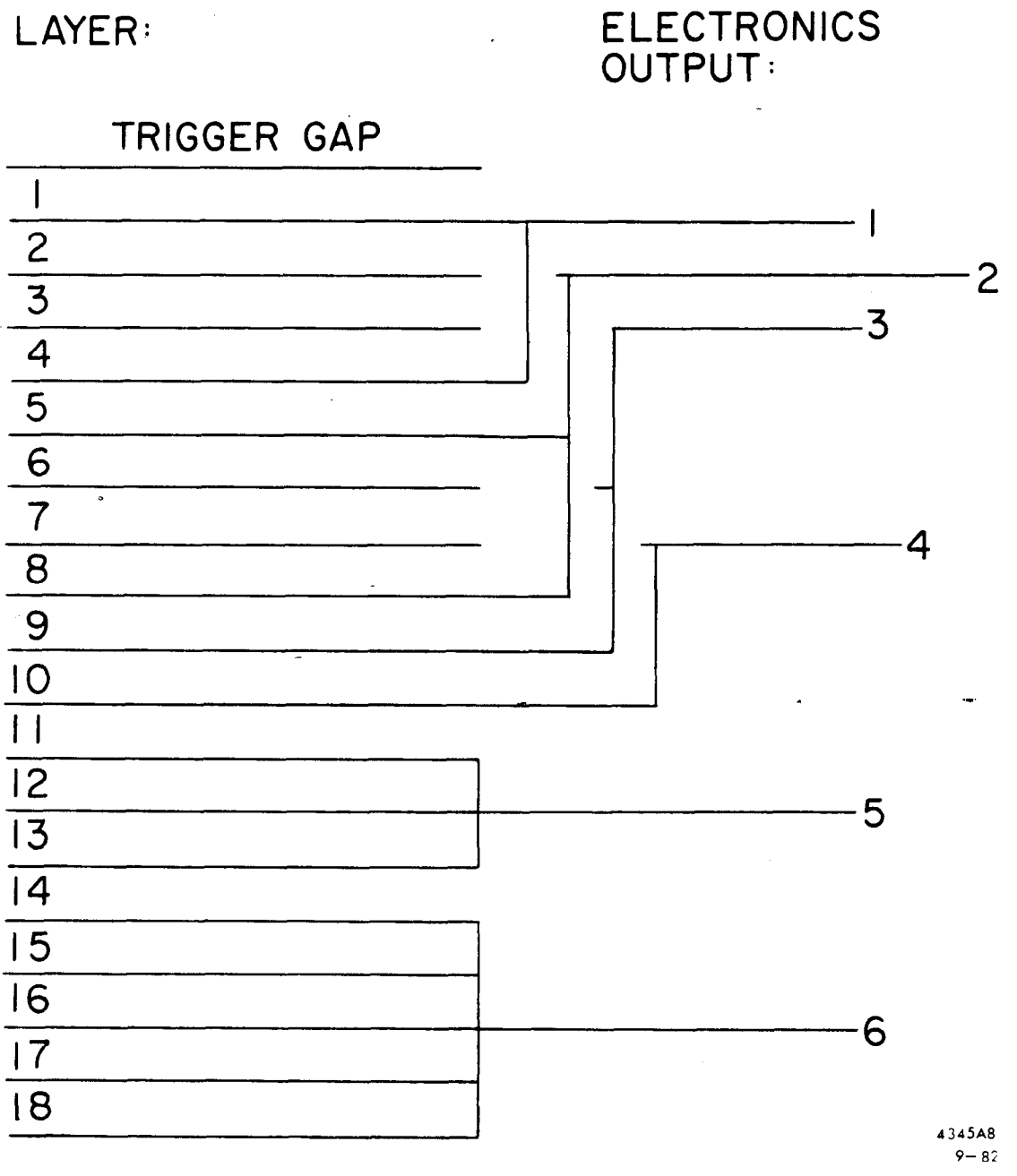

Fig. 5.2: Ganged schematic of the liquid argon shower counter readout.

In all cases a fixed number of charged tracks were required and no more than that number were allowed. A charged track is defined as at least 9 hits in the drift chamber. The track must define a helix and project back to the beam crossing point within 15cm in z which is the direction in which the positron beam travels, and 7 cm in $r=\sqrt{(x^2+y^2)}$. A charged track is only used if the time of flight counter along its radially outward projected path has been hit and a good time of flight measurement made. The drift chamber covers 85% of 4π sterradians. The angle θ is defined as the angle between the z direction, and the direction of the track. The acceptance for charged tracks falls off sharply with θ and a conservative cut of $\cos\theta < .64$ is made on all tracks.

The time of flight scintillation counters are rectangular and therefore have edges. If a charged particle goes through the edge of a counter, the pulse height measured may be too small to be regarded as a signal. The edges are inefficient, therefore tracks which are projected within 2mm of one of the four edges of a TOF counter are excluded.

In all analyses a cut was made on the square of the missing mass in the event recoiling from the charged tracks, where the masses of the charged tracks were assumed. This cut was made to exclude events in which the missing mass was greater than the pion mass. Events were rejected which had missing momentum < 160 MeV/c in order to exclude events with either a missing photon or no particles missing. In many of the analyses a cut was made on the variable $U = |E_m - P_m|$, where E_m is the missing energy from the charged tracks, and P_m is the missing momentum. This cut is a finer cut on the mass of the missing particle than

the missing mass cut. Note that $M_m^2 = (E_m+P_m)\times U$. Since U is linear in E_m the error in U does not depend to first order on the magnitude of the missing energy. This cuts' purpose is to assure that no more than one π^0 is missing.

In all analyses, a kinematic fit was made by the program SQUAW to the events. Squaw is a kinematic fitting program originally written for the analysis of bubble chamber data. It has been converted for use in the analysis of electron-positron annihilation data. It uses Mark II track information and readjusts the track momentum and energy, within measured errors and resolutions, in such a way as to conserve energy and momentum and minimize the χ^2 of the fit. Given a hypothesis such as $\psi \rightarrow \pi\pi\gamma\gamma$, it will make its best fit to the hypothesis and output fitted momenta, masses, and measures of goodness of fit. In these analyses a four constraint fit was made since all final state particles were detected. It is possible to further constrain the events by requiring that two of the outgoing particles have a particular invariant mass. For instance, that two photons have the mass of a π^0. No fits were made in these analyses with 5 constraints because the invariant mass spectrum of the two gammas was of interest in estimating the background to the hypothesised decay.

Squaw makes its own set of internal cuts on each track in the event, and on the events themselves. They are programmable, and those used in the analysis which are additional cuts on data follow.

1. The time of flight measurement must be consistent with the mass hypothesised and the measured momentum to within 600 psec, or 660 psec if the TOF counter associated with the track was doubly hit. The 600 picosecond cut is a 2σ cut on the TOF residual defined as,

$$T_r = t_m - t_e$$

where the expected time t_e = pathlength of particle/measured velocity.

2. Photons found within 36 cm of a charged track are not regarded as real photons in a fit. (This cut is not performed in all analyses and will be mentioned when it is.) It is used to exclude photons associated with charged hadron tracks from being considered real photons.

3. No more than four photons are allowed per liquid argon module.

4. Corrections are made for energy loss of the charged particles in the material the particle traverses before going through the drift chamber. The momenta of the particles are corrected accordingly. The corrections are:

$$\text{For } \beta = v/c > .93 \quad , \quad dE/dx = .0041/\sin\theta$$

where $\sin\theta = p_{xy}/p$.

$$\text{For } \beta < .93 \quad , \quad dE/dx = .825 \times (.0041/\sin\theta)/\beta^{2.65} \quad .$$

5. The liquid argon resolution used is $\delta E/E = 14\%/\sqrt{E}$ and the angular error used is ±8 milliradians.

In analyses, where mentioned, a cut has been made to exclude muons. This is done using the muon detection system. If a particle has a momentum which projects through the muon detector and passes through as many layers as is consistent with it being a muon of momentum p then it is called a muon, and the event is rejected.

Electron/Pion Separation

All of the liquid argon information, shower shape, total energy deposited, energy in each layer, etc, are used to discriminate electrons from pions and kaons. The method is based on a statistical idea of recursive partitioning.[1] We want to distinguish between two classes of events. An n-dimensional space is formed by the variables describing each event. We take a pure sample of electrons and a pure sample of pions and see where they fall in this n-dimensional space.

The space is then partitioned by a coordinate hyperplane in n dimensions which maximizes the separation between the two classes. This partitioning is repeated until either the space is completely separated into the two classes or there are only ten events left in each partitioned volume. Eventually, for every small volume of this partitioned space there is an associated probability of an event from the data in question falling into it being an electron or a pion. The real data sample is now mapped onto this n-dimensional space and each event is classified as electron or pion. Misidentification probabilities are at the level of 3% that an electron is called a pion and 5% that a pion is called an electron.

All of the above cuts are made in each of the five final state analyses. The cuts change in magnitude for the different decays and some further cuts are made in particular cases. These will be discussed separately in each case.

---

[1] J. Friedman, IEEE Transactions on Computers C26, 404 (April 1977) and SLAC-PUB-1573.

Chapter VI

MEASUREMENT ERRORS

There are both systematic and statistical errors in the measurement of the branching ratio, which is calculated as:

$$B(\psi \rightarrow X) = \frac{\#\text{ events observed} - \#\text{ events background}}{(\#\text{ produced } \psi\text{'s}) \cdot (\text{detection efficiency})}$$

The systematic error in the number of produced events was discussed earlier. The error on the number of produced ψ's is 5% and the error in the number of produced ψ''s is 17%. The detection efficiency or acceptance for each decay was calculated by generating a large number of Monte Carlo events and performing the data analysis on them. The statistical error in this number is in all cases less than 60% the error in the number of observed events. The systematic error in determining the acceptance comes from the failure of the Monte Carlo to perfectly simulate the Mark II detector. We discuss only those Monte Carlo distributions which we make restrictions on.

1) We ask that the event trigger the detector. The trigger efficiency for the detector and the Monte Carlo were measured to be within 1.5% of each other.

2) We make a loose vertex cut on charged tracks. The difference in the number of events cut out in the data and the Monte Carlo is $<$ 2%.

3) We make a 2σ consistency cut on the time of flight residual of each track. The Monte Carlo underestimates the tails of this distribution. We estimate a 4% systematic error due to this effect.

4) We did not include pion punch through in the Monte Carlo. This leads to a 5% systematic in rejecting μ's.

5) The Monte Carlo does not perfectly model multiple scattering and nuclear interactions in the material before the particles reach the drift chamber. The Monte Carlo underestimates this effect. Therefore the χ^2 distributions of fits to charged tracks from the data and the Monte Carlo will differ. This means that the cut on χ^2 or tail-end probability of fits will introduce a systematic error. This error increases with the number of charged particles in the event give a fixed χ^2 cut. We loosen the χ^2 cut as the multiplicity increases so that we estimate a constant systematic error of 5% due to this cut. The statistical errors on the acceptance are added separately in each decay.

The number of background events for each decay mode is estimated by hand and is assumed to be a flat function. In all cases we subtract $<$ 5% of the signal. We estimate a 50% background estimation error throughout. These systematics are calculated individually for each decay mode and added to the total error in quadrature.

The statistical error in the number of events seen varies greatly with the decay mode and in some cases (7π and $p\bar{p}\pi^0$) dominate the total error. There is a systematic error in the number of events observed due to the misidentification of electrons as pions or kaons by the liquid argon system. This is only true in those analyses which reject electrons specifically. This is calculated to be a 1% systematic error.

Adding all the common errors in quadrature gives a 10% error for ψ decays and a 19% error for ψ' decays. To check whether this estimate makes sense we took one decay mode, $\psi \to 2\pi^+2\pi^-\pi^0$ and measured it four different ways, as follows:

1. We required no photons and made a 1-constraint fit to the hypothesis $\psi \to 2\pi^+2\pi^-$ (missing π^0).
2. We required no photons and did not make a fit.
3. We required two photons and made a 4-constraint fit to the hypothesis $\psi \to 2\pi^+2\pi^-\gamma\gamma$.
4. We required two photons and did not make a fit.

In the cases where a fit was made TOF cuts and vertex cuts were made. In the other cases they were not. We find agreement of these four results for branching ratios to within 14%. If we add statistical and background subtraction errors to our $\psi \to 2\pi^+2\pi^-\pi^0$ estimate we get a 13% error. This estimates the systematic error and is in reasonable aggreement with our previous estimation.

Chapter VII

DATA ANALYSIS

7.1 $\psi \to \pi^+\pi^-\pi^0$

We find from experiment that this decay proceeds predominantly through the intermediate state $\rho\pi$,

$$\psi \to \rho\pi \quad , \quad \rho \to \pi\pi$$

The ρ can be neutral, (ρ^0), or charged, (ρ^+ or ρ^-). The charged and neutral modes were measured separately. The efficiency for detecting π^0's is strongly energy dependent due the steeply rising photon detection efficiency. Figure 7.1 shows a plot of detection efficiency for π^0's and photons versus energy. The efficiency for detecting π^0's from the decay $\psi \to \rho^0\pi^0$ is greater than that for detecting them from the decay $\psi \to \rho^+\pi^-$ because the π^0 in the former decay has a greater momentum on average than in the latter. Figure 7.2 shows diagramatically both interactions in the laboratory reference frame.

In selecting events for both decays, two oppositely charged tracks were required in the central drift chamber, and at least two photons which were not identified as fakes were required in the liquid argon system. We required that pions have time of flight measurements consistent within 2σ with the pion mass hypothesis. Neither of the two charged tracks were allowed to be identified as electrons by the liquid

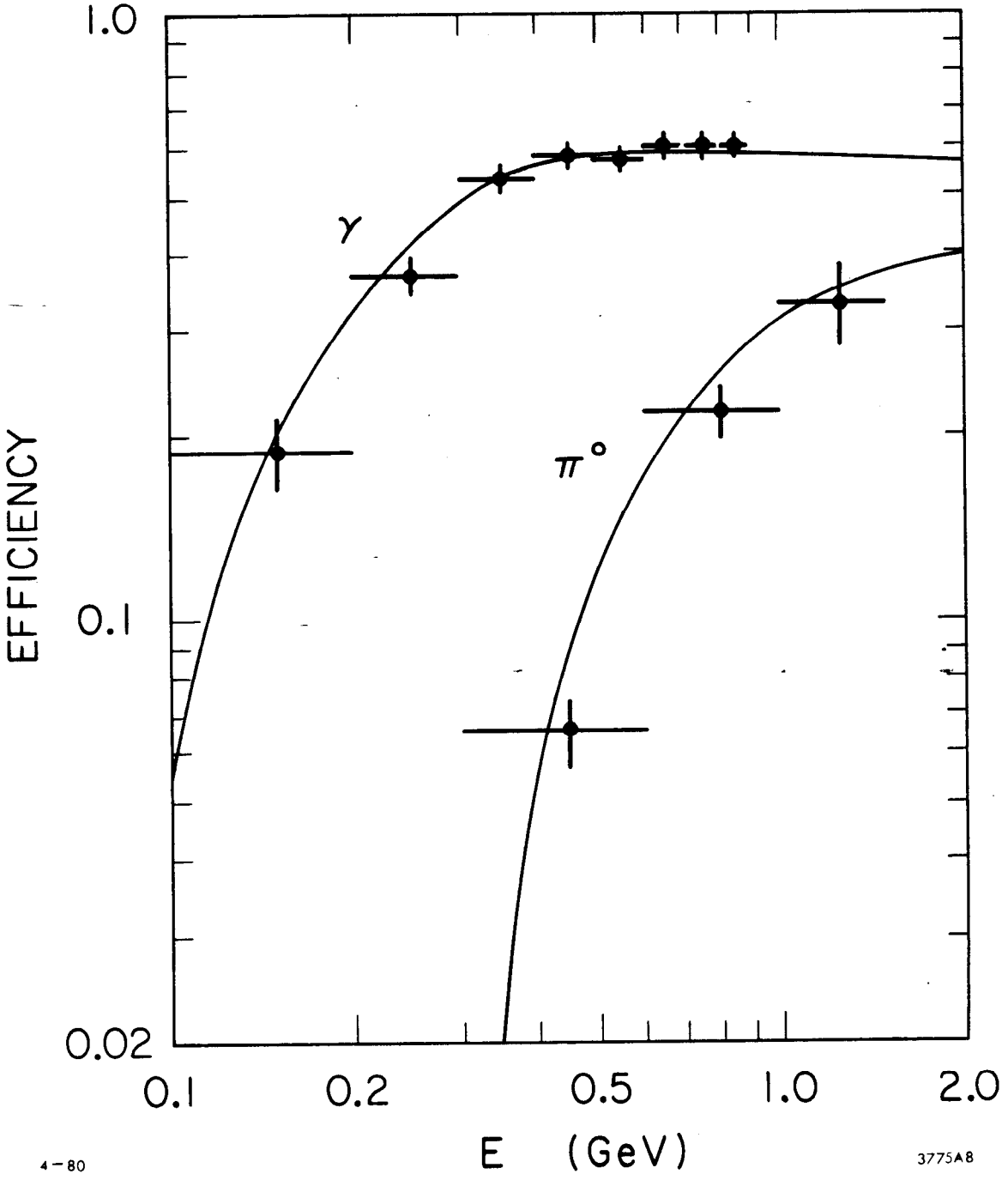

Fig. 7.1: Detection efficiency for photons and π^0's versus energy.

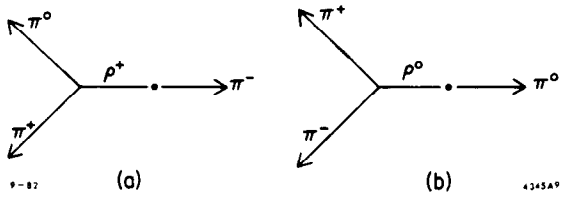

Fig. 7.2

argon system, nor were either allowed to be called μ's by the muon system. This means that events in which either pion decayed inside the detector, via $\pi \rightarrow \mu\nu$, or in which either pion punchs through the muon steel without interacting, were rejected. The Monte Carlo program models the muon detection system faithfully, knows the lifetime of the pion and the probability of pion "punch-through" and therefore calculates correctly the loss of events in the sample due to this cut on muons. The proximity of the photon to a charged track is also a variable of restriction. The photons used to reconstruct the π^0 were required to be at least 36 cm from any charged track. This distance was measured at the inner face of the liquid argon shower counters.

The data was kinematically fit with four constraints using SQUAW to the hypothesis $\psi \rightarrow \pi^+\pi^-\gamma\gamma$. The tail-end probability P or confidence level of the fit defined as

$$P \equiv \int_{\chi^2}^{\infty} \frac{1}{2^h\,\Gamma(h)} (\chi^2)^{h-1} \exp(-\chi^2/2)\, d\chi^2$$

where χ^2 is the goodness of the 4 constraint fit and h equals one half times the number of degrees of freedom in the fit. Figure 7.3 is a plot of this tail-end probability distribution. Ideally the signal events will populate the plot as a uniform distribution on the interval 0 to 1. The background events will populate the lowest region in P. A cut is made which maximises both the rejection of background events and the acceptance of signal events. In this case the requirement is that $P > .05$.

The total branching ratio to 3π was measured by simply requiring a π^0 in the event. Figure 7.4 shows the invariant mass spectrum of the two photons from the ψ and the ψ'(shaded). A clear π^0 signal (166 events) can be seen with no background in the ψ decay. Four events consistent with including π^0's are seen from the ψ' decay. The detection efficiencies were generated by a Monte Carlo thrown as $\psi \rightarrow \rho\pi$, with the correct two body, spin one angular distributions[1]. The ψ efficiency is ϵ=2.68% and the ψ' efficiency is ϵ'= 4.60%. The branching ratio is:

$$B(\psi \rightarrow \pi^+\pi^-\pi^0) = (1.45\pm.19) \times 10^{-2}.$$

A measurement is made for the branching ratio from the ψ':

$$B(\psi' \rightarrow \pi^+\pi^-\pi^0) = (.85\pm.46) \times 10^{-4}$$

The ratio of branching ratios is:

$$B(\psi')/B(\psi) = (.58 \pm .40)\%$$

---

[1] The ψ was decayed with the distribution, $f(\theta) = 1 + \cos^2\theta$, where θ is the polar angle with respect to the beamline, and the ρ was decayed to two π's with the distribution $f(\theta) = \sin^2\theta'$, where θ' is the polar angle with respect to the direction of the ρ.

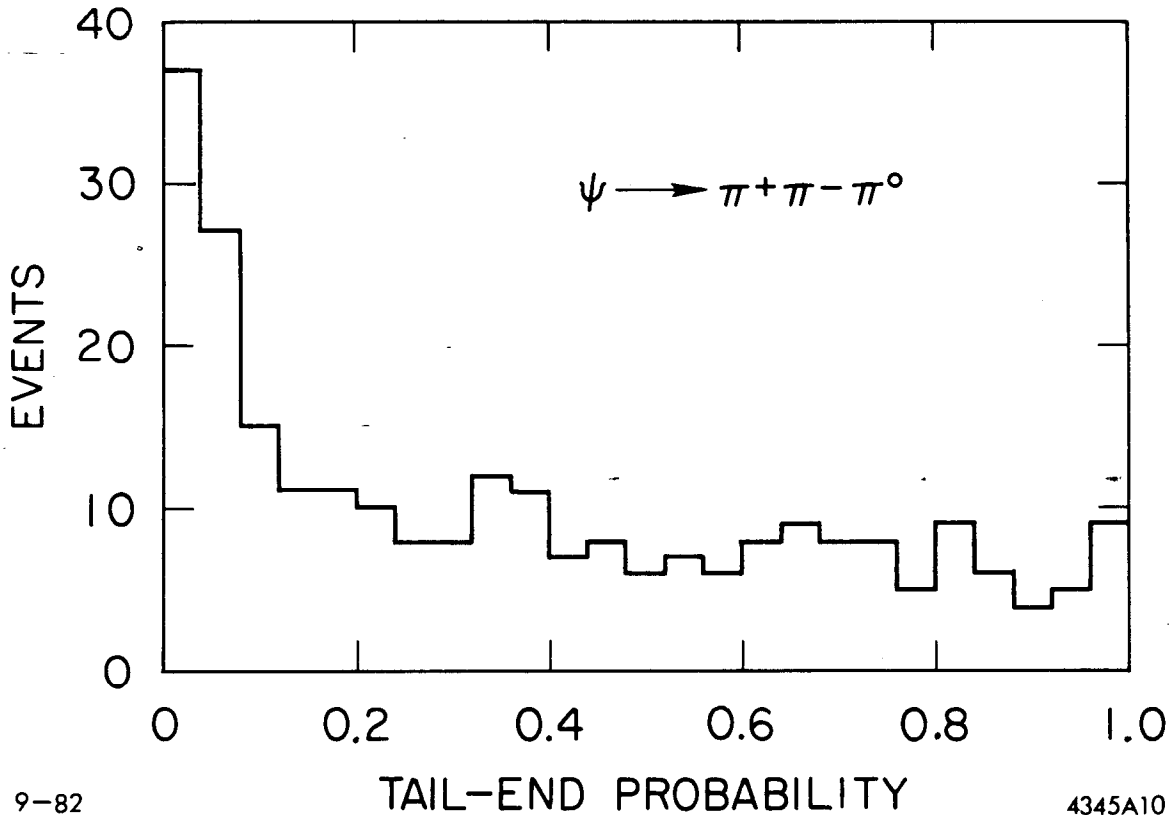

Fig. 7.3: Tail-end probability for events, fit with four constraints to the hypothesis, $\psi \to \pi^+\pi^-\gamma\gamma$.

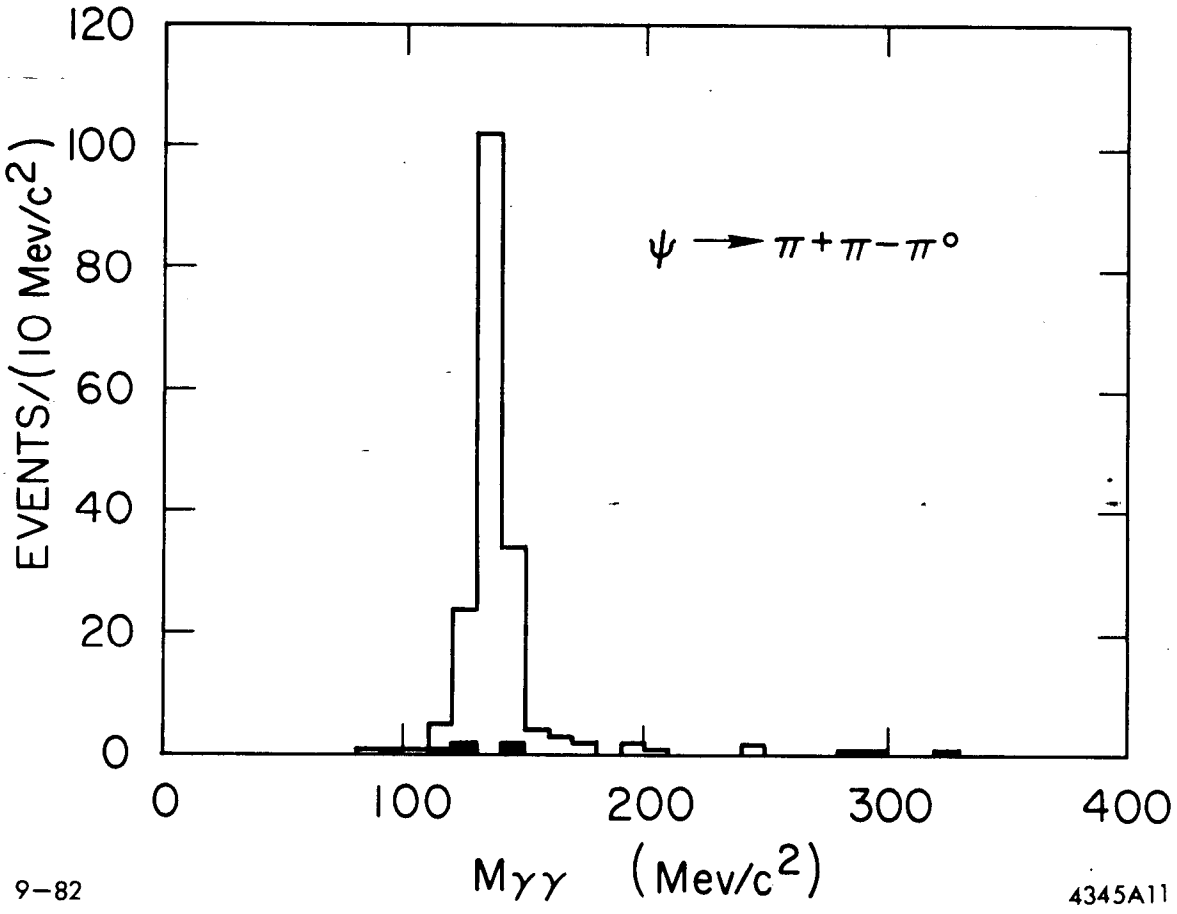

Fig. 7.4: $\gamma\gamma$ invariant mass for events $\psi \to \pi^+\pi^-\gamma\gamma$ (and ψ' data in shaded region).

The Dalitz plot describing the invariant mass squared of the $\pi^0\pi^+$ system versus the invariant mass squared of the $\pi^+\pi^-$ system, Fig. 7.5, shows no events with both a neutral and a charged ρ. There is a band of ρ^0's, a band of ρ^+'s and a cluster of events with ρ^-'s in them. The Dalitz distribution is consistent with all events occuring through the $\rho\pi$ intermediate state. Figure 7.6 is the invariant mass distribution of the $\pi^+\pi^-$ pair. A ρ^0 signal is evident as well as the reflection from the events with charged ρ's in them at around 2 GeV/c^2.

The Neutral Mode

The neutral mode was measured by requiring that there be a neutral ρ in the event. That is, events in which,

$$530 < M(\pi^+\pi^-) < 1010 \text{ MeV}/c^2$$

were selected. This corresponds to a 3σ cut on the mass of the ρ. The invariant mass of the photons was required to be within the mass bounds set by the Monte Carlo

$$115 < M(\gamma\gamma) < 165 \text{ MeV}/c^2.$$

65 events of the produced 427,378 events taken at the $\psi(3095)$ survive all the above cuts with no background. Approximately 20,000 Monte Carlo event were generated, as

$$\psi \rightarrow \rho^0\pi^0$$

These were thrown with two body Lorentz invariant phase space modified to give the correct spin one angular distribution for the decay products of the ρ. The detection efficiency for the neutral decay from the ψ is $\epsilon = 3.71\%$.

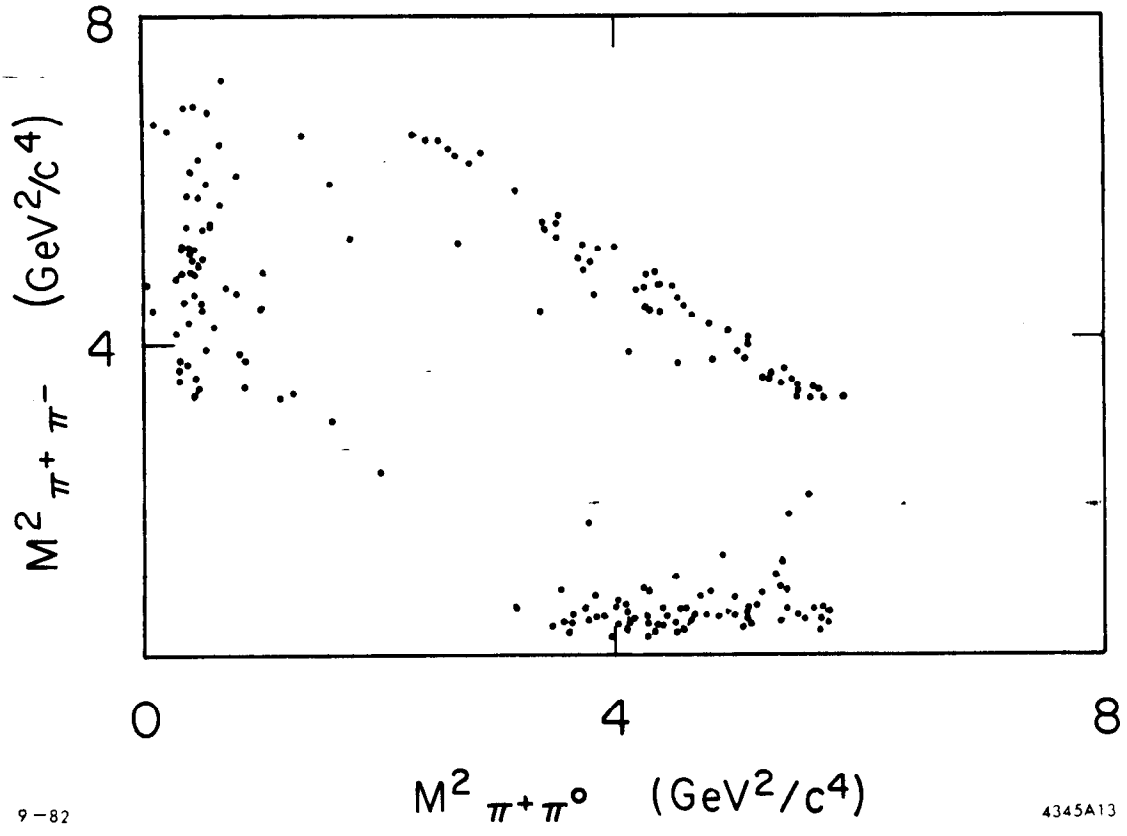

Fig. 7.5: Dalitz plot of the $M^2(\pi^+\pi^0)$ vs. $M^2(\pi^+\pi^-)$. Evidence for $\rho^\pm$ and ρ^0.

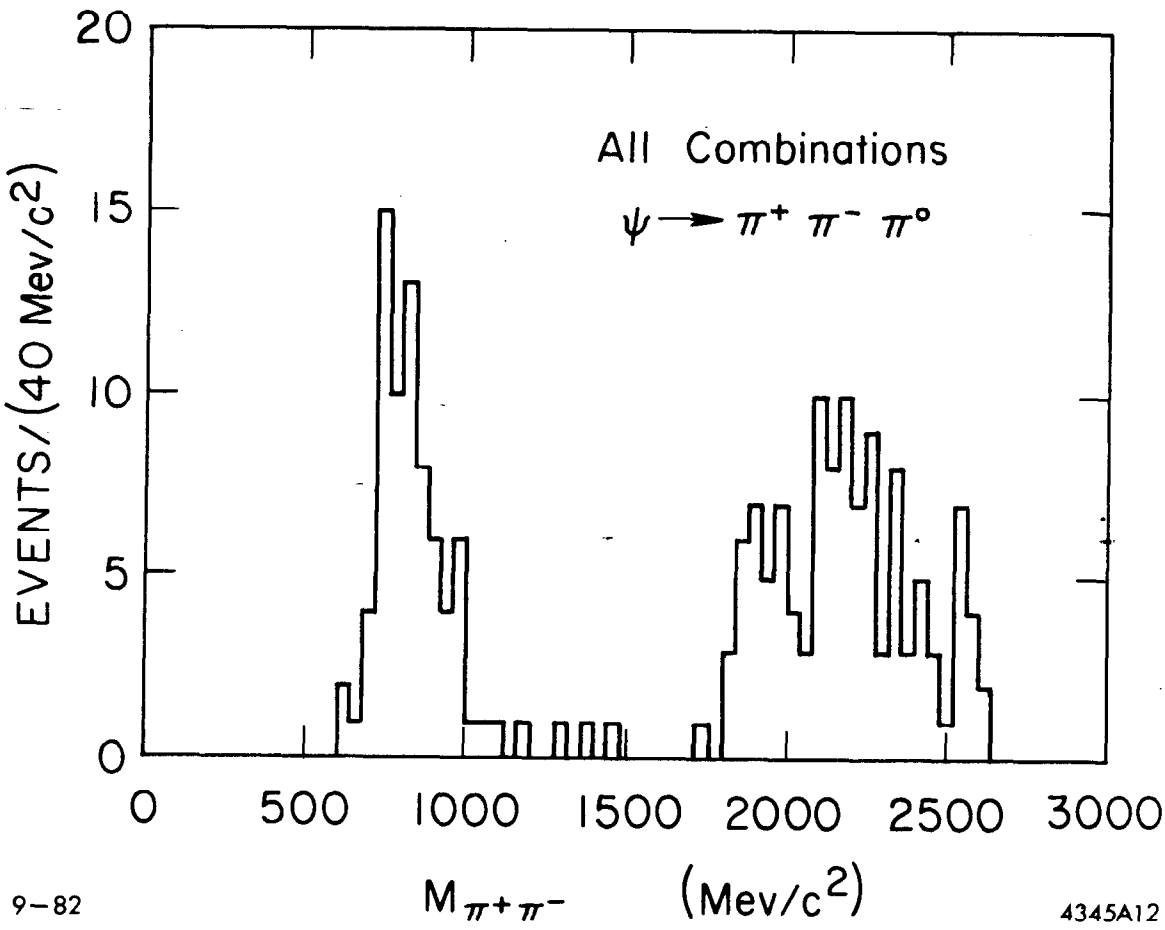

Fig. 7.6: Invariant mass of the $\pi^+\pi^-$ system in events of the type $\psi \to \pi^+\pi^-\pi^0$.

The branching ratio is:

$$B(\psi \to \rho^0\pi^0) = (4.10 \pm .66) \times 10^{-3}$$

Figure 7.7 is a plot of the invariant mass of the two photons.

The same analysis was performed on the data taken at the $\psi'(3684)$, where the beam energy for calculating the various kinematic variables is taken to be 1.842 GeV. There were no events surviving this analysis. About 8,000 Monte Carlo events of the type $\psi' \to \rho^0\pi^0$ were generated giving an efficiency of $\epsilon' = 6.35\%$. Because no events were seen, an upper limit has been set on the branching ratio. Assuming Poisson statistics at the 90% confidence level 2.3 events could fluctuate down to 0 events. Therefore an upper limit is made on the branching ratio assuming 2.3 events.

$$B(\psi' \to \rho^0\pi^0) < 3.55 \times 10^{-5} \qquad 90\% \text{ C.L.}$$

The ratio of the branching ratios at the ψ and ψ' is

$$B(\psi')/B(\psi) < .87\% \qquad 90\% \text{ C.L.}$$

where 13% was expected from the the non-relativistic perturbative QCD calculation.

The Charged Mode

$$\psi \to \rho^{\pm}\pi^{\mp}$$

The charged mode, $\psi \to \rho^{\pm}\pi^{\mp}$, was measured by requiring that there was a charged ρ in the event. We achieved this by selecting events in which

$$530 < M(\pi^+\pi^0) \text{ or } M(\pi^-\pi^0) < 1010 \text{ MeV}/c^2$$

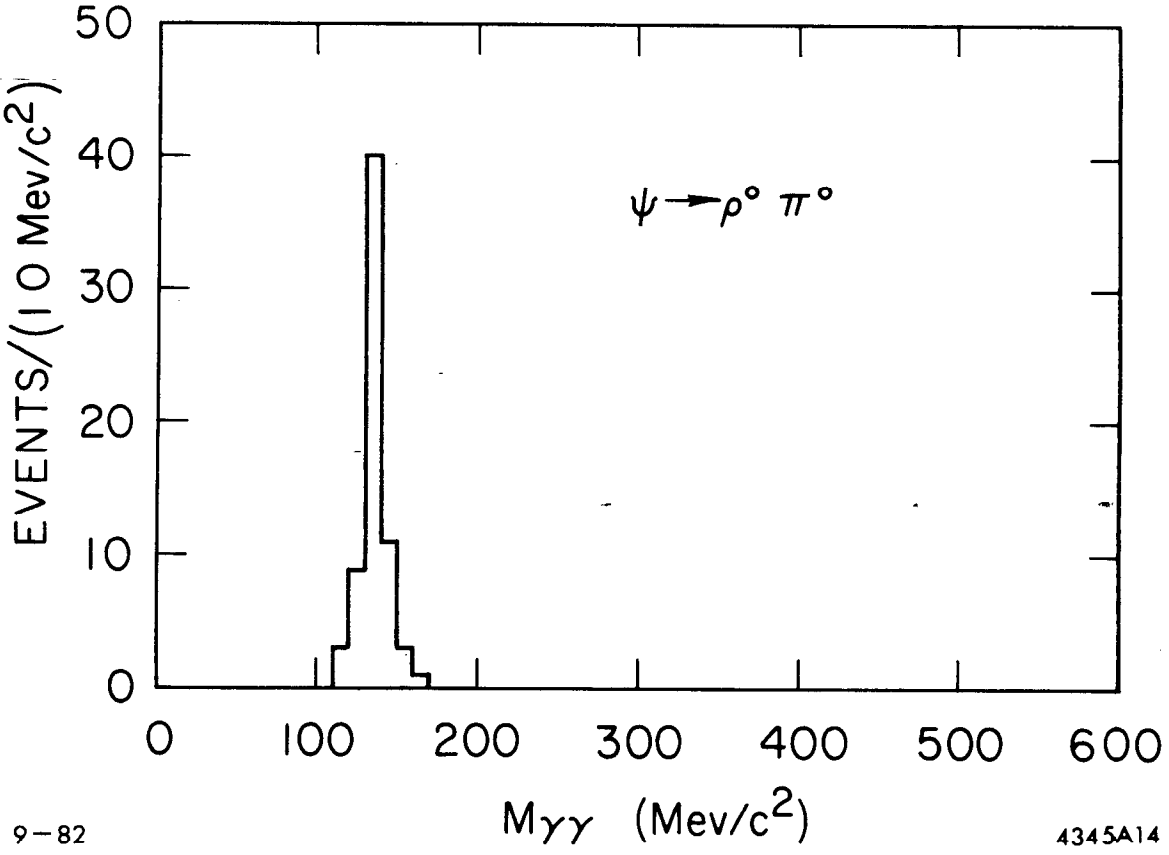

Fig. 7.7: $\gamma\gamma$ invariant mass for $\psi \to \pi^+\pi^-\gamma\gamma$ events in which a ρ^0 is required. No such events are seen from the ψ'.

Again, the invariant mass of the two photons is restricted to the π^0 mass defined as;

$$115 < M(\gamma\gamma) < 165 \text{ MeV}/c^2$$

There are 88 events which survive the cuts in the ψ data. The background is estimated to be flat at the level of .66 events per 10 MeV bin. We therefore subtract 3.3 events from the signal region. Figure 7.8 shows the invariant masses of the $\gamma\gamma$ pair. A charged ρ signal is evident in the Dalitz plot, Fig. 7.5. 16,000 Monte Carlo events of the form $\psi \to \rho^{\pm}\pi^{\mp}$ were generated with a spin one angular distribution for the ρ. The detection efficiency was found to be $\epsilon = 2.16\%$. The branching ratio measured is:

$$B(\psi \to \rho^{\pm}\pi^{\mp}) = (9.18 \pm 1.56) \times 10^{-3}$$

The same analysis was performed on the ψ' data resulting in one candidate event. Figure 7.8 includes the $\gamma\gamma$ mass spectrum from the ψ'. The efficiency for detecting events of this type at the ψ' was calculated by the Monte Carlo,

$$\epsilon' = 3.72\%$$

An upper limit was set on the branching ratio from the ψ' assuming 3.9 events could fluctuate down to 1 event at the 90% confidence level.

$$B(\psi' \to \rho^{\pm}\pi^{\mp}) < 1.0 \times 10^{-4} \text{ at the 90\% C.L.}$$

The ratio of the branching ratios is;

$$B(\psi')/B(\psi) < 1.05\% \text{ where } 13\% \text{ is expected.}$$

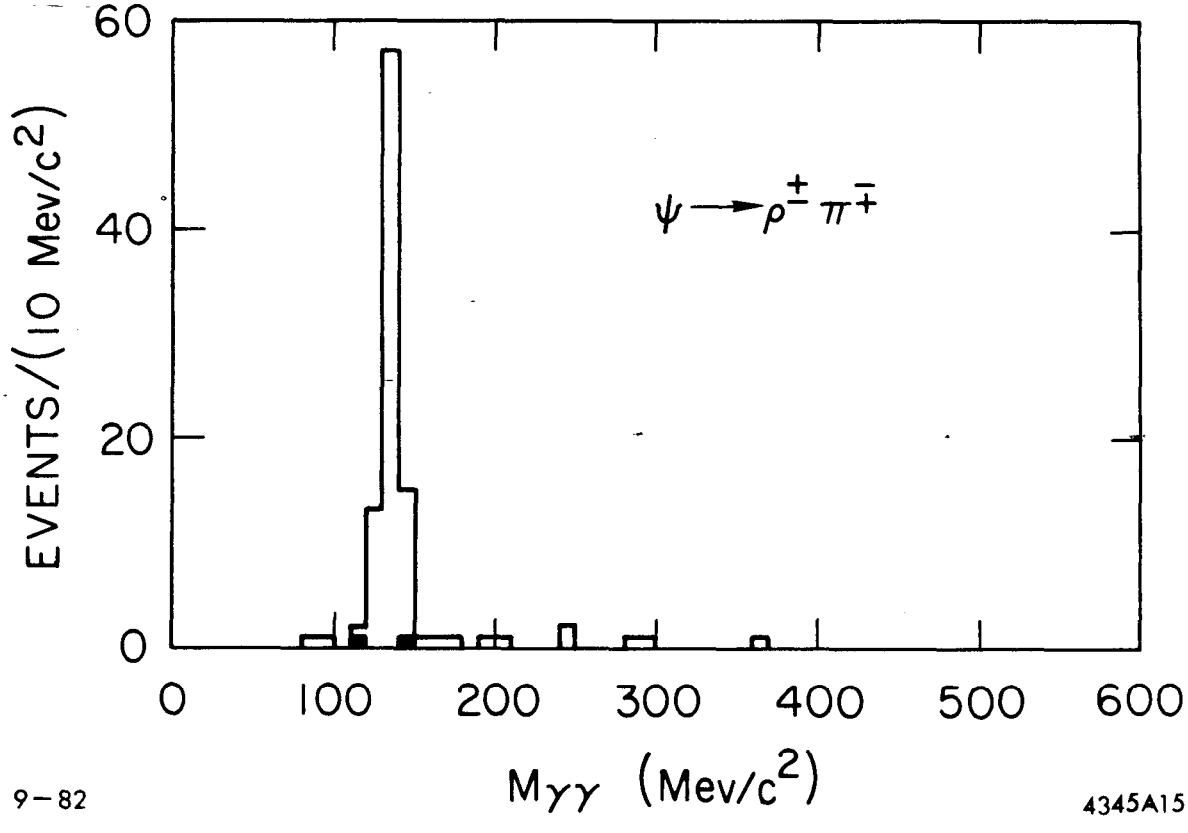

Fig. 7.8: $\gamma\gamma$ invariant mass for events of the type $\psi \to \pi^+\pi^-\gamma\gamma$ (ψ' data is shaded) in which a charged ρ is required.

We have also incidentally measured the combined branching ratios,

$$B(\psi \to \rho\pi) = (1.33 \pm .32) \times 10^{-2}$$

and

$$B(\psi' \to \rho\pi) < .0083 \times 10^{-2}$$

giving a total ratio,

$$B(\psi')/B(\psi) < .62\%$$

In conclusion, we find no evidence for a signal in either the neutral or charged decay modes of the $\psi'(3684)$ to $\rho\pi$. This result is inconsistent with the predictions of the naive non-relativistic quark model discussed in chapter II.

7.2 $\psi \to K^+K^-\pi^0$

The analysis of this decay is similar in many respects to that of the decay $\psi \to \pi^+\pi^-\pi^0$, because they both occur predominantly through a resonant intermediate state. In this case the decay occurs through the K*(892).

$$\psi \to K^*K \quad , \quad K^* \to K\pi^0$$

The TOF cuts are made so that the charged tracks are consistent with the kaon hypothesis; the restriction on U changes so that E_m is calculated with kaon masses. Again if either particle is identified as a muon or an electron the event is rejected. Approximately 30% of the charged kaons produced decay, via $K \to \mu\nu$, inside the detector. These tracks are then identified by the muon system as μ's. This means that $\simeq$ 9% of the

events will be lost due to the cut on the number of muons in the event. The data was fit with four constraints to the event hypothesis;

$$\psi \rightarrow K^+K^-\gamma\gamma$$

and events in which tail end probability P > .05 were rejected.

A large K* signal can be seen in the invariant mass spectrum of the $K^{\pm}\pi^0$ systems in Fig. 7.9. There is no apparent resonant structure in the invariant mass spectrum of the charged kaon pair. A plot of cosθ where θ is the angle between the two charged particles, Fig. 7.10, shows the distribution steeply peaked at high cosθ. The kaons tend to be strongly collinear as the charged pions are in the decay $\psi \rightarrow \rho^{\pm}\pi^{\mp}$. This fact corroborrates the claim that the decay occurs via a K*, since for such a two body decay, we would expect the charged tracks to be highly collinear. The solid line in Fig. 7.10 shows the Monte Carlo distribution where the Monte Carlo has been generated as

$$\psi \rightarrow K^{*\pm}K^{\mp}$$

The $\gamma\gamma$ mass spectrum, Fig. 7.11, shows a large π^0 signal consisting of 25 events with no background. The detection efficiency was calculated by a Monte Carlo thrown as

$$\psi \rightarrow K^*(892)K^{\pm}$$

with the correct spin 1 angular distributions. The K* was decayed to $K^0\pi$ 2/3 of the time and $K^{\pm}\pi^0$ 1/3 of the time. The efficiency for detecting events of the type, $\psi \rightarrow K^{*\mp}K^{\pm}$, $K^{*\mp} \rightarrow \pi^0K^{\mp}$ was calculated to be;

$$\epsilon = 6.39\% \quad .$$

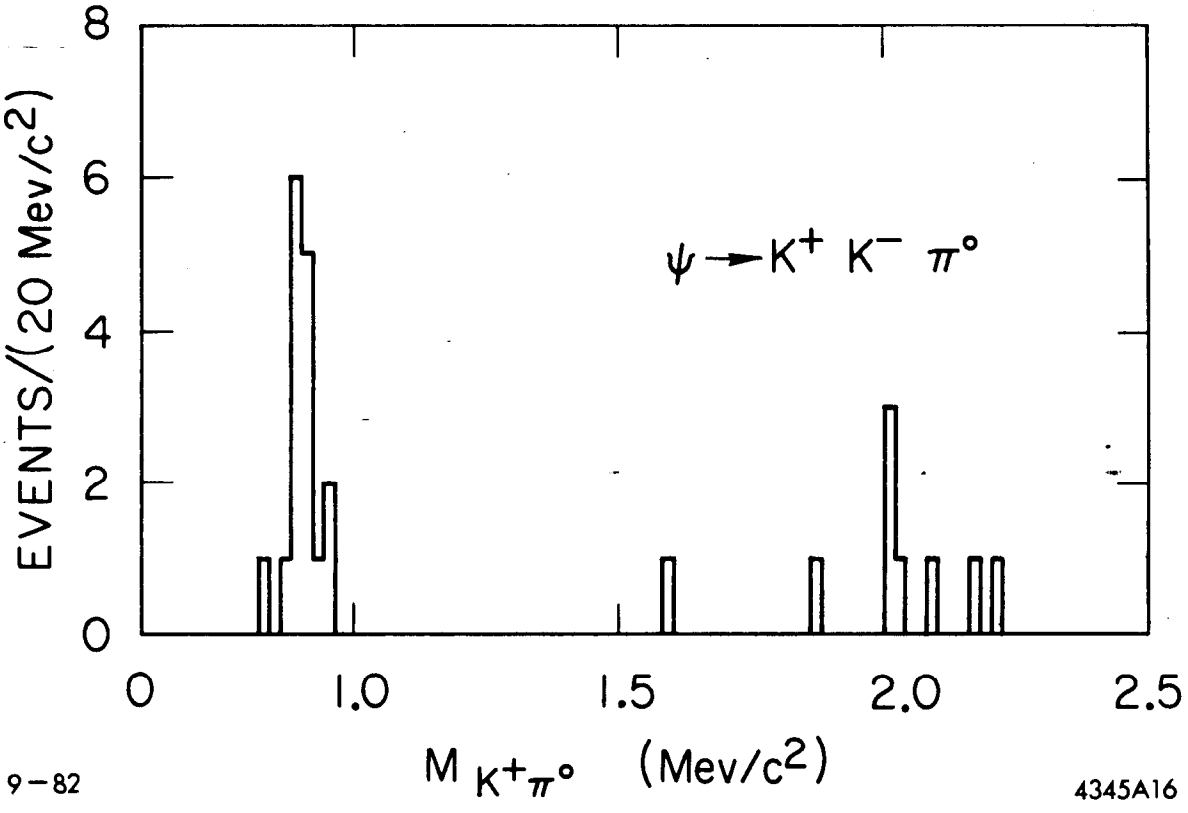

Fig. 7.9: Invariant mass of the $K^+\pi^0$ system in the decay $\psi \to K^+K^-\gamma\gamma$. A K*(892) signal is evident.

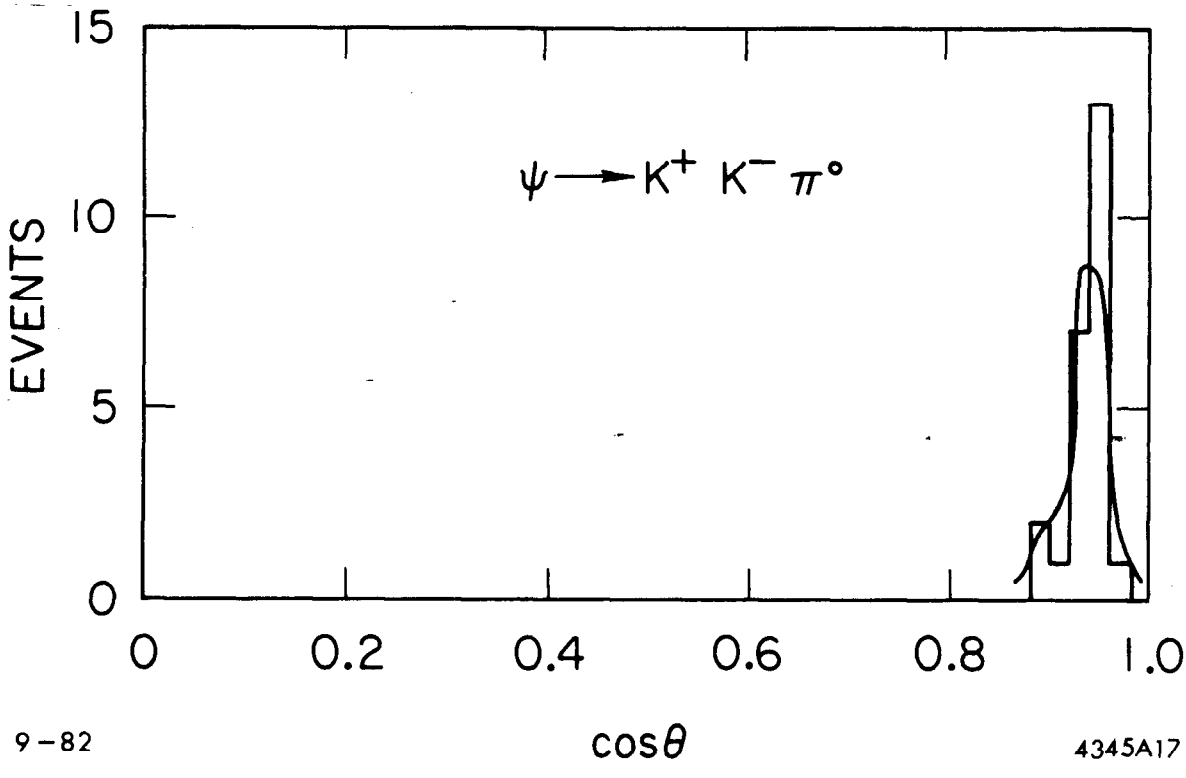

Fig. 7.10: Acollinearity distribution for the charged K's from $\psi \rightarrow K^+K^-\gamma\gamma$ decays. The solid line is from a resonant $\psi \rightarrow K^*(892)K$ Monte Carlo.

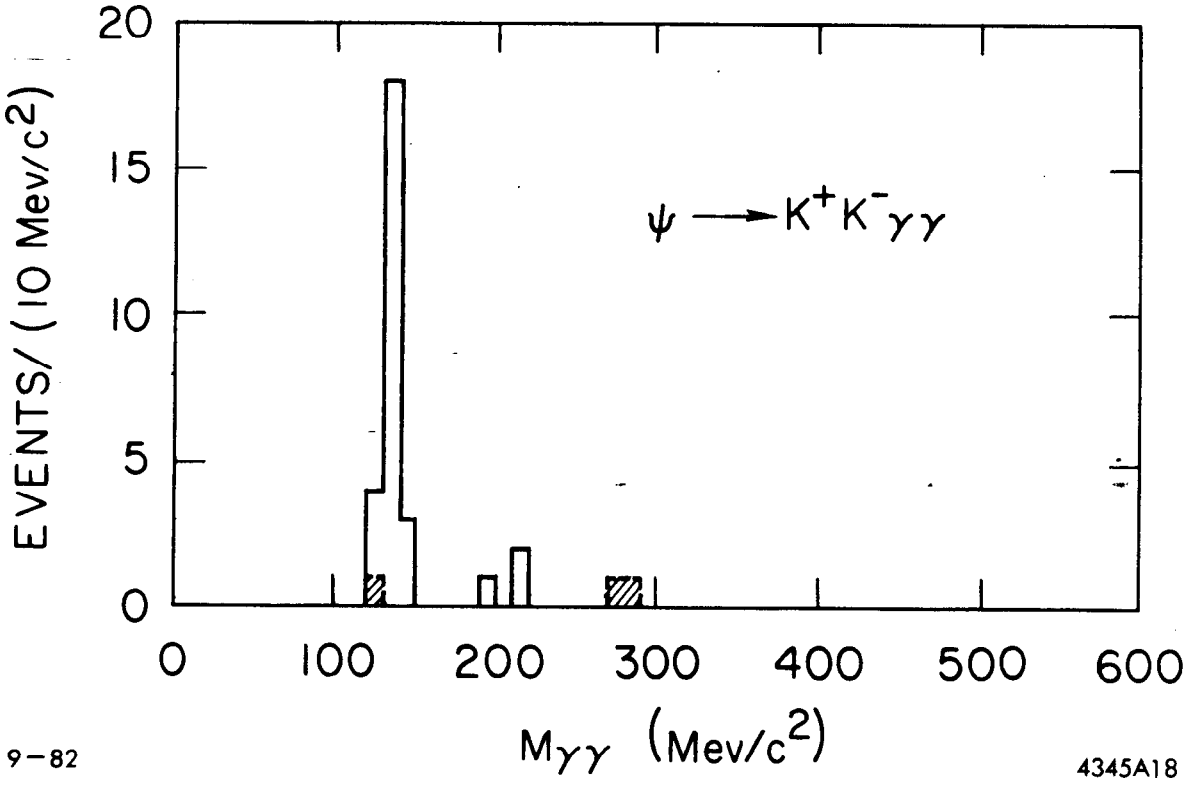

Fig. 7.11: $\gamma\gamma$ invariant mass spectra for ψ (and ψ' shaded) $\rightarrow K^+K^-\gamma\gamma$.

The branching ratio from the ψ is then,

$$B(\psi \to K^+K^-\pi^0) = (9.15 \pm 2.01) \times 10^{-4}$$

Then we demand that a K* is in the event, that is, that the invariant mass of the $\pi^0K^\pm$ system be consistent with the K* mass,

$$780 < M(K^\pm\pi^0) < 1000 \text{ MeV}/c^2$$

Figure 7.12 shows the $\gamma\gamma$ invariant mass spectrum in this case. There are 24 π^0's in the signal. The detection efficiency is as above and the branching ratio is:

$$B(\psi \to K^*(892)K) \times B(K^* \to K\pi^0) = (8.8 \pm 1.9) \times 10^{-4}$$

<u>$\psi' \to K^+K^-\pi^0$</u>

The analysis at the ψ' is identical to that performed at the ψ. Before the cut demanding a K*(892) in the event, there is 1 event seen. Figure 7.11 includes the $\gamma\gamma$ invariant mass spectrum from the ψ'. The detection efficiency calculated assuming all decays occur via an intermediate K*(892) is;

$$\epsilon' = 12.6\%$$

We set an upper limit on the branching ratio based on one event.

$$B(\psi' \to K^+K^-\pi^0) < (2.96 \times 10^{-5}) \quad 90\% \text{ C.L.}$$

We again required that a K* be present in the final state, by making the cut,

$$780 < M(\pi^0K^\pm) < 1000$$

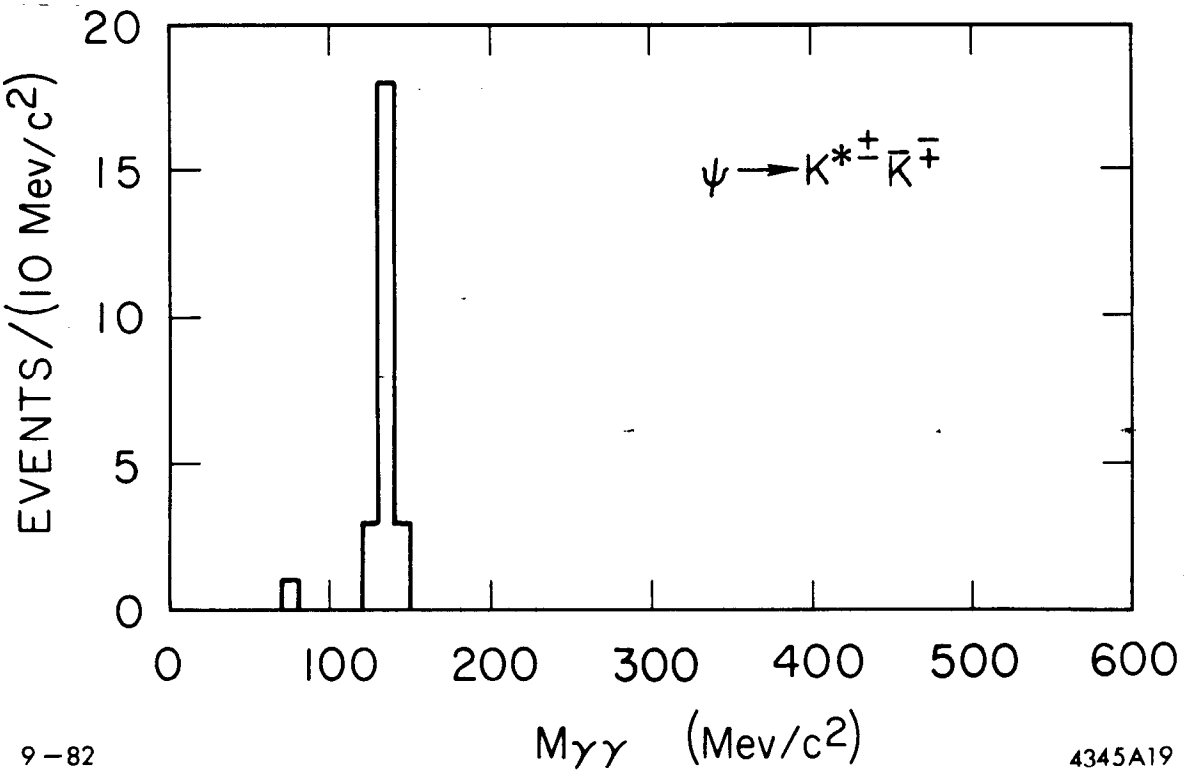

Fig. 7.12: $\gamma\gamma$ invariant mass distribution for decays $\psi \to K^+K^-\gamma\gamma$ in which a K*(892) is required. There are no events observed from the ψ'.

No events involving a π^0 survived this cut. Therefore we place an upper limit at the 90% confidence level, on the branching ratio,

$$B(\psi' \rightarrow K^*K) \times B(K^* \rightarrow K^{\pm}\pi^0) < 1.79 \times 10^{-5} \quad 90\% \text{ C.L.}$$

The ratio of branching ratios from the ψ and ψ' is,

$$B(\psi')/B(\psi) < 2.03 \times 10^{-2} \quad 90\ \% \text{ C.L.}$$

Again, this result is not consistent with the theoretical prediction.

7.3 $\psi \rightarrow p\bar{p}\pi^0$

This analysis, although quite similar to the analysis of the decay $\psi \rightarrow \pi^+\pi^-\pi^0$, is simpler due to a lack of significant backgrounds and the ease with which the TOF system separates protons from kaons, pions and electrons.

Two oppositely charged tracks with TOF measurements consistent within 2σ, with the proton hypothesis, must be detected in the central drift chamber. At least two good photons must be found in the liquid argon shower counters. The kinematic variable $U = |E_m - P_m|$ must be $< .1$ GeV. Finally, the data was kinematically fit, with four constraints to the hypothesis $\psi \rightarrow p\bar{p}\gamma\gamma$. We demanded that

$$\chi^2 < 20 \quad \text{or} \quad \chi^2 \text{ per degree of freedom} < 5 \ .$$

This cut is less stringent than in previous cases due to the lack of background.

The invariant mass spectrum of the two photons is shown in Fig. 7.13. There is a π^0 signal, where a π^0 is defined by

$$115 < M(\gamma\gamma) < 165 \text{ MeV}/c^2,$$

consisting of 16 events with no background on either side. The detection efficiency is $\epsilon = 3.72\%$. The branching ratio:

$$B(\psi \to p\bar{p}\pi^0) = (1.0 \pm .3) \times 10^{-3}$$

<u>$\psi' \to p\bar{p}\pi^0$</u>

The analysis of such events from the $\psi'(3684)$ is completely similar to those from the ψ. The possible additional background, $\psi' \to \pi^0\pi^0\psi$, $\psi \to \bar{p}p$, requires that a π^0 go undetected. The restriction on the variable U prevents the inclusion of events with more than one π^0 missing. Figure 7.13 includes the invariant mass spectrum of the two photons. There are 9 events involving π^0's (as defined above) with no background. The Monte Carlo generated efficiency is

$$\epsilon' = 6.2\%$$

The branching ratio is:

$$B(\psi' \to p\bar{p}\pi^0) = (1.4 \pm .5) \times 10^{-4}$$

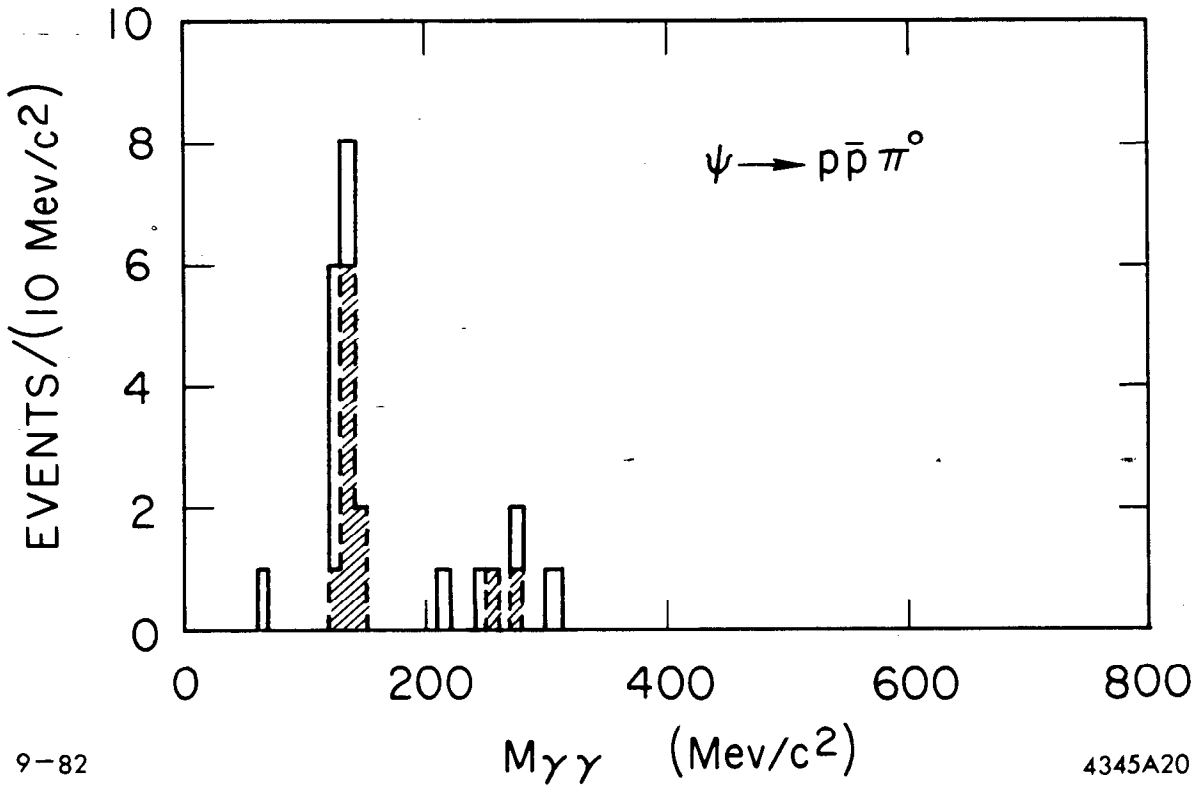

Fig. 7.13: $\gamma\gamma$ invariant mass spectra for decays ψ (and ψ' shaded data) $\rightarrow p\bar{p}\pi^0$.

The ratio of the branching ratios is:

$$B(\psi')/B(\psi) = (14.0 \pm 6.3)\% \quad ,$$

where 13% was expected.

7.4 $\psi \rightarrow 2\pi^+2\pi^-\pi^0$

The 5π decay mode of the ψ occurs through various intermediate resonant states such as $\omega\pi\pi$, ωf, ρA_2 and $\rho\pi\pi\pi$. We include all such final states in the data sample. In selecting events we ask that 4 charged tracks with total charge 0 be detected in the central drift chamber. The tracks were required to be consistent, within 2σ, with the pion mass hypothesis, by time of flight. The missing mass recoiling from the four charged pions was required to be less than 500 MeV/c^2 , a loose cut to make sure the missing mass was not far greater than a π^0 mass.

The kinematic variable U, desribed in the event selection section, was restricted to U < .1 GeV. This was made as a tighter cut on the mass of the neutral particle. It also rules out events of the form, $\psi \rightarrow p\bar{p}\pi^+\pi^-\pi^0$, and $\psi \rightarrow K^+K^-\pi^+\pi^-\pi^0$ which were not rejected by TOF cuts from contaminating the sample.

The data was kinematically fit, with four constraints, to the hypothesis $\psi \rightarrow \pi^+\pi^-\pi^+\pi^-\gamma\gamma$. Events with $\chi^2 > 20$ were rejected. A relatively loose cut is made in this case on the goodness of fit χ^2, because the number of pions in the final state increases the probability that

one particle in the event will interact or scatter and therefore have a large χ^2. The Monte Carlo was generated with a Lorentz invariant phase space distribution, although there are resonances in the final state. These resonances do not change appreciably the efficiency calculated by this Monte Carlo. The efficiency for detecting these events from the ψ is

$$\epsilon = 1.09\% \quad .$$

After all cuts have been made on the ψ sample, 152 events remain. Figure 7.14 is a plot of the $\gamma\gamma$ invariant mass showing a clear π^0 signal. The background is approximately flat, at the level of 1.5 events per 20 MeV bin. Subtracting the background of 4.5 events leaves a π^0 signal of 147.5 events, which gives a branching ratio;

$$B(\psi \rightarrow 2\pi^+2\pi^-\pi^0) = (3.17 \pm .42) \times 10^{-2}$$

$$\psi' \rightarrow 2\pi^+2\pi^-\pi^0$$

In the case of the ψ' decay there is one further large background from the decay $\psi \rightarrow \pi^+\pi^-\psi$, $\psi \rightarrow \pi^+\pi^-\pi^0$. This is considered a background because we are measuring the strong decays of the ψ which occur via a three gluon annihilation. This decay does not. We beleive it occurs by one of the quarks in the ψ' emitting two gluons, transforming the ψ' into a ψ and two pions. See Chapter II, reaction e. The ψ then decays via a three gluon annihilation to three pions. These events are rejected by making a cut on the invariant mass of all $\pi^+\pi^-\pi^0$ systems such that,

$$3.080 < M(\pi^+\pi^-\pi^0) < 3.120 \text{ GeV/c}^2$$

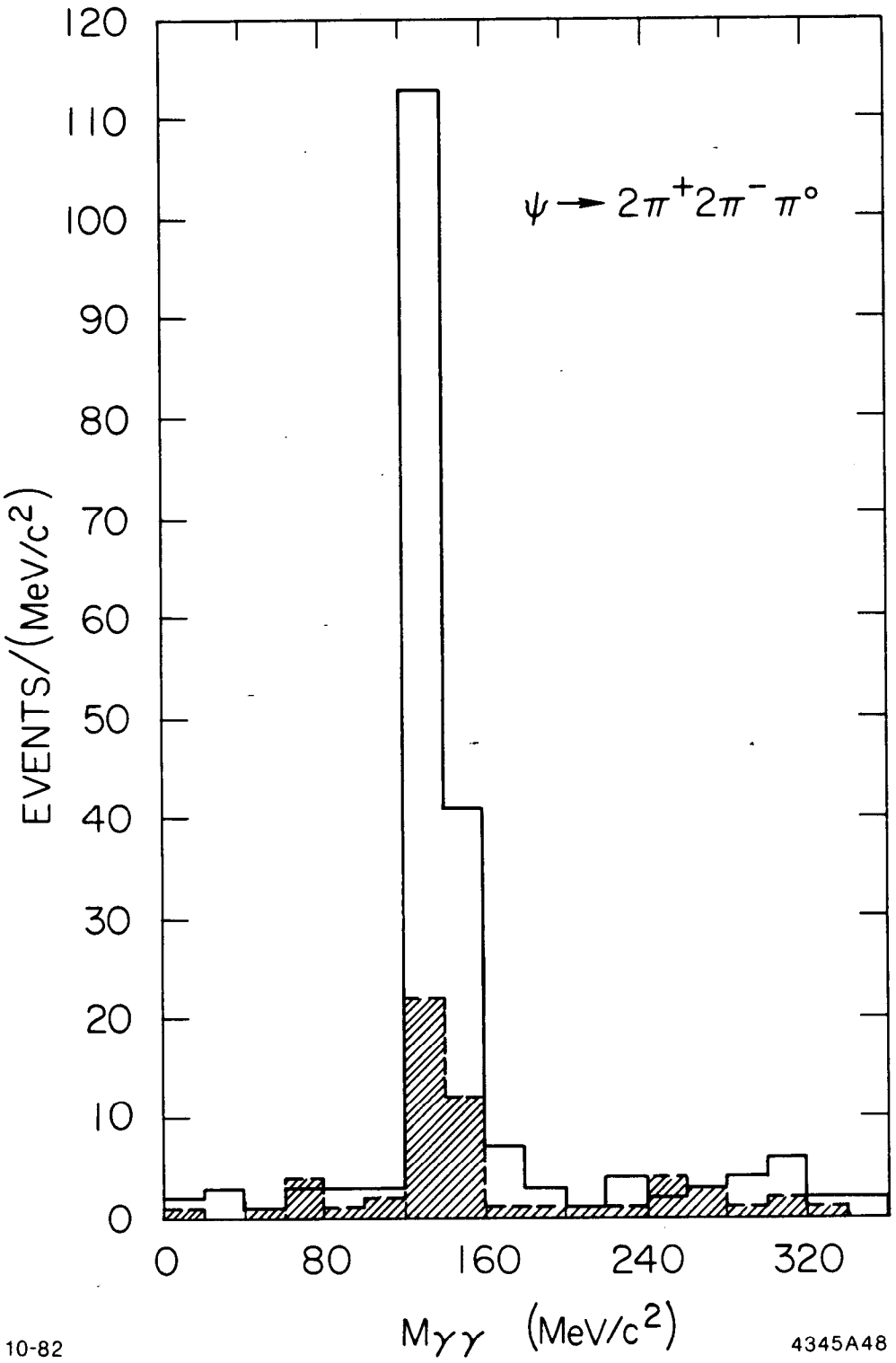

Fig. 7.14: $\gamma\gamma$ invariant mass spectra from the decay ψ and ψ'(shaded) $\rightarrow$ $2\pi^+2\pi^-\gamma\gamma$.

Figure 7.15 shows this 3π invariant mass spectrum before the cut. All combinations are plotted. A clear ψ signal is visible. Figure 7.14 includes the $\gamma\gamma$ spectrum from the ψ'. A clear π^0 signal is seen with 46 signal events and aprroximately 4 background events. The detection efficiency from the ψ' was calculated from Monte Carlo to be

$$\epsilon' = 1.39\ \%$$

Giving a branching ratio:

$$B(\psi' \rightarrow 2\pi^+2\pi^-\pi^0) = (.30 \pm .08) \times 10^{-2}$$

The ratio of branching ratios from the ψ and ψ' is:

$$B(\psi')/B(\psi) = (9.5 \pm 2.7)\% \quad .$$

7.5 $\psi \rightarrow \omega\pi^+\pi^-$

One of the intermediate states through which the ψ decays to five pions is $\omega\pi^+\pi^-$. This includes the intermediate state ω f(1270). Figure 7.16 is a plot of all $\pi^+\pi^-\pi^0$ combinations. An ω signal is evident at the mass of the ω, 780 MeV/c^2. We required that at least one of the 3 pion combinations be consistent with the ω mass, i.e.,

$$630 < M(\pi^+\pi^-\pi^0) < 900\ \text{MeV}/c^2.$$

Figure 7.17 is a plot of the $\gamma\ \gamma$ invariant mass, which shows a clear π^0 signal of 30 events. We estimate 2 events due to background and

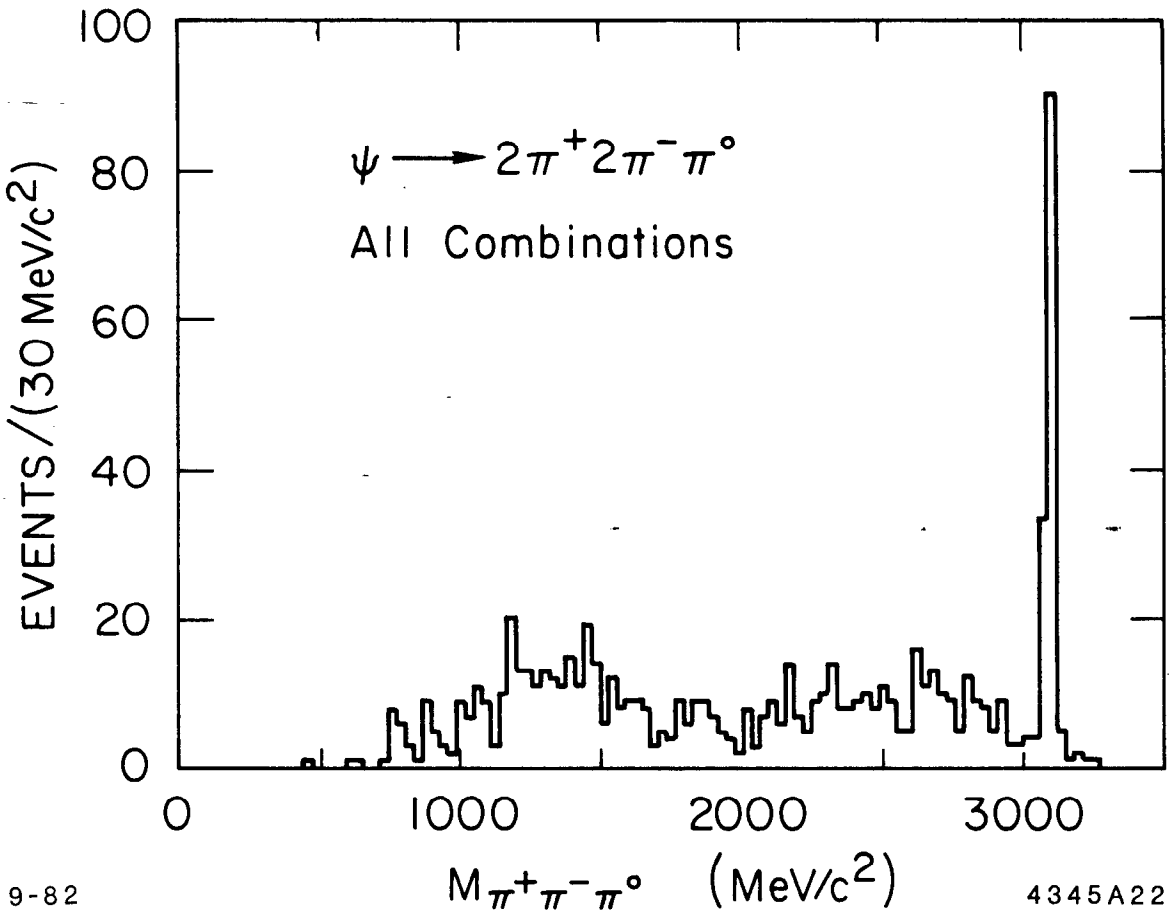

Fig. 7.15: Invariant mass distribution of all $\pi^+\pi^-\pi^0$ combinations from $\psi' \rightarrow 2\pi^+2\pi^-\pi^0$ decays, showing a clear ψ signal.

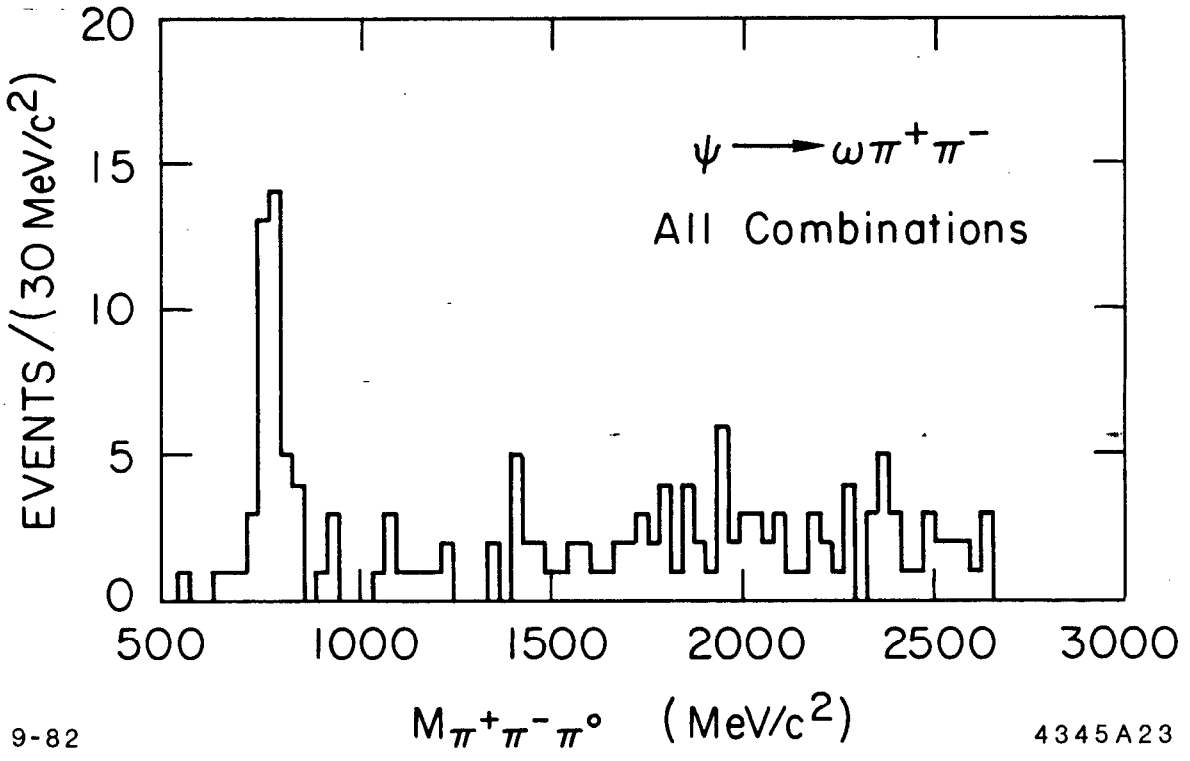

Fig. 7.16: Invariant mass of all $\pi^+\pi^-\pi^0$ combinations in events $\psi \to 2\pi^+2\pi^-\pi^0$ in which an ω is required.

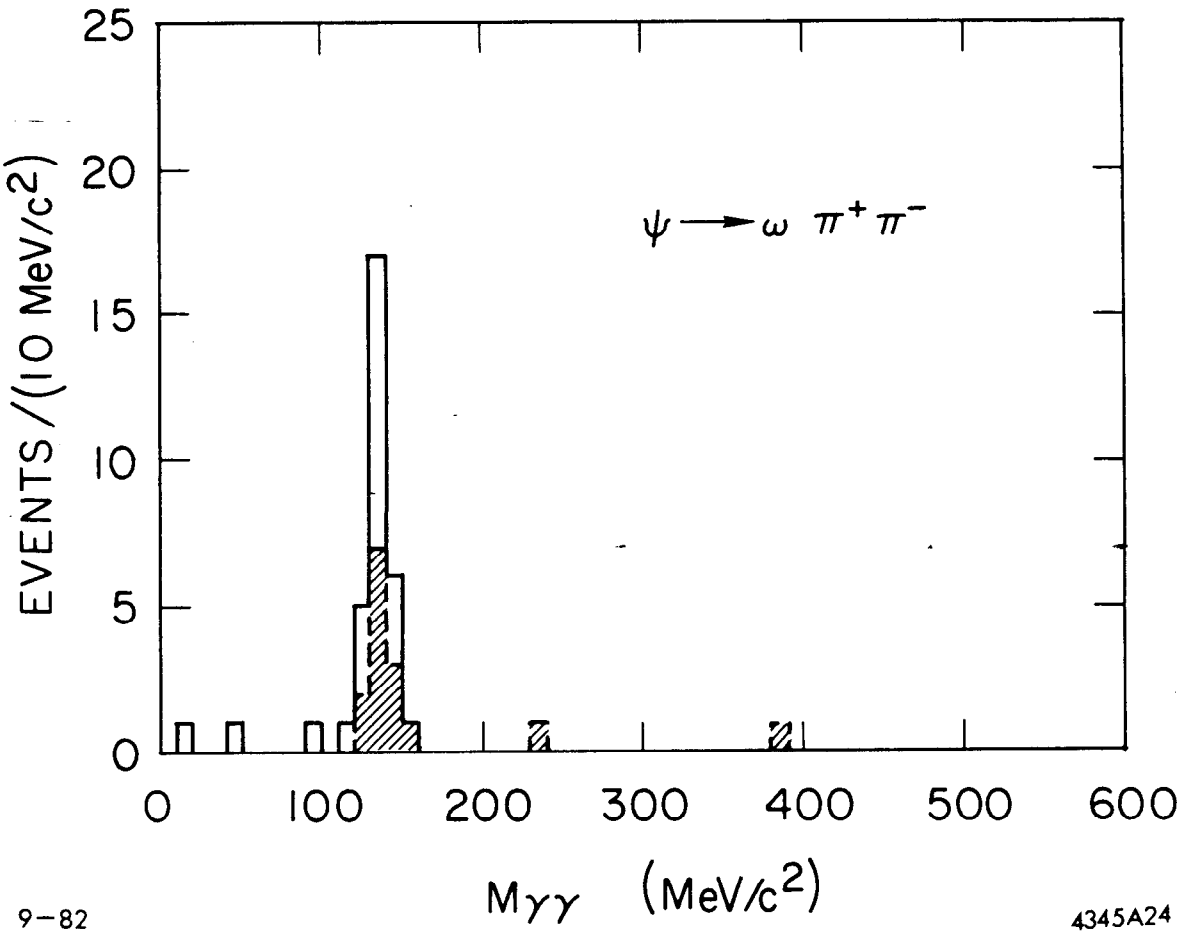

Fig. 7.17: $\gamma\gamma$ invariant mass distribution for events from the decay $\psi \to 2\pi^+2\pi^-\pi^0$ (and ψ' shaded data) when an ω is required.

subtract these from the signal. The detection efficiency for these events was calculated by Monte Carlo,

$$\epsilon = 1.10\ \%$$

This gives a branching ratio from the ψ of

$$B(\psi \to \omega\pi^+\pi^-) = (6.6 \pm 1.5) \times 10^{-3}.$$

For the analagous decay from the ψ', Fig. 7.18 shows a plot of all $\pi^+\pi^-\pi^0$ invariant mass combinations. A small ω signal is apparent. Figure 7.18 is a plot of the $\gamma\gamma$ invariant mass showing 9 events which include π^0's. We estimate one background event which we subtract.

The detection efficiency was assumed to be approximately equal to the detection efficiency measured for the decay $\psi' \to 2\pi^+2\pi^-\pi^0$,

$$\epsilon' = 1.39\%$$

leading to a branching ratio of:

$$B(\psi' \to \omega\pi^+\pi^-) = (6.3 \pm 2.5) \times 10^{-4}.$$

The ratio of branching ratios equals:

$$B(\psi')/B(\psi) = (9.5 \pm 4.4)\% \quad .$$

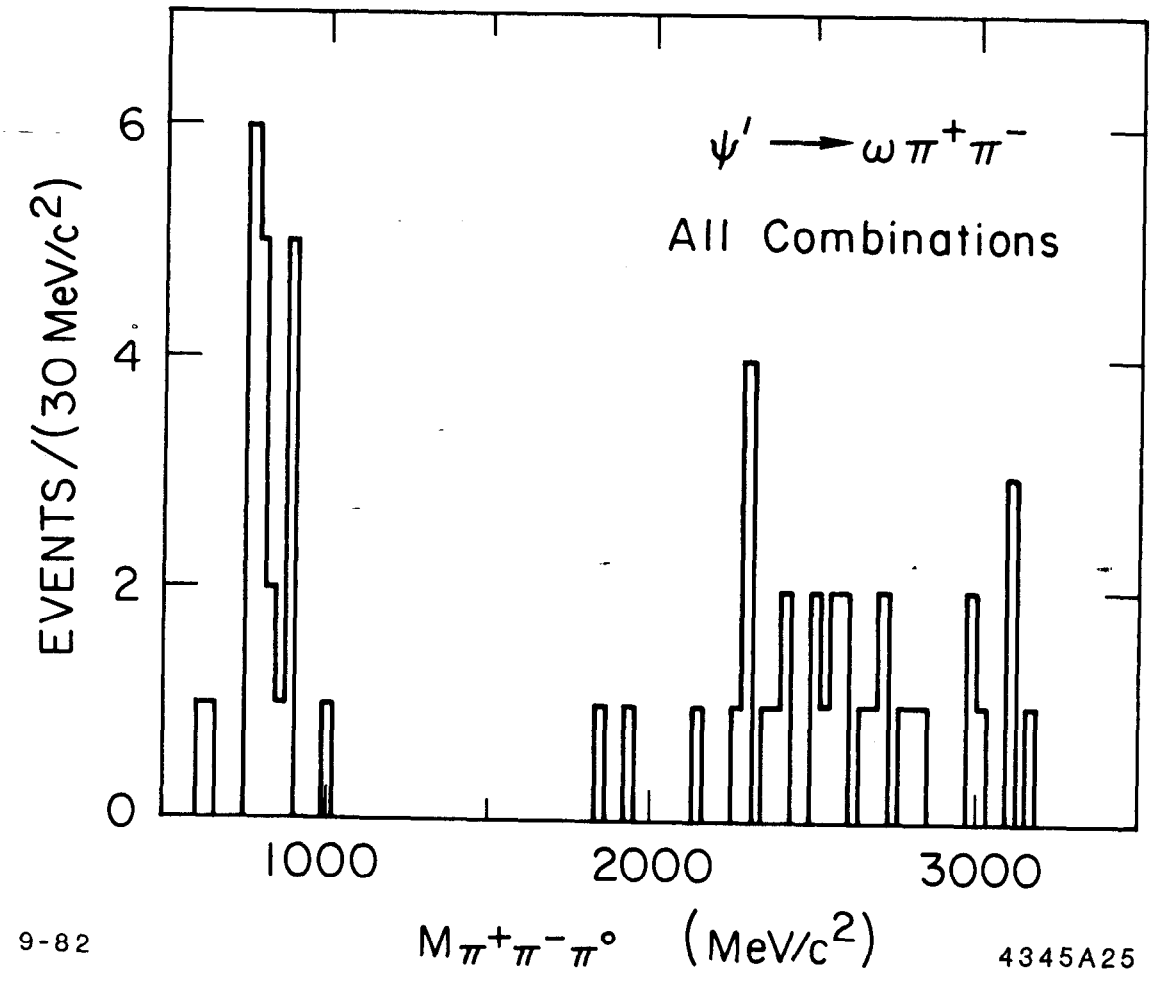

Fig. 7.18: All $\pi^+\pi^-\pi^0$ invariant mass combinations from events $\psi \rightarrow 2\pi^+2\pi^-\pi^0$ in which an ω is required.

7.6 $\underline{\psi \to 3\pi^+3\pi^-\pi^0}$

This decay is treated in the same manner as the decay $\psi \to 2(\pi^+\pi^-)\pi^0$. An additional cut is made on the invariant mass of all $2\pi^+2\pi^-\pi^0$ combinations to exclude events of the type $\psi' \to \pi^+\pi^-\psi$, $\psi \to 2\pi^+2\pi^-\pi^0$ in the ψ' decays.

Events are selected which pass the four constraint kinematic fit with $\chi^2 < 20$. Figure 7.19 shows the two photon invariant mass spectra from the ψ and the ψ' (shaded region). There are clear π^0 signals in each case. 11 events survive the ψ analysis and 6 events survive the ψ' analysis, therefore the statistical errors on the branching ratios are high, around 30-40%.

The detection efficiencies for these decays were generated using Lorentz invariant phase space distributed Monte Carlo data. The efficiencies were insensitive, within errors, to the addition of the ω resonance to the final state in the Monte Carlo. The efficiency at the ψ is $\epsilon = .09\%$ giving the corresponding branching ratio;

$$B(\psi \to 3\pi^+3\pi^-\pi^0) = (2.8 \pm .9) \times 10^{-2}$$

In the case of the ψ' decay the efficiency was found to be

$$\epsilon' = .17\%$$

giving a branching ratio of;

$$B(\psi' \to 3\pi^+3\pi^-\pi^0) = (3.5 \pm 1.6) \times 10^{-3}.$$

The ratio of branching ratios is,

$$B(\psi')/B(\psi) = (13 \pm 7)\% \quad .$$

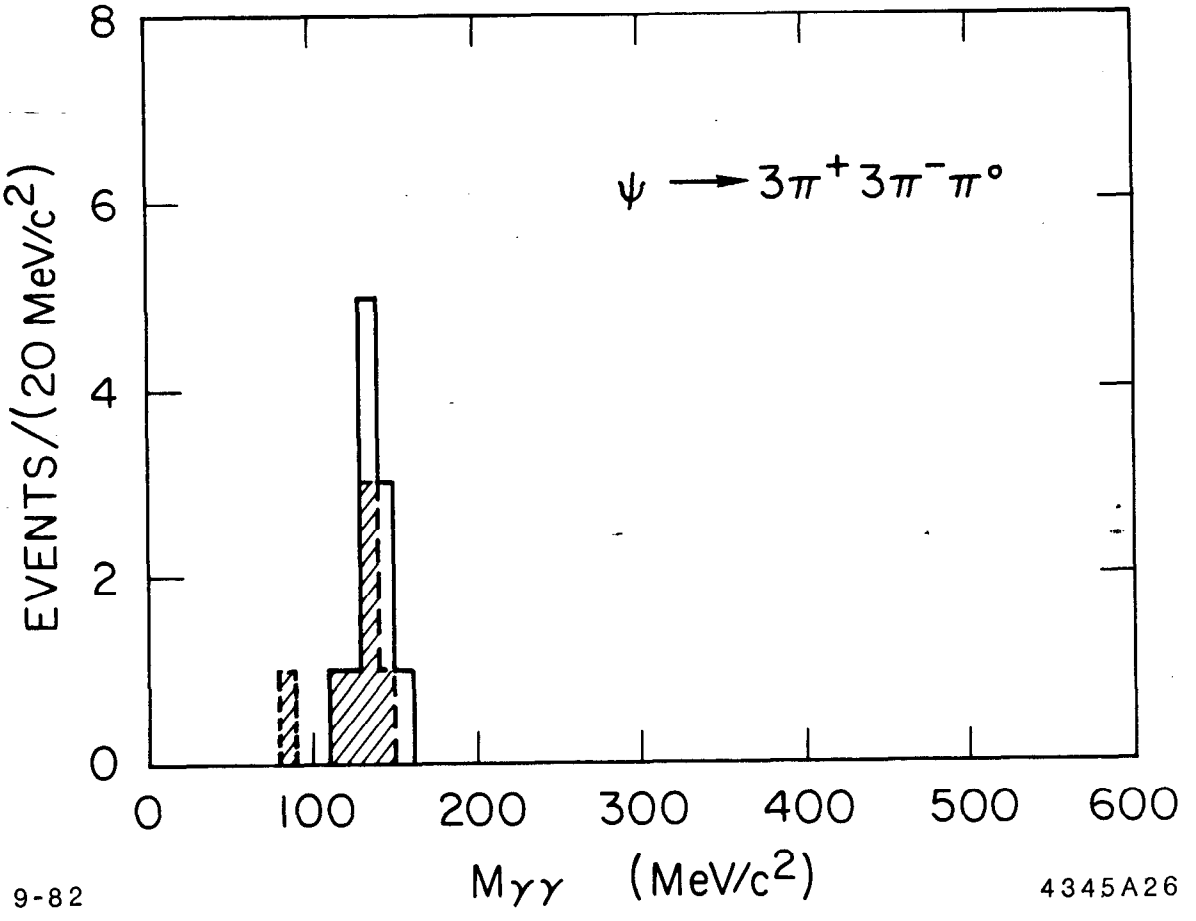

Fig. 7.19: $\gamma\gamma$ invariant mass spectra for events ψ (and ψ' shaded region) $\rightarrow 3\pi^+3\pi^-\pi^0$.

Chapter VIII

SUMMARY: PART 1

We have found that, of the six decay modes studied, four are consistent with our theoretical prediction based on perturbative quantum chromodynamics, and two are not. The two decays which differ significantly from prediction are $\psi' \to \pi^+\pi^-\pi^0$ and $\psi' \to K^+K^-\pi^0$. We find no evidence for these decays. Table 8.1 shows the results of all modes, including for comparison, a mode we did not measure, $\psi' \to p\bar{p}$, and previous measurements where they exist.

In the decay to three π's we found that the decay takes place predominantly through the intermediate state $\rho\pi$. And in the decay to $K\bar{K}\pi$ we found that it occurs through the intermediate state K*K. These are both quasi- two body decays occuring through a spin one resonance to three pseudoscalars. There is as yet no theoretical explanation for the lack of a significant signal in these cases. The suppression from prediction is more than a factor of ten. Brodsky and Lepage[1] predict a ratio[2],

$$\frac{B(\psi' \to \rho\pi)}{B(\psi \to \rho\pi)} \sim \left[\frac{M_\psi}{M_{\psi'}}\right]^6 \qquad (1)$$

---

[1] S.J.Brodsky and G.P.Lepage, Phys. Rev. D24, 2848 (1981).
[2] Brodsky and Lepages branching ratios are defined differently than the authors. They define it as the partial width divided by the width into light quark hadrons. This is consistent with our definition within a factor of 2.

Table 8.1

Mode	$B(\psi \to X)\%$	$B(\psi \to X)\%$ Previous*	$B(\psi' \to X)\%$	$B(\psi' \to X)\%$ Previous*	$B(\psi')/B(\psi)\%$
$p\bar{p}$	0.22±0.02	Same	0.023±0.005	Same	10.5±2.4
$p\bar{p}\pi^0$	$(1.0\pm0.3)\times10^{-1}$	$(1.00\pm.15)\times10^{-1}$	$(1.4\pm0.5)\times10^{-2}$	--	14.0±6.3
$2\pi^+2\pi^-\pi^0$	(3.17±0.42)	(3.72±.50)	(.30±0.08)	(.35±.15)	9.5±2.7
$\omega\pi^+\pi^-$	$(6.6\pm1.5)\times10^{-1}$	(0.68±.21)	$(6.3\pm2.5)\times10^{-2}$	--	9.5±4.4
$3\pi^+3\pi^-\pi^0$	(2.8±0.9)	(2.9±.7)	$(3.5\pm1.6)\times10^{-1}$	--	13.0±7.0
$K^{*\pm}K^{\mp}$ $\hookrightarrow K^{\pm}\pi^0$	$(8.8\pm1.9)\times10^{-2}$	$(1.13\pm.20)\times10^{-1}$	$< 1.79\times10^{-3}$	--	< 2.03
$K^+K^-\pi^0$	$(9.2\pm2.0)\times10^{-2}$	--	$< 2.96\times10^{-3}$	--	< 3.2
$\rho^0\pi^0$	$(4.1\pm0.7)\times10^{-1}$	$(5.34\pm.88)\times10^{-1}$	$< 3.60\times10^{-3}$	< .1	< 0.87
$\rho^{\pm}\pi^{\mp}$	(0.92±0.16)	--	$< 1.0\times10^{-2}$	--	< 1.05
$\pi^+\pi^-\pi^0$	(1.45±0.19)	--	$(8.5\pm4.6)\times10^{-3}$	< .1	0.6±0.4
$\rho\pi$	(1.3±0.3)	(1.23±.14)	< 0.0083	--	< 0.63

* Particle Data Group, Rev. Mod. Phys. Vol. 52 (1980).
All upper limits are at 90% confidence level.

assuming quark helicity is conserved in strong interactions. This includes a suppression proportional to the ratio of masses to the fourth power. This suppression is not large enough, though, to account for the data. The exponent in (1) would have to be about 23 to explain it.

In the theoretical calculation made in chapter I we assumed that the only differences between the ψ and the ψ' which were relevant were their wavefunctions at the origin and their masses. The ratio of the masses is

$$\frac{M_\psi}{M_{\psi'}} = .84$$

Any suppression due to the difference in masses would require an exponent of about 25 to be consistent with the data. It is important to note that perturbative QCD will only work when $\alpha_s^2 << 1$. The charmonium system may well be in a region where such a perturbation expansion is invalid. In this case, our original theoretical prediction is invalid and QCD is unscathed. If this is a regime in which perturbative QCD should be applicable then our result is a problem for that theory. In any case, the suppression is a mystery.

Chapter IX

RADIATIVE DECAY OF THE ψ

9.1 INTRODUCTION

In the summer of 1981 the Crystal Ball collaboration reported the observation[1] of a resonant state in the decay, $\psi \to \eta\eta\gamma$. This resonance, which they labelled the θ, is seen to decay to $\eta\eta$, with a width of 220±100 MeV and invariant mass M = 640±50 MeV. They have measured the branching ratio

$$B(\psi \to \theta\gamma)\ B(\theta \to \eta\eta) = (4.9 \pm 1.4 \pm 1.0) \times 10^{-4} \quad .$$

and have found that spin 2 is favoured at the 95% confidence level. This discovery prompted us to look more closely at the decays,

$$\psi \to K^+K^-\gamma \quad \text{and} \quad \psi \to \pi^+\pi^-\gamma \quad .$$

This second analysis is itself divided into two parts. The first method of analysis makes a completely constrained analysis of the decay $\psi \to K^+K^-\gamma$, requiring the detection of all final state particles. The second method does not require that the photon be detected thus utilising the entire data sample.

---

[1] C. Edwards et al., Phys. Rev. Lett. 48, 458, (1982).

9.2 METHOD I: $\psi \to K^+K^-\gamma$

Event Selection

To study the decay $\psi \to K^+K^-\gamma$, we selected events in which all particles in the final state were observed. We identified the K's by time of flight measurements and by the kinematics of the decay. The photons were identified with the liquid argon system.

The following restrictions were made on the data sample of all events with two charged prongs in data sample 2, corresponding to 627,000 produced ψ's.

1. Two and only two oppositely charged tracks in the central detector were required. This excludes events in which the γ converts in the beam pipe.
2. We selected events with at least one γ, with energy E > 200 MeV, not identified as a fake, found in one of the eight liquid argon barrel modules.
3. Only events in which the charged tracks have good time of flight measurements associated with them are used.
4. We required that

$$\sqrt{[\Delta t_1]^2 + [\Delta t_2]^2} \; < \; 600 \text{ picoseconds}$$

where

$$\Delta t_1 \equiv [t_1(\text{measured}) - t_1(\text{expected})] \quad ,$$

The expected time is calculated assuming K masses for the charged particles. This cut assures that both charged tracks are consistent, within 2σ (or 600 ps), with the K mass hypothesis.

5. We required the charged tracks to be acollinear. That $\cos(\theta_a) < .86$, or equivalently $\theta_a > 30°$. The acollinearity angle between the two charged tracks is defined as:

$$\theta_a \equiv \cos^{-1}(\vec{p}_{K1} \cdot -\vec{p}_{K2})/|\vec{p}_{K1} \cdot \vec{p}_{K2}| \quad .$$

This cut attempts to exclude backgrounds which are characteristically collinear, such as Bhabhas, μ pairs and K*K events.

6. We require that $U = |E_m - P_m| < 100$ MeV. This cut selects events in which only a π^0 or a γ is missing.

7. We required that

$$P_t^2 < .0015 \quad , \text{ where } P_t^2 = [2P_m \sin(\theta/2)]^2 \quad .$$

θ is the angle between the missing momentum vector $\vec{P}_m$ and the direction of the observed photon. This variable is described in detail elsewhere[2]. P_t^2 distinguishes between π^0's and photons. The photons concentrate at low P_t^2 whereas the events which contain π^0's are spread out in P_t^2, therefore we can cut out much of the π^0 background by requiring events to have a low P_t^2. The rest of the π^0's can be subtracted. In this case almost all the π^0 background comes from the decay, $\psi \rightarrow K^+K^-\pi^0$, which we know occurs predominantly through the intermediate state, K*(892)K. We know also that the K's from this decay are highly collinear (see Fig. 7.10). We have made a cut on the acollinearity of the K's above, which cuts out about 94.9% of these events. Therefore there is very little data at P_t^2 above 0.003 GeV^2 and a π^0 background subtraction is unnecessary. Figure 9.1 shows the P_t^2 distribution after the

---

[2] Himel et al., Phys. Rev. Lett. 45, 1146 (1980).

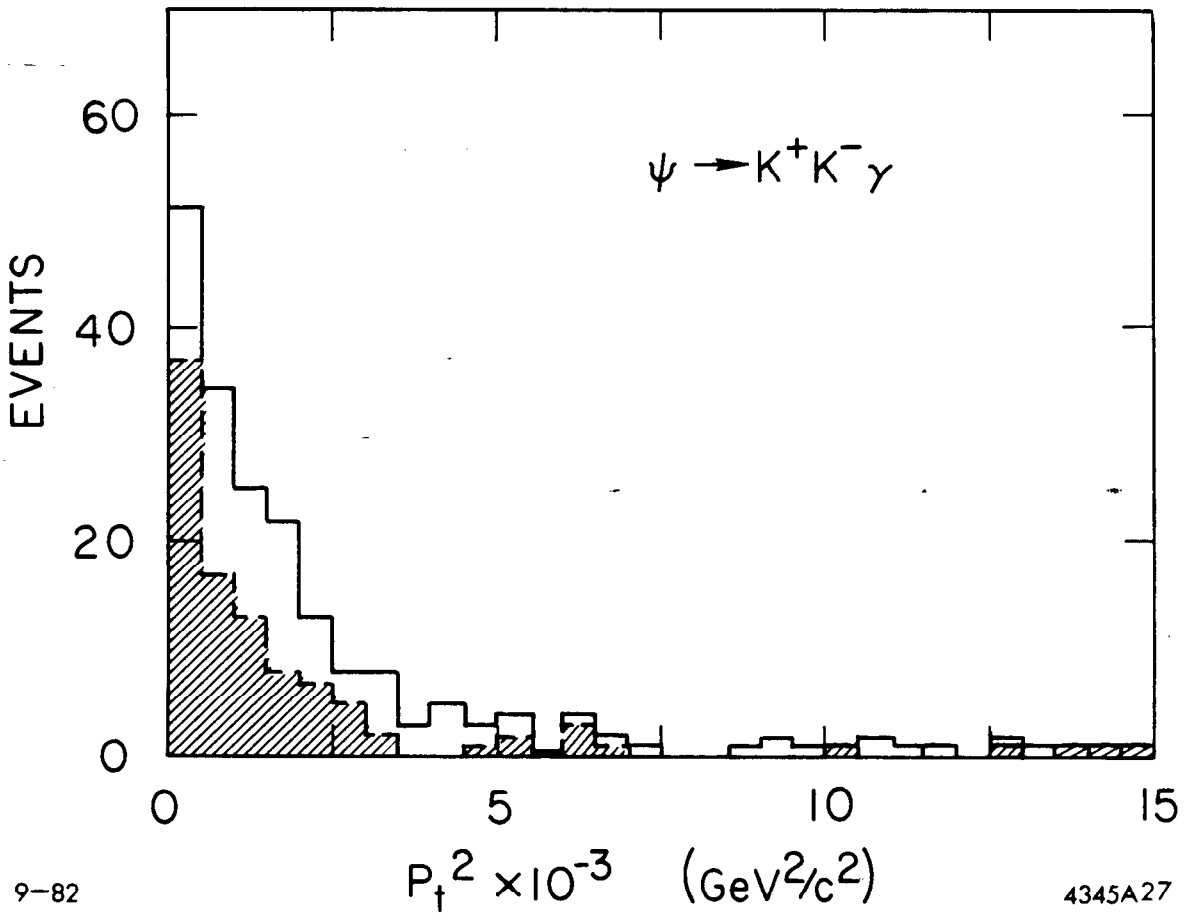

Fig. 9.1: Number of events versus p_t^2. The unshaded historgram is after acollinearity cut cosθ < .96. The shaded histogram is after acollinearity cut cosθ < .86.

cut on U is made and after the acollinearity cut is made. Figure 9.2 shows the U distribution after all cuts on photons including the cut on P_t^2.

8. Finally the data is kinematically fit with four constraints, (energy and momentum conservation), by the program SQUAW, to the hypothesis, $\psi \to K^+K^-\gamma$ and events in which $\chi^2 < 15$ are kept. The invariant mass spectrum of the 56 events which passed these cuts is shown in Fig. 9.3. A resonance is clearly seen in the invariant mass spectrum of the K^+K^- at around 1.65 GeV/c^2. There is very little background.

9.3 BACKGROUNDS AND FITS

The following is a consideration of six of the most obvious and possibly large backgrounds to the signal $\psi \to K^+K^-\gamma$. We have estimated an upper limit to each of their contributions.

1. $\psi \to K^\pm\pi^\mp K^0$

This final state could contribute as a background if the π is misidentified as a K and the K^0 is misidentified as a γ. This decay, however, occurs predominantly through the intermediate state, $K^{*0}\bar{K}^0$, by isospin rotation of the decay $\psi \to K^+K^-\pi^0$ analysed previously. If the π is misidentified as a K, the K*(892) peak will appear in the K^+K^- invariant mass distribtion as a peak at about 1.05 GeV/c^2. We see no evidence for a peak at that mass in the data of Fig. 9.3. At most one event could be considered consistent with being due to this background.

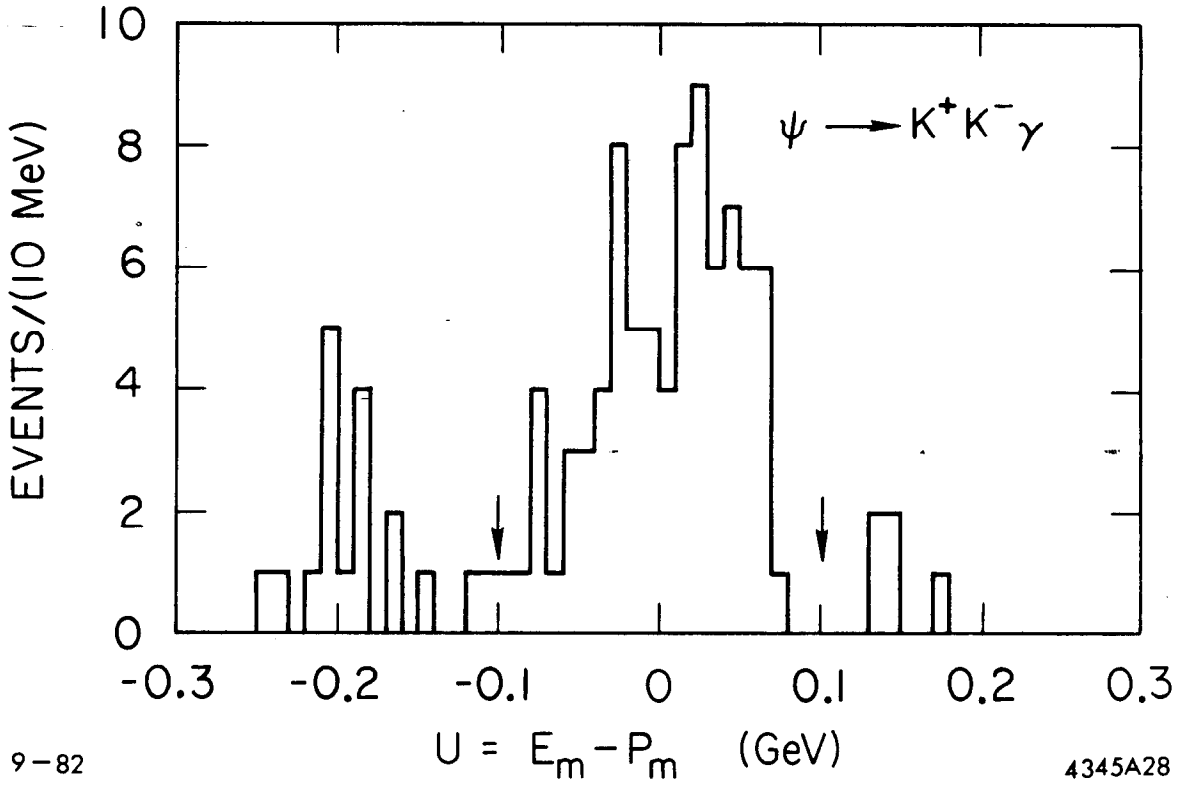

Fig. 9.2: Plot of the variable $E_m - P_m$. We cut at ±.1.

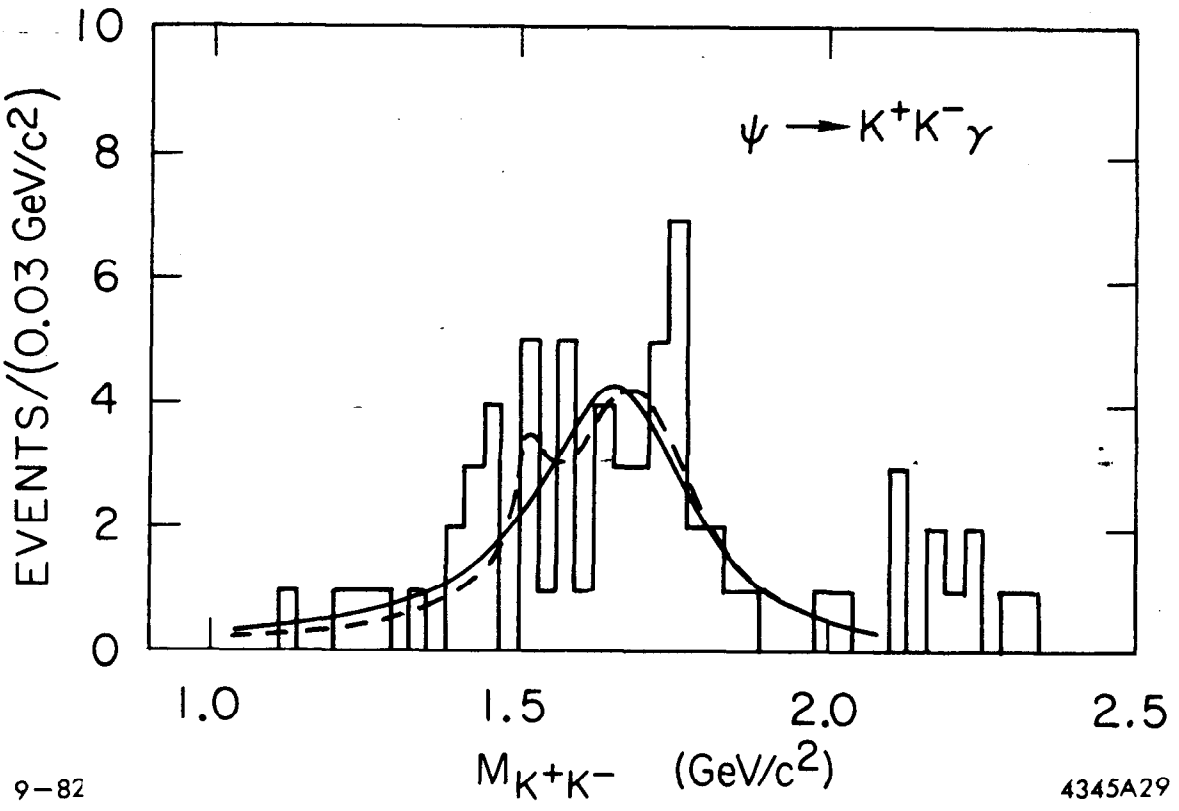

Fig. 9.3: All events surviving analysis of Method I. The dashed line is a fit to 2 Breit-Wigners, f′ and X. The solid line is the fit to X (undetermined resonance Breit-Wigner) only.

If this final state were a background, all the events from it would be concentrated in a peak far below the region of interest, defined as $1.3 < M(K^+K^-) < 1.9$ GeV/c^2. We estimate this background as being responsible for less than .1% of the signal we see.

2. $\underline{\psi \to \pi^+\pi^-\gamma}$

In particular we consider events of the type $\psi \to f(1270)\gamma$, $f \to \pi^+\pi^-$. The magnitude of the contribution to the data sample from events of the type $\psi \to f(1270)\gamma$ is important to estimate because if the π's are misidentified as K's, then the f(1270) appears as a resonance in the invariant mass of the K^+K^- system at about 1620 MeV/c^2. This is exactly the region in which we are looking for the $\theta(1640)$. The background is largely excluded by kinematic cuts since both π's must be misidentifed both by time of flight and kinematics as K's.

To determine the level of contribution we take a sample of Monte Carlo generated events, $\psi \to f(1270)\gamma$, and make the kinematic cut $U < .1$. This reduces the sample by 97.9%. Applying all analysis cuts reduces the sample by 99.9%. We have measured the branching ratio, $B(\psi \to f(1270)\gamma)\ B(f \to \pi\pi) = (1.3 \pm 0.3) \times 10^{-3}$.[3] The data sample we are working with corresponds to approximately 627,000 produced ψ's and the detection efficiency for these events is about 15%. Therefore we expect, given the reductions, < 2f's to contaminate our signal after the U cut and < .1 event after all cuts. This exercise suggests that this can be regarded as a negligible background, at the level of < 1% of the

---

[3] Mark II, unpublished.

signal. However, the Monte Carlo does not reproduce the tails of the time of flight residual distribution perfectly and so it is not entirely correct to use Monte Carlo data as a control sample when making time of flight cuts. To skirt this problem we estimate the level of background contribution by another Monte Carlo independent method. We pick a sample of real f events from the data by making the TOF requirement on a sample of two oppositely charged prongs plus a photon, that both charged particles be consistent, at the 2σ level, with the π mass hypothesis, and that the invariant mass of the two charged particles assuming π masses, be consistent with the f(1270) mass:

$$1170 < M(\pi^+\pi^-) < 1370 \quad .$$

Events which pass these cuts are labelled $\psi \rightarrow$ "f"γ events. The number of these that pass the U cut, where U is calculated using K masses, is counted. Note that there will be events in this sample which are not $\pi^+\pi^-\gamma$ events but rather $K^+K^-\gamma$ events in which both K's have low TOF's. This means the number of "f"'s that survive the U cut will be an upper limit on the number of f's which contaminate our signal. We find 4 such events and conclude that the number of f's contaminating our signal is < 7%.

3. $\underline{\psi \rightarrow \pi^+\pi^-\pi^0}$

Events of this type are excluded by both the U kinematic cut, and the P_t^2 cut. This background can be monitored by noting that the decay proceeds predominantly through the ρ resonance (see Fig. 5.5) and looking for neutral and charged ρ's in the invariant mass of all 2π combinations

in the event. We look at the possibility that both charged π's from the decay $\psi \to \rho^0\pi^0$ are misidenitifed as K's. The ρ resonance would then appear as a peak in the K^+K^- invariant mass distribution at a mass of about 1.1 GeV/c^2. There is no evidence for such a signal in Fig. 9.3 and so we conclude that this background $\psi \to \rho\pi$, contributes less than 1% of the signal.

4. $\underline{\psi \to K^+K^-\pi^0}$

A large part of this background is cut out with the P_t^2 cut, which discriminates between π^0's and photons, and a larger part cut out by the acollinearity cut. This decay proceeds almost entirely through the intermediate state $K^*(892)\bar{K}$. A plot of the invariant mass spectrum of the K^+K^- pair from decays $\psi \to K^*K$ is shown in Fig. 9.4. The distribution begins above 1.9 GeV/c^2. This is because the K^+K^- mass reflects the K*(892) mass seen in the $K^\pm\pi^\mp$ spectrum. This means that this background does not contribute significantly to the signal region. We estimate the level of this background by noting the branching ratio $B(\psi \to K^{*\pm}K^\mp)\ B(K^{*\pm} \to K^\pm\pi^0) = 9.15 \times 10^{-4}$, the efficiency for detecting these events after all cuts is $\epsilon = .4\%$. This means that we expect to observe 2.3 such events, 10% of which will have K^+K^- masses below 2 GeV, or < 1% of the signal.

5. $\underline{\psi \to e^+e^-\gamma}$

These are Bhabha events where one of the electrons bremsstrahlungs a photon in the final state. Since there are a great many such QED events, they provide a significant background. We required that neither

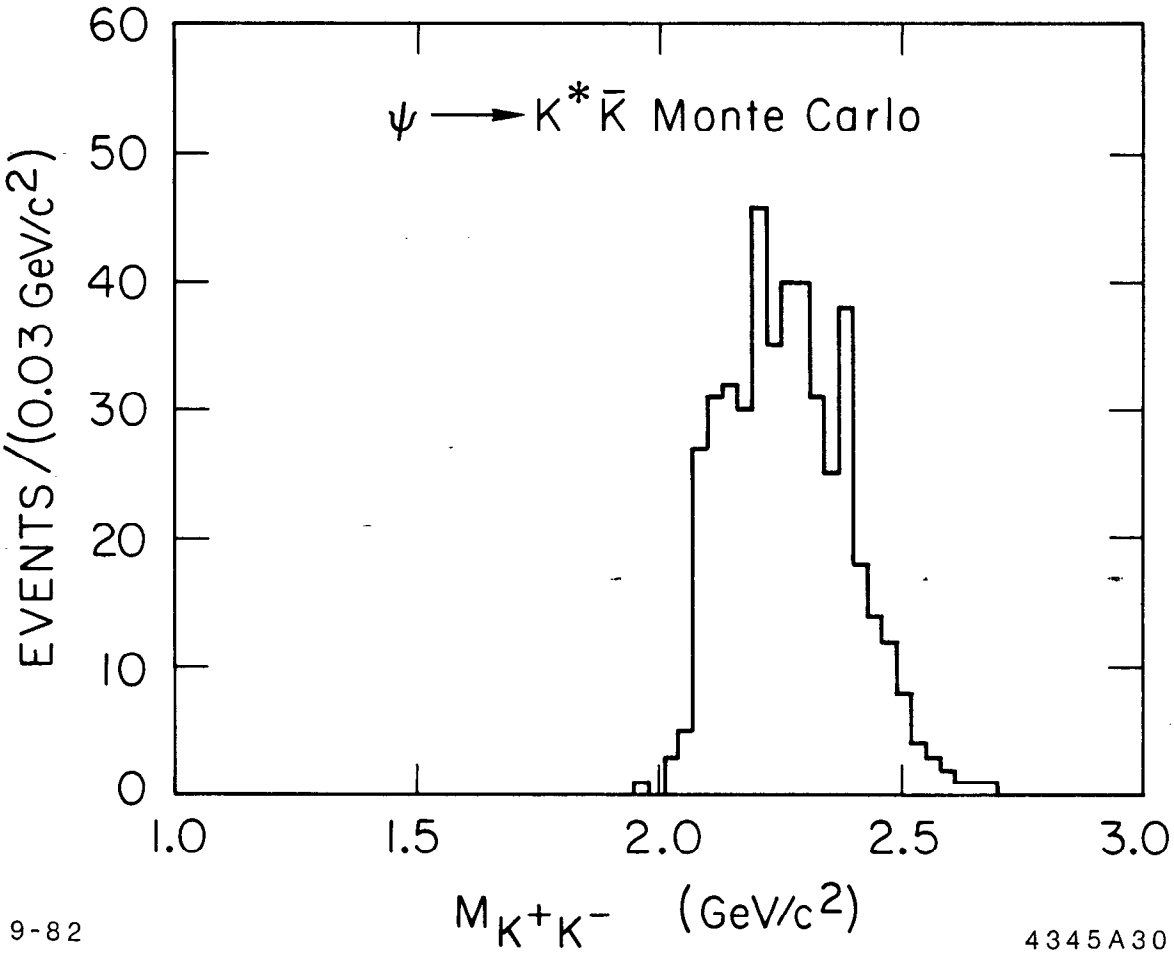

Fig. 9.4: Invariant mass of the K^+K^- from Monte Carlo generated decays of $\psi \rightarrow K^{*\pm}K^{\mp}$.

charged particle be identified as an electron by the liquid argon electron-pion separation program described in Chapter 3. The probability that we call an electron a π is calculated to be 5%. When we do not make the cut separating electrons from π's we gain only 1 event. This means that the background due to Bhabha's is $<$ .1% of the signal.

6. $\underline{\psi \to \mu^+\mu^-\gamma}$.

Since the K's often decay into $\mu\nu$ we do not cut out events with tracks in the muon counters. However the μ's radiate hard photons far less often than the electrons and there are no events in the final sample that are identified by the muon system as $\mu^+\mu^-\gamma$ events. The probability that both μ's are misidentified as π's is the probability that both μ's are not contained in the muon systems solid angle, which is $<$ 2%. We conclude that this is a negligible background at the level of $<$ .1%.

Efficiencies

The efficiency for detecting events of the type $\psi \to K^+K^-\gamma$ was measured using both phase space and resonant Monte Carlo data. The phase space model was used to measure the variation of efficiency with the invariant mass of the K^+K^- pair. The efficiency is consistent with being flat in the region $1.3 < M(K^+K^-) < 1.9$ GeV/c^2 and a correction was not necessary. Figure 9.5 is a plot of the efficiency as a function of mass. The resonant Monte Carlo was thrown with an isotropic angular distribution for the γ. The assumption of isotropy adds $\simeq$ 20% to the

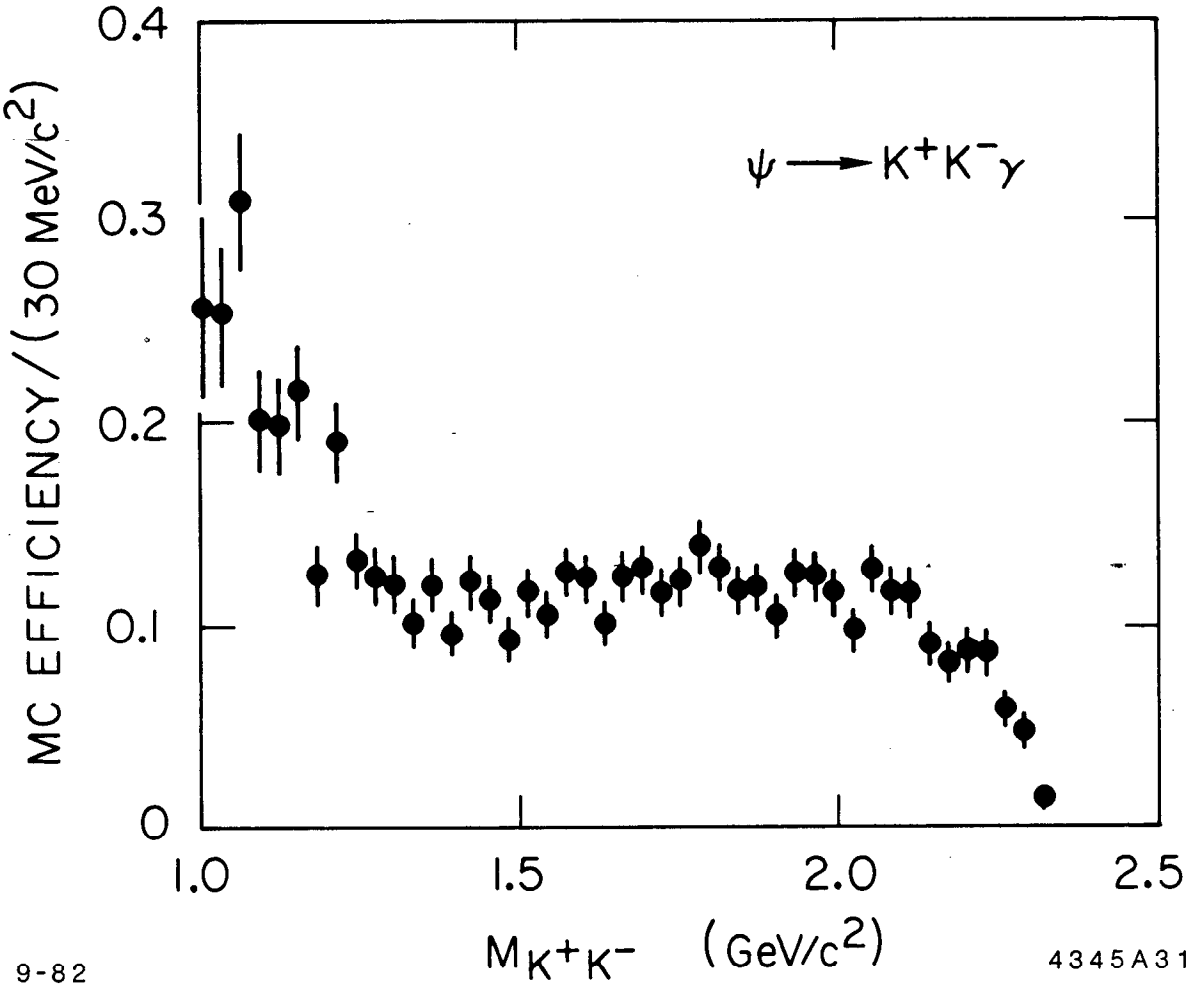

Fig. 9.5: Detection efficiency versus K^+K^- invariant mass from events $\psi \to K^+K^-\gamma$.

systematic error in the branching ratio. This Monte Carlo was used to measure the efficiency for finding events of the type

$$\psi \rightarrow \theta\gamma \quad , \quad \theta \rightarrow K^+K^- \quad .$$

The efficiency is $\epsilon = 14\%$.

Fits to the Data

We are looking for a particular particle, the $\theta(1640)$. We will assume for simplicity that the resonance we observe is the θ now although we have presented no evidence for this. Later we will discuss the similarity of the resonance we measure to the θ.

A maximum liklihood fit using the full data sample of 627,000 produced ψ's, to the hypothetical function f, where

$$f(x) = \frac{a}{[(x^2 - M_r^2)^2 + M_r^2\,\Gamma_r^2]} + b$$

was made where M_r is the mass of the resonance, Γ_r is its width, and a and b are constants. This is a relativistic Breit-Wigner function which describes a resonant state. The fit is the solid line in Fig. 9.3. The flat background term b was found to be consistent with zero. The mass and width of the Breit-Wigner were found to be:

$$M(\theta) = 1655 \pm 30 \text{ MeV}/c^2 \quad , \quad \Gamma(\theta) = 295 \pm 30 \text{ MeV} \quad .$$

We note that SU(3) predicts that the decay,

$$\psi \rightarrow f'\gamma \quad , \quad f' \rightarrow K^+K^- \text{ will occur.}$$

The mass of the f′ is 1516 MeV/c^2 and the width is $\Gamma(f') = 60$ MeV.[1] If it is produced, the f′ will be present in the signal region. We take this into consideration and a fit is made to the above function f(x) plus a relativistic Breit-Wigner with mass and width fixed to those of the f′(1516). The new function is;

$$g(x) = f(x) + \frac{c}{[(x^2 - M_{f'}{}^2)^2 + M_{f'}{}^2 \Gamma_{f'}{}^2]} \quad .$$

This fit gives $M(\theta) = 1680 \pm 30$ MeV/c^2 and $\Gamma(\theta) = 265 \pm 30$ MeV. The dotted line in Fig. 9.3 shows g(x) from this fit. The goodnesses of fit for these two hypotheses are comparable. However there is no statistically significant f′(1516) signal in the data.

The branching ratio is calculated, using the sample of 427,000 produced ψ events, and making a cut on mass (K^+K^-) such that all events are in the region, 1.450-1.850 GeV/c^2. Here we assume that there is only one resonance. We find

$$B(\psi \rightarrow \theta\gamma)\cdot B(\theta \rightarrow K^+K^-) = (6.7 \pm 1.3 \pm 1.7) \times 10^{-4} \quad .$$

Where the first error is statistical and the second systematic. If we measure the branching ratio from the second fit, including the f′(1516), then we find:

$$B(\psi \rightarrow \theta\gamma)\cdot B(\theta \rightarrow K^+K^-) = (6.3 \pm 1.2 \pm 1.9) \times 10^{-4} \quad .$$

---

[1] Particle Data Group, Reviews of Modern Physics, Vol. 52, (1980).

The systematic errors are large and break down as follows: There is a 17% uncertainty in the number of signal events due to background. This is because we do not know how many events to attribute to a possible f′ signal discussed previously. There is a 5% uncertainty due to the error in the number of produced ψ′s. There is a 24% uncertainty due to the Monte Carlo having a flat angular distribution and not precisely simulating the data in other respects. All together this introduces a 29% systematic error.

Chapter X

METHOD II: $\psi \rightarrow K^+K^-\gamma$

Background

It is clear from the plot of P_t^2 (Fig. 9.2) that there is very little π^0 background in our final data sample. Less than 5% of the data is π^0 background. This background is concentrated in events in which the K^+K^- mass is > 1.9 GeV/c^2 as has already been shown. We do not see all these $K^+K^-\pi^0$ events in the P_t^2 plot because most of these events have collinear charged tracks and we have already made a tight cut of 30° on the collinearity of the charged tracks. The lack of a significant π^0 background suggests that an analysis can be done to look for the θ without requiring a cut on P_t^2 and without requiring an observed photon. The data sample from method I was reanalysed, removing all cuts using the liquid argon counter information. The background resulting was about 40% of the signal. We demanded that the charged tracks come from a vertex and the background was reduced to about 25% of the signal. We took the data sample with liquid argon information and analysed it without making any cuts on the photon information. We analysed it with and without the cut which rejects electrons. We found that the electron background is approximately 10.5% of the data. This background splits into three categories. There is 2% electron background in the region of $M(K^+K^-)$ below 1.44 GeV/c^2, 1% background in the signal region, and 10% background in the region $M(K^+K^-)$ above 1.83 GeV/c^2. From this study we

conclude that, in the data sample without liquid argon shower counter information, there will be a 10.5% electron background overall, and a 1% background in the region of the signal. The remaining 20-25% background can be attributed to a collection of final states and mistracked events.

The new analysis, by not requiring a photon, increases the data sample by a factor of two (half of the ψ data was taken with unresponsive liquid argon counters) and increases the efficiency for detection by a factor of 1.5. This gives a total data sample increase of a factor of 3. The sample corresponds to $\simeq 1.27 \times 10^6$ produced ψ's.

Event Selection Requiring no Photons

The same cuts were made on this data sample as in the previous analysis except

1. No photon was required.
2. Both charged tracks were required to come from a vertex at beam crossing.
3. The data was kinematically fit with 1 constraint to the hypothesis

$$\psi \rightarrow K^+K^- \text{ (+ a missing } \gamma)$$

The U cut was made tighter, such that $U < .08$. This was done to better reject $e^+e^-\gamma$ and $\pi^+\pi^-\gamma$ events. Figure 9.2 shows the invariant mass (K^+K^-) plot for the surviving events. A clear θ signal is seen as well as an apparent f'(1516) signal sitting on the θ's left hand shoulder.

A maximum liklihood fit to the form was made where a, b and c are constants. Again the measured mass and width of the f' were fixed.

Figure 10.1 shows the surviving events. A clear θ and f′(1516) signal are seen. The solid line is the fit to two Breit-Wigners. The fit was made over the restricted region,

$$1.2 < M(K^+K^-) < 1.9 \text{ GeV}/c^2$$

because:

1. At about 1.05-1.10 GeV/c^2 there is a signal from the background,

$$\psi \rightarrow K^{0*}\bar{K}^0$$

in which the K^{0*} decays to $K^{\pm}\pi^{\mp}$. If the π is misidentified as a K then the resonance in the mass(Kπ) ≃ 892 MeV/c^2 moves up to a mass(K^+K^-) ≃ 1.05 GeV/c^2.

2. There appear to be signs of structure above 1.9 GeV/c^2, for instance at 1.95 GeV/c^2. This is also where the known backgrounds start contributing substantially. We are not making the claim that there are indeed resonances in this region, but rather that this portion of the mass spectrum is not understood well enough to assume a form for a background in this region.

The fit results are:

$$M(\theta) = 1700 \pm 30 \text{ MeV}/c^2 \quad , \quad \Gamma(\theta) = 156 \pm 20 \text{ MeV}$$

The flat background was found to be approximately 2.4 events per 30 MeV bin. In the signal region this corresponds to 25% of the events. The branching ratios of the θ and f′ were found to be:

$$B(\psi \rightarrow \theta\gamma) \times B(\theta \rightarrow K^+K^-) = (6.0 \pm .9 \pm 2.5) \times 10^{-4}$$

and

$$B(\psi \rightarrow f'\gamma) \times B(f' \rightarrow K^+K^-) = (.9 \pm .3 \pm .5) \times 10^{-4}$$

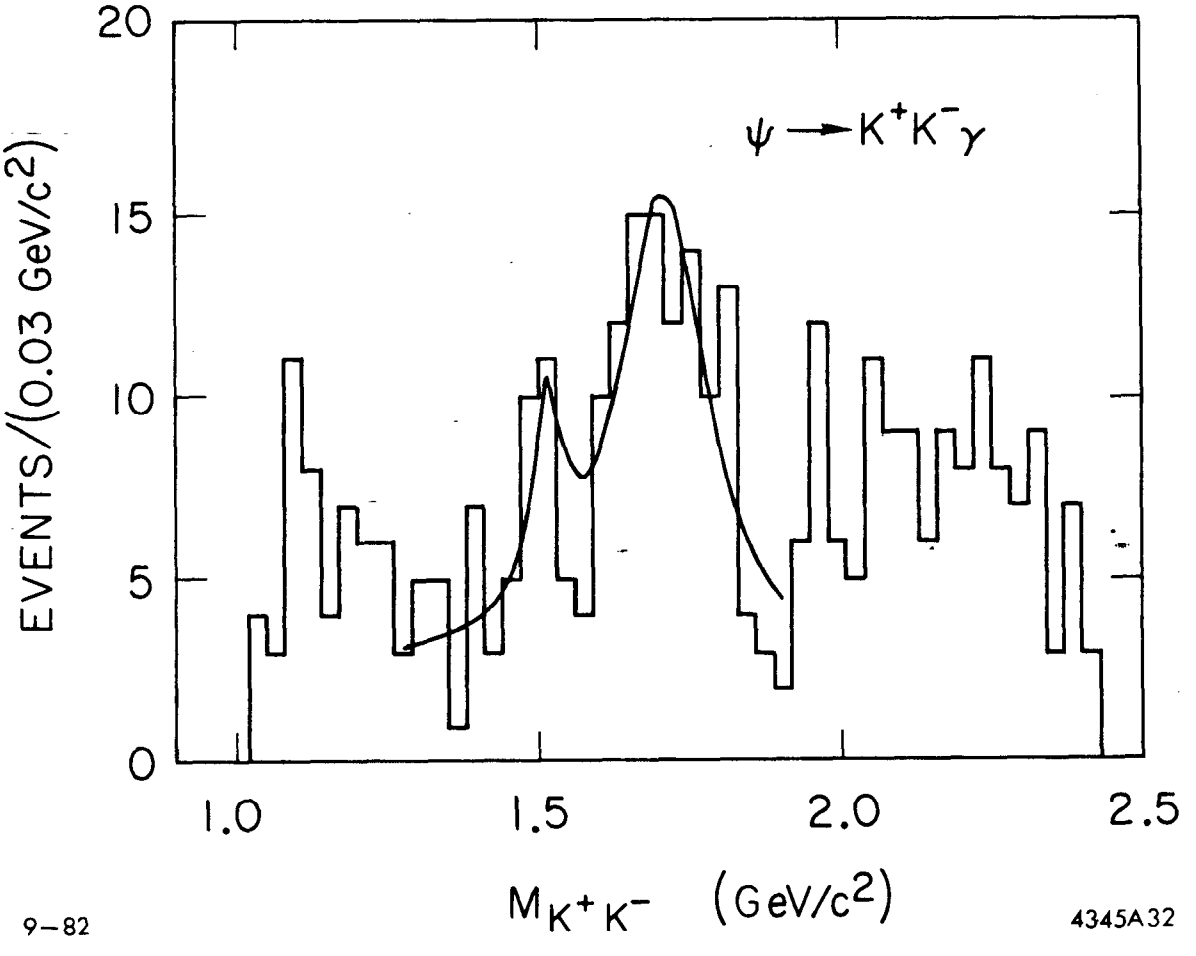

Fig. 10.1: K^+K^- invariant mass spectrum of events which survive the analysis of Method II.

The large systematic errors are due to great uncertainty in the content and form of the background. By this second method of analysis we get better statistics and more background which enables us to separate the f′ from the θ but does not allow us to measure the spin of either.

Chapter XI

SPIN DETERMINATION FOR BOTH METHODS

Spin Determination of the θ(1640)

We have attempted to measure the spin of the θ resonance in the radiative decay, $\psi \to \gamma\theta$, $\theta \to K^+K^-$. There are three angles which describe the decay: θ_1 is the angle between the direction of the γ and the positron beam direction z. Consult Fig. 3.1. θ_2 and ϕ are the polar angles of one of the kaons in the center of mass frame of the θ with respect to z′. Where the z′ axis is the direction opposite to the γ direction.

It has been shown[1] that the angular distribution describing the decay of the ψ to a γ and a spin 2 meson, is a function of θ_1, θ_2 and ϕ. The function has two parameters, x and y which are defined as

$$x = A_1/A_0 \quad , \quad y = A_2/A_0$$

where A_0, A_1 and A_2 are the helicity amplitudes for the three possible helicities of a spin 2 particle. The function is:

---

[1] Kabir and Hey, PRD 13, 3161 (1976).

$$W_{xy}(\theta_1,\theta_2,\phi) = (1 + \cos^2\theta_1)(3\cos^2\theta_2 - 1)^2$$

$$+ 4\sqrt{3}\, x \sin\theta_1 \cos\theta_1 \sin\theta_2 \cos\theta_2 (3\cos^2\theta_2 - 1) \cos\phi$$

$$+ \sqrt{6}y \sin^2\theta_1 \sin^2\theta_2 (3\cos^2\theta_2 - 1) \cos 2\phi$$

$$+ 12x^2 \sin^2\theta_1 \sin^2\theta_2 \cos^2\theta_2 + 3/2 (1+\cos^2\theta_1) \sin^4\theta_2$$

$$- 6\sqrt{2}\, xy \sin\theta_1 \cos\theta_1 \sin^3\theta_2 \cos\phi \cos\theta_2 \quad .$$

The distribution of the photon must be:

$$f(\theta_1) = 1 + \alpha\cos^2\theta_1 \quad ,$$

where $\alpha = (1 + y^2 - 2x^2)/(1 + y^2 + 2x^2)$. For a spin 2 particle, $-1 < \alpha < 1$. A spin 0 particle decays isotropically and so the function describing the decay, $\psi \to \theta\gamma$, $\theta \to K^+K^-$ is, $W(\theta_1,\theta_2,\phi) = 1 + \cos^2\theta_1$.

To determine the spin of the θ, we first note that the possibilities for spin parity assignments are reduced to

$$J_{pc} = 0_{++},\ 2_{++},\ \text{etc.} \quad ,$$

by the characteristics of the final state, K^+K^-. Two pseudoscalars can have $J_{pc} = 0_{++},\ 1_{--},\ 2_{++},\ 3_{--}$, etc. The state we produce in the radiative decay must have charge conjugation +1, so the odd angular momentum states, 1_{--} , 2_{--}, etc., which are C^- states, are excluded. Then we make a maximum liklihood fit to the two most probable spin hypotheses, that is, spin 0 and spin 2. We maximize the logarithm of the liklihoods in both cases and compare them.

The liklihood $\mathcal{L}$ is the probability of observing an event with a given θ_1, θ_2 and ϕ:

$$\mathcal{L} = \frac{\epsilon(\theta_1,\theta_2,\phi)\ W_{xy}(\theta_1,\theta_2,\phi)}{\iiint d\cos\theta_1\ d\cos\theta_2\ d\phi\ [\epsilon(\theta_1,\theta_2,\phi)\ W_{xy}(\theta_1,\theta_2,\phi)]}$$

where ϵ is the detection efficiency for an event with angles (θ_1,θ_2,ϕ). The denominator normalises the probability to 1.

We sum the logarithm of the liklihoods of all events in the sample:

$$\sum_{\text{events}} \ln \mathcal{L} = \sum_{\text{events}} \ln\left[\frac{W_{xy}(\theta_1,\theta_2,\phi)}{\iiint [\ \ldots\ ]}\right] + \sum_{\text{events}} \ln \epsilon(\theta_1,\theta_2,\phi)\ .$$

The second term does not depend on x and y and does not vary between the spin 0 and spin 2 hypotheses, therefore we neglect it in our comparison. The integral in the denominator is equivalent to a sum over the Monte Carlo events which pass the analysis cuts, of the function W normalised by the number of Monte Carlo events.

$$\sum_{\text{events}} \ln \mathcal{L} = \sum_{\text{events}} \ln\left[\frac{W_{xy}(\theta_1,\theta_2,\phi)}{1/N_{MC} \sum\limits_{\substack{MC\\ \text{events}}} W_{xy}(\theta_1,\theta_2,\phi)}\right]\ .$$

This is the function we have maximized.

For the data from the first method of analysis, that is requiring an observed photon in the event, and analysing the data in the region $1.55 < M(K^+K^-) < 1.85\ GeV/c^2$, we find:

$$x = 1.2 \pm .6 \quad \text{and} \quad y = -.9 \pm .6$$

and $\alpha = -.23 \pm .97$

$$\ell n \, \mathcal{L} = 63.0 \qquad \text{for the spin 2 hypothesis}$$

and

$$\ell n \, \mathcal{L} = 60.5 \qquad \text{for the spin 0 hypothesis}$$

A contour plot of y vs x is shown in Fig. 11.1. The contours are in steps of 1σ.

To compare liklihood, note that the fit done to the spin 2 hypothesis has two more degrees of freedom than the spin 0 case. This makes it easier to have a good fit. To correct for this we subtracted 2 from the equivalent χ^2, where $\chi^2 \equiv -2\log\mathcal{L}$, for the former fit. If the probability of spin 2 being true is normalised to 1 then the probability of spin 0 is found to be .22. That is, spin 2 is the slightly favoured hypothesis at the 78% confidence level.

The same fit is performed on the data sample from method II where we have a large (25%) background. We do not know the angular distribution of this background. Because of this we can make no spin measurement in this case.

Problems with θ spin determination:

In the small sample 1, the sample size is too small, on the order of 25 events in the fitting region, to make a statistically significant spin assignment. The f'(1516) has already been identified as a spin 2^+ meson. This means that both the large and small samples are further reduced in size by requiring that the f' does not contribute a significant background. The third problem is due to not understanding the background in the larger sample well enough to know what spin it has.

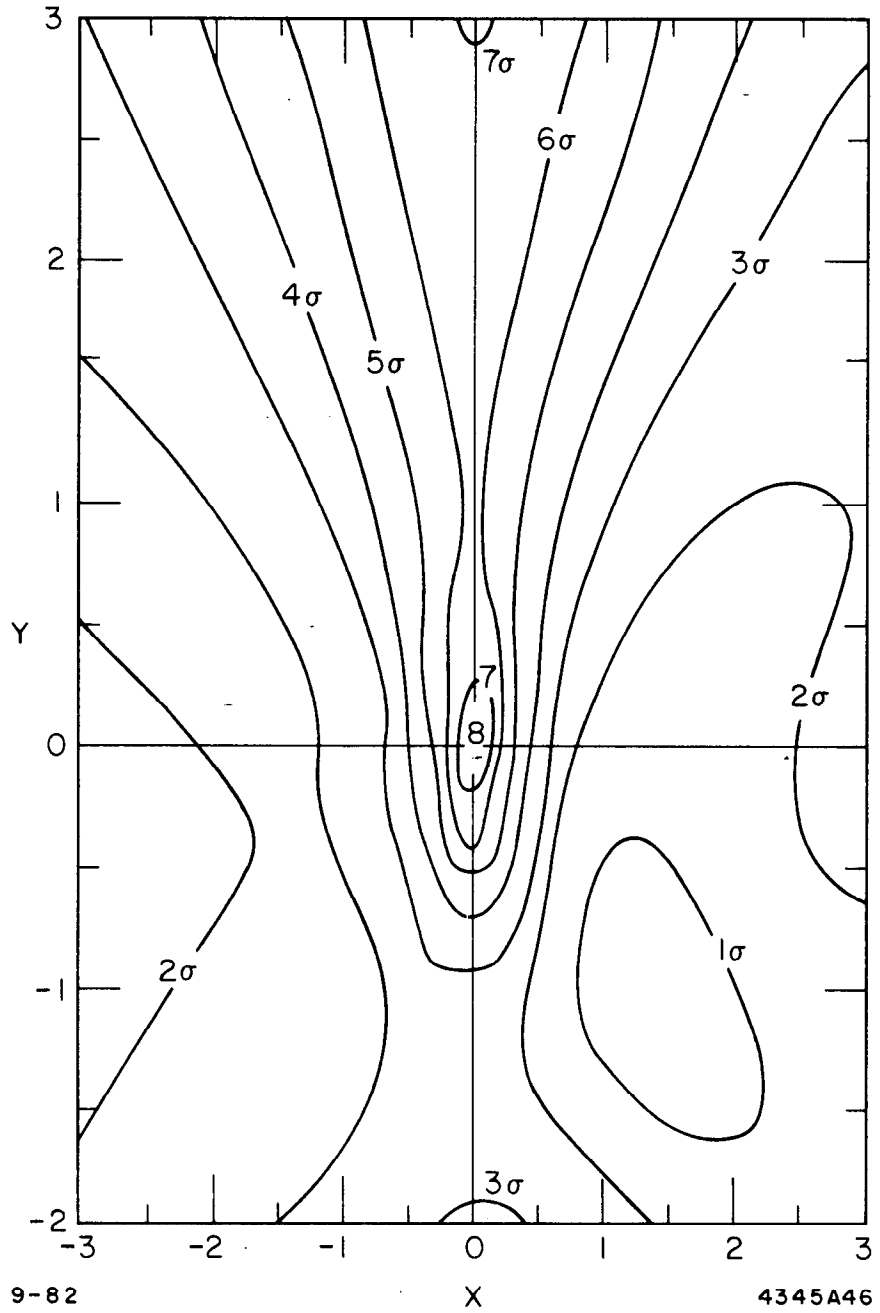

Fig. 11.1: Contour plot of helicity amplitude ratios Y versus X. The contours are 1σ apart. The minimum value is determined by maximum liklihood.

A 25% background which has unknown spin increases the systematic error of the spin measurement sufficiently to preclude measurement.

This result, spin 2 favoured at the 78% C.L., was obtained from the first analysis, and is consistent with the previous measurement by the Crystal Ball of spin 2 favoured at the 95% C.L. in the decay $\psi \rightarrow \eta\eta\gamma$.

Chapter XII

NEUTRAL DECAYS

We also expect the θ to decay via $\theta \rightarrow K_S K_S$. We searched for it in the decay

$$\psi \rightarrow K_S^0 \, K_S^0 \, \gamma.$$

We expect to observe about a factor of four fewer events from this decay than from the charged K decay because there are two final states for K^0K^0 and only one for $K^{\pm}K^{\mp}$ and because there are 4 charged particle in the final state compared to 2 in the charged case. We look for a final state with four charged pions, total charge zero, in which there are two pairs of oppositely charged pions, each pair must have an invariant mass consistent with the K_S mass. We demand that one of the pairs reconstruct as a v in the drift chamber, consistent with coming from the decay of a K^0. This analysis was performed on data sample 1, with 427,000 produced ψ's. A signal was not found. However an upper limit on the branching ratio was set at the 90% confidence level assuming all events in the region, $1.45 < M(\pi^+\pi^-\pi^+\pi^-) < 1.85$ were signal events. This gives,

$$B(\psi \rightarrow \theta\gamma) \times B(\theta \rightarrow K_S^0 K_S^0) < 1.9 \times 10^{-3} \text{ 90\% C.L.}$$

This limit is consistent with the charged mode branching ratio. Figure 12.1 is a plot of the invariant mass of the four π's after all cuts have been made.

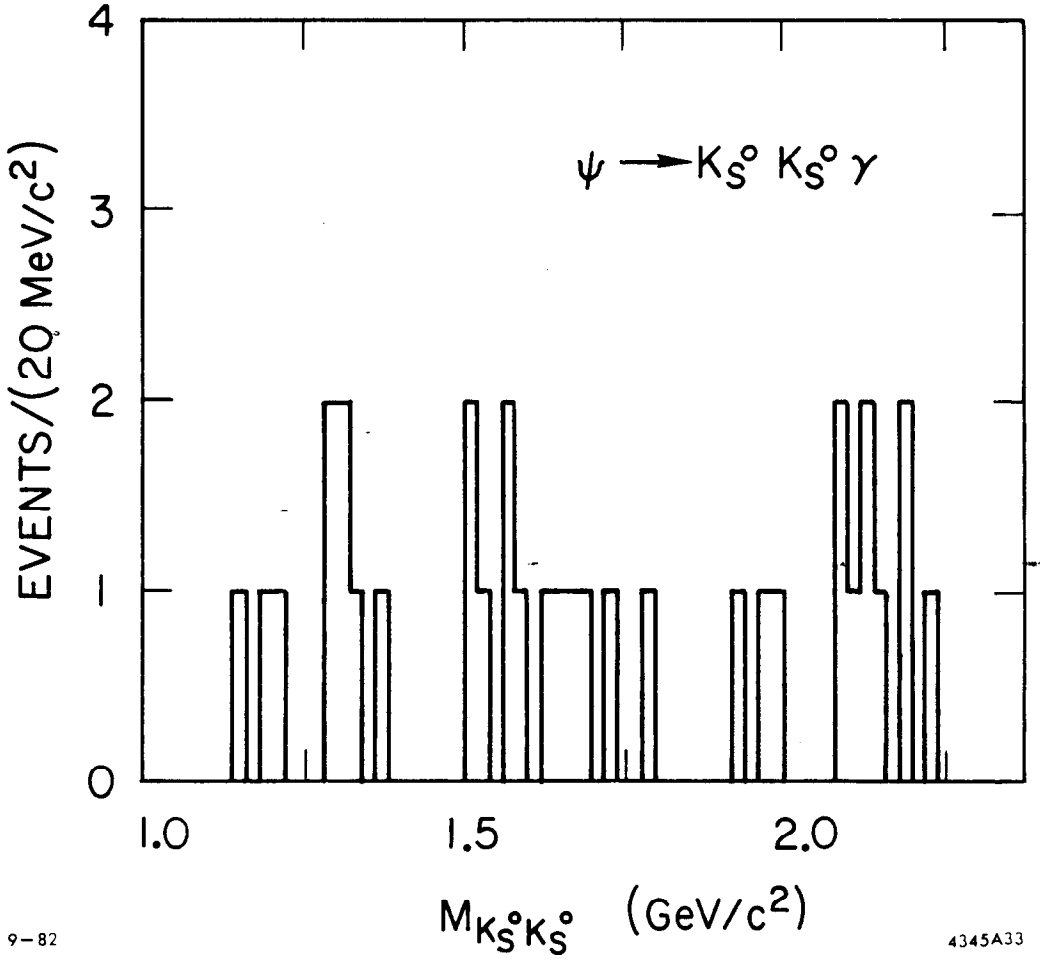

Fig. 12.1: Invariant mass spectrum of the K_sK_s pair from events $\psi \rightarrow K_sK_s\gamma$.

Chapter XIII

SUMMARY: PART II

We have observed a resonance in the radiative decay, $\psi \rightarrow K^+K^-\gamma$, with invariant mass 1700 MeV/c^2 and width 156 MeV. We find the spin assignment to be 2^{++} favoured at the 78% confidence level. These values are consistent with those of the $\theta(1640)$ resonance observed in the decay $\psi \rightarrow \eta\eta\gamma$. Table 13.1 summarises the findings of both experiments for the purpose of comparison.

Table 13.1

EXPERIMENT	M(θ) MeV/c^2	Γ(θ) MeV	B($\psi \rightarrow \gamma\theta$) B(θ →)	
Crystal Ball	1640 ± 50	220^{+100}_{-70}	$(4.9\pm1.4\pm1.0) \times 10^{-4}$	$\|\eta\ \eta\rangle$
Mark II Sample I	1655 ± 30	295 ± 60	$(6.7\pm1.3\pm1.7) \times 10^{-4}$	$\|K^+K^-\rangle$
Sample I with f′	1680 ± 30	265 ± 60	$(6.3\pm1.2\pm1.9) \times 10^{-4}$	$\|K^+K^-\rangle$
Sample II with f′	1708 ± 30	156 ± 60	$(6.0\pm0.9\pm2.5) \times 10^{-4}$	$\|K^+K^-\rangle$

We conclude that the resonance seen by the Mark II in K^+K^- is likely to be the same as that seen in $\eta\eta$ by the Crystal Ball. The data concerning the θ has so far been inconclusive as to the spin of the resonance and its species. The θ may be one of the following:

1. A Glueball

It could be a gluon bound state. There are bag model[1] predictions of 2^{++} and 0^{++} bound states at various masses between 1 and 2 GeV/c^2, including a state at 1590 MeV/c^2. These predictions however, depend on the bag model used and its characterisitc constants. We expect naively, that glueball will decay in a flavour independent manner because it is a half-Zweig suppressed decay. See Fig. 13.1.

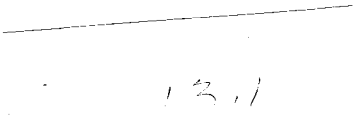

Figure 13.1

Therefore we expect to see the θ decay to $\pi\pi$, $\eta\eta$ and KK. However two upper limits have been set[2,3] on the branching ratio

$$B(\psi \to \theta\gamma) \times B(\theta \to \pi\pi) \quad .$$

The first limit was set by looking at the neutral decay, $\theta \to \pi^0\pi^0$, to be:

$$B(\psi \to \theta\gamma) \times B(\theta \to \pi\pi) < 6 \times 10^{-4} \quad 90\% \text{ C.L.}$$

---

[1] R.Jaffe and K.Johnson, Phys. Lett. 60B, 201 (1976).
[2] C. Edwards et al., Phys. Rev. Lett. 48, 458 (1982).
[3] Mark II unpublished.

and the second by looking at the charged decay mode, $\theta \to \pi^+\pi^-$, which sets the limit,

$$B(\psi \to \theta\gamma) \times B(\theta \to \pi\pi) < 3.2 \times 10^{-4} \quad 90\% \text{ C.L.}$$

No θ signal is seen in the invariant mass plots in either case. Figure 13.2 shows the Mark II, π^0 subtracted, $\pi^+\pi^-$ mass spectrum from the decay $\psi \to \pi^+\pi^-\gamma$. A clear $f^0(1270)$ peak is seen. The upper limit on the $\theta \to \pi\pi$ decay mode is set after the tail of the f(1270) has been subtracted, and with the θ parameters assumed as measured. Figure 13.3 shows the Crystal Balls' $\pi^0\pi^0$ mass spectrum from the decay $\psi \to \pi^0\pi^0\gamma$. Again a clear f(1270) mass peak is seen. A small signal at the θ mass cannot be ruled out. We would expect from SU(3) that the decay of a glueball to $\pi\pi$ would be three times that to $\eta\eta$. The lack of the $\pi\pi$ decay suggests that the θ is not a glueball, or at least not entirely a glueball. It does not strictly rule out the possibility since the behaviour of glueballs is not yet well known.

2. A $Q\bar{Q}Q\bar{Q}$ State

The second candidate species is the four quark state. Jaffe[4] also predicts masses for various 0^{++} and 2^{++} 4 quark states in the bag model. In this case the state would be,

$$1/\sqrt{2}\ |uu + dd\rangle\ ss$$

This state has the property that it does not decay to $\pi\pi$, while it does decay to $\eta\eta$ and $K\bar{K}$. Chanowitz[5] using this model predicts the ratio of

---

[4] R. Jaffe, Phys. Rev. D15, 267,281 (1977).
[5] M. Chanowitz, LBL-13398 (1981).

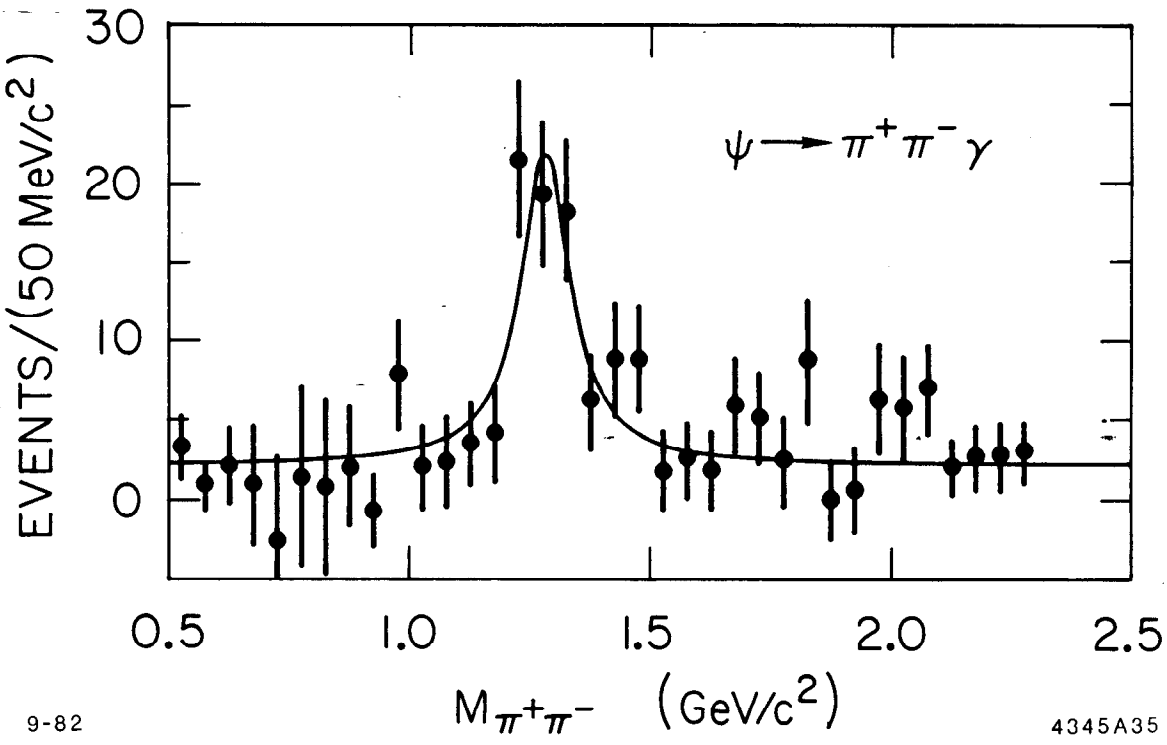

Fig. 13.2: $\pi^+\pi^-$ invariant mass spectrum, π^0 subtracted, for events of the type $\psi \to \pi^+\pi^-\gamma$. Mark II data.

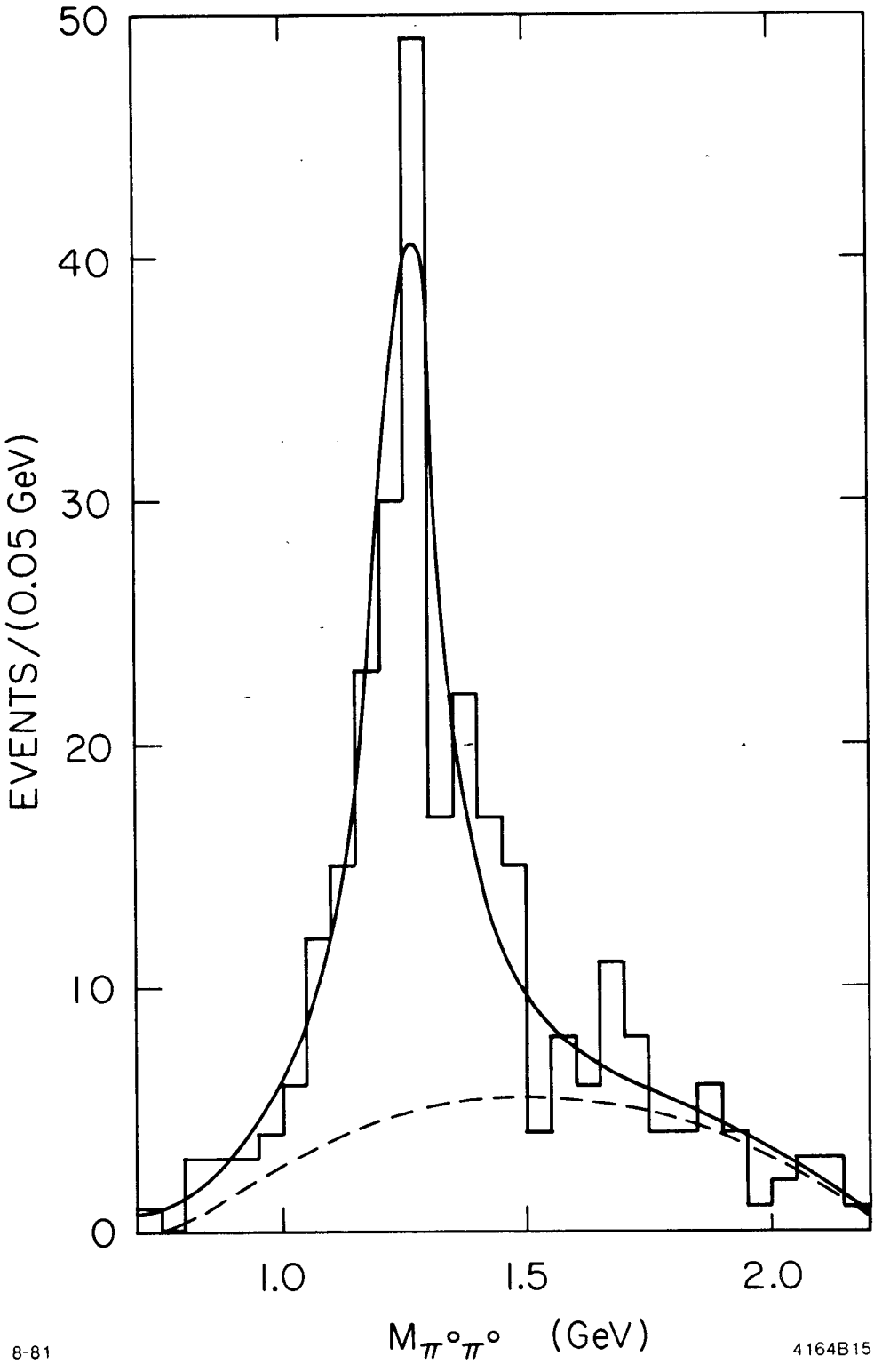

Fig. 13.3: The $\pi^0\pi^0$ invariant mass spectrum from events $\psi \to \pi^0\pi^0\gamma$. Crystal Ball Data.

branching ratios,

$$B(\theta \to K^+K^-) = B(\theta \to K^0K^0) = B(\theta \to \eta\eta) \quad .$$

From the data, the ratio $B(\theta \to K^+K^-):B(\theta \to \eta\eta)$ is,

$$1.2 \pm .5 \; : \; 1.0 \pm .4 \quad .$$

So the data are in good agreement with this prediction, but the data have large errors and therefore other models are not excluded.

3. A $|s\bar{s}\rangle$ state

The θ cannot be a conventional $|s\bar{s}\rangle$ state in the 2^{++} nonet since all those states are known and accounted for. It could be a conventional state in the 0^{++} nonet since that nonet is poorly understood as to its constituents. It could be a radially excited $|s\bar{s}\rangle$ state. Lipkin, Cohen and Isgur[6] suggest that the θ could be a radially excited $|s\bar{s}\rangle$ state which interferes with the f(1270) and the f'(1516). However their prediction for the shape of the K^+K^- invariant mas spectrum for this state, Fig. 13.4, based on the shape of the $\eta\eta$ mass spectrum, is not consistent with the spectrum found by this analysis.

4. A $|qq\rangle + |q\bar{q}\rangle$ state

Rosner[7] proposes a model which mixes a glue-glue state with $q\bar{q}$ states. He predicts a ratio of widths:

$$\Gamma(\theta \to K\bar{K}) \approx 5.7\, \Gamma(\theta \to \eta\eta) \quad .$$

This model is not ruled out.

---

[6] Cohen et al., ANL-Hep-pr-81-45 (1981).
[7] J.L.Rosner, Phys. Rev. D24, 1347 (1981) and private communication.

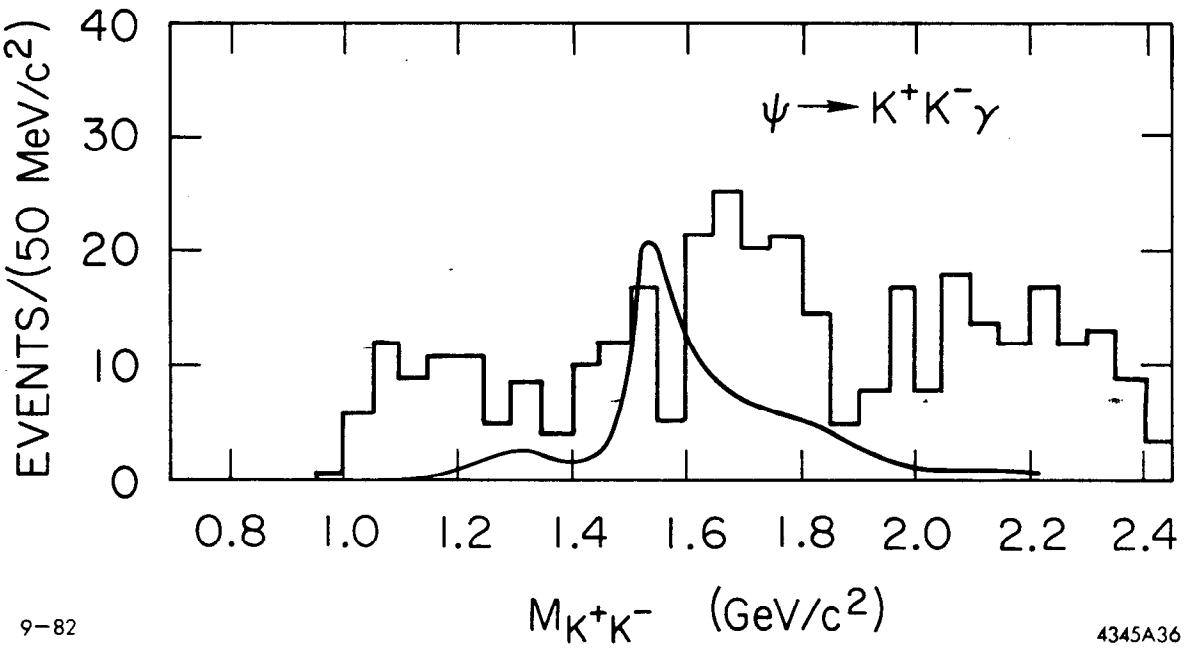

Fig. 13.4: Invariant mass of the K^+K^- in $\psi \to K^+K^-\gamma$ events, predicted by the radial excitation model of Cohen et al. The histogram is the data from analysis of $\psi \to K^+K^-\gamma$, Method II.

Finally the species of the θ is still unknown. A more convincing measurement of the spin must be made before assigning the θ its place.

$\psi \to f'(1516)\gamma$

We have observed the decay, $\psi \to f'(1516)\gamma$, for the first time. We have made a measurement of the branching ratio,

$$B(\psi \to f'\gamma) \times B(f' \to K^+K^-) = (.9 \pm .5) \times 10^{-5} \quad .$$

If we assume that $f' \to KK$ is the dominant decay of the f', that is $B(f' \to KK) \geq .75B(f' \to all)$ then we find from the data that,

$$B(\psi \to f'\gamma)/B(\psi \to f\gamma) \leq 0.16 \pm 0.10 \quad .$$

and

$$B(\psi \to f\gamma) : B(\psi \to f'\gamma) \cong 6.3 \pm 2.1 : 1.0 \pm .5 \quad .$$

We have used the fact that the branching ratio[9], $B(\psi \to f\gamma) = (1.5 \pm .5) \times 10^{-3}$. The assumption for the $K\bar{K}$ branching ratio from the f' is made for two reasons. The first is that there is no measurement of the decay $f' \to \eta\eta$. The upper limit on the branching ratio $B(f' \to \eta\eta)$ has been set[9] at < 50% and the other decay modes have been measured to be very small. The second is that SU(3) predicts the ratio

$$f' \to \eta\eta / f' \to KK = 1/9 \quad .$$

---

[9] Particle Data Group, Rev. fo Modern Physics, Vol. 52, (1980).

Lipkin and Rubinstein[10] compare the ratio of branching ratios,

$$\psi \rightarrow f, \gamma f \text{ and } \gamma A_2$$

for three final state production mechanisms. The first, shown in Fig. 13.5 is a decay of the ψ through a virtual photon to a quark and antiquark, one of which emits a photon.

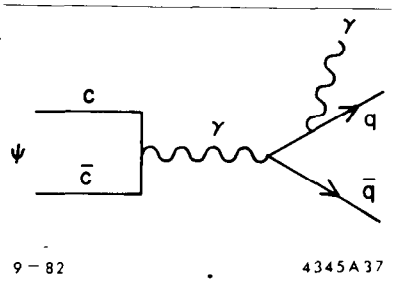

Figure 13.5

The ratio for this mode of production is,

$$f:f':A_2 \quad = \quad 25:2:9 \text{ by SU(3)} \quad ,$$

which is clearly ruled out by our data.

The second, shown in Fig. 13.6, is the decay of the ψ through three gluons to a quark and an antiquark, one of which emits a photon in the final state.

---

[10] Lipkin and Rubinstein, Phys. Lett. 76B, 324 (1978).

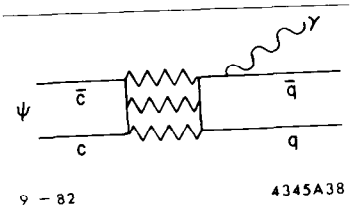

Figure 13.6

The ratio for this production mechanism is predicted by SU(3) to be

$$f:f':A_2 = 1:2:9 \quad .$$

Again this is inconsistent with our data if it is the dominant mechanism. The third possibility is the the ψ annihilated to two gluons and a photon. See Fig. 13.7.

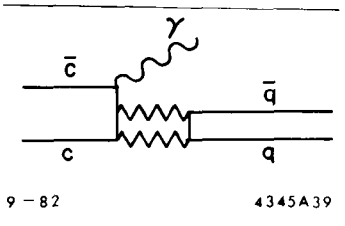

Figure 13.7

The ratio for this production mechanism is,

$$f:f':A_2 = 4:2:0 \text{ by SU(3)} \quad .$$

This prediction is consistent with our data. We conclude that if there is one dominant production mechanism of the f anf f′ in radiative ψ decays then the only data consistent one is the third possibility presented, the annihilation to two gluons and a photon.